Czech Technical University in Prague

Faculty of Electrical Engineering
Department of Computer Science and Engineering

Optimisation of Hydrological Models Using Adaptive Heuristic Search Algorithms

Doctoral Thesis

by

Martin Chlumecký

PhD Programme: Electrical Engineering and Information Technology
Branch of Study: Information Science and Computer Engineering

Doctoral thesis statement for obtaining the academic title of "Doctor",
abbreviated to "Ph.D."

Prague, March 2018

Abstract and Contributions

The rainfall-runoff model is a theoretical physical model based on principles of water movement in a watershed. This thesis focuses on the conceptual rainfall-runoff SAC-SMA model which can estimate various aspects of modelled basins. The most common use of the model is to assess parameters that are not readily measured or to predict the future behaviour of the modelled basin. The model should be well calibrated to return useful information. The model calibration is performed using dozens of parameters and their correct setting is a complex issue even for experienced hydrologists.

Therefore, it is necessary to use optimisation techniques which are able to find an appropriate setting of model parameters very fast. We aim to use the genetic algorithm (GA) which is one of the global search algorithms that use the heuristic procedures. The goal is to calibrate the model so that it returns the most accurate results.

Even though many optimisation methods already exist, there are still cases of calibrations where the current optimisation techniques fail. Moreover, some parameters are in correlation that is different for each modelled basin and period. Typically, these are parameters which describe continuous natural processes that are defined by discrete values. The continuous process is then specified by several coordinates that are deformed by the optimisation. The result is an inapplicable calibration. The random number generator (RNG) plays a significant role in this since it estimates values of optimised parameters. However, the software RNG just generates pseudo-random numbers (PRNG) which means that sequences of "random" numbers might begin to repeat. The goal of the thesis is to analyse and design a solution for the problems described above.

The SAC-SMA model defines two hydrological phenomena that can be specified by continuous functions instead of the discrete values. The continuous function is expressed by parameters whose optimisation does not disturb the continuous course. Hydrological data are an appropriate source of real random numbers which can be a base for the PRNG. The new concept of the RNG based on hydrological data (HRNG) has been developed for the optimisation of the SAC-SMA model.

The results indicate that parameters defined by the continuous function provide a better solution since the GA preserves a mutual relationship between the correlated parameters. The optimisation using the HRNG brings a significant improvement of the model calibration. The most significant contribution of the HRNG is acceleration of the optimisation and that the HRNG is able to find better solutions in comparison with the PRNG. Moreover, the HRNG reduces mutual dependence of the optimisation quality and GA parameter setting.

The achieved results contribute to efficient calibration of the rainfall-runoff models. Hydrological data can be used as a source of random numbers to improve the optimisation process. The newly designed methods and principles will be able to be applied to other optimisation problems which are a subject for further research. Furthermore, the distribution function of the HRNG can influence the optimisation direction and thereby optimisation speed so that the additional research will be focused on the distribution function of the RNG and its effect on optimisation quality.

Anotace

Srážko-odtokové modely jsou teoretické modely založené na fyzikálních principech pohybu vody. V této práci se zabýváme konceptuálním srážko-odtokovým modelem Sacramento Soil Moisture Accounting Model (SAC-SMA), pomocí kterého je možné, sledovat a odhadovat různé aspekty povodí. Model je také schopný odhadovat rozličné fyzikální veličiny, jejichž měření je finančně či časově náročné a v některých případech dokonce nemožné. Aby byl model schopen vracet užitečné informace, musí být model správně kalibrován. Kalibrace modelu se provádí pomocí až desítek parametrů a jejich správné nastavení je velmi složitá úloha i pro zkušeného hydrologa.

Z těchto důvodů je nutné použít optimalizační techniky, které jsou schopné velmi rychle najít správnou konfiguraci modelových parametrů. Největší zastoupení mají globální vyhledávací algoritmy, které využívají heuristické postupy. V této práci se zaměřujeme na genetické algoritmy (GA), které se ukázaly jako vhodný nástroj pro automatickou kalibraci srážko-odtokových modelů. Cílem je tedy nakalibrovat model tak, aby vracel co nejpřesnější výsledky.

Ačkoliv bylo vyvinuto několik optimalizačních postupů, stále se objevují případy kalibrací, kde současné optimalizační techniky selhávají. Analýzou bylo zjištěno, že některé parametry modelu jsou ve vzájemné korelaci, která je ovšem jiná pro každé modelované povodí a dokonce i období. Typicky jde o parametry, které popisují spojité přírodní procesy, které jsou definovány pomocí diskrétních hodnot. Spojitá vlastnost je pak popsána pomocí několika bodů, které ale optimalizační techniky deformují. Výsledkem je pak nereálná kalibrace modelu. Klíčovou roli také hraje generátor náhodných čísel, který odhaduje hodnoty optimalizovaných parametrů. Softwarové generátory ale pouze generují pseudo-náhodná čísla (PRNG), která se důsledkem konečného prostoru paměti počítače a sekvence generovaných čísel mohou začít opakovat. Cílem práce je tedy analyzovat a navrhnout řešení pro výše uvedené problémy.

SAC-SMA model zde definuje dva hydrologické procesy, které lze popsat spojitou funkcí, místo množiny diskrétních hodnot. Spojitá funkce je definována parametry, jejíchž optimalizace nenaruší spojitý průběh funkce. Hydrologická data jsou dobrým zdrojem skutečných náhodných čísel. Data mohou pomoci při optimalizaci tím, že budou podkladem pro PRNG. Pomocí těchto dat byl vyvinut nový generátor náhodných čísel, který je založený na principu hydrologických dat (HRNG).

Výsledky naznačují, že pokud jsou parametry definovány pomocí spojité funkce, optimalizační algoritmus udržuje vzájemný vztah mezi korelovanými parametry a výsledky kalibrace jsou použitelné v praxi. Optimalizace přináší výrazné zlepšení při použití HRNG. Velmi významným příspěvkem HRNG je zrychlení optimalizace a to, že HRNG je schopné najít lepší řešení. Navíc při použití HRNG se snižuje závislost kvality optimalizace na nastavení parametrů GA.

Dosažené výsledky přispěly k efektivní kalibraci srážko-odtokových modelů. Hydrologická data je možné použít jako zdroj náhodných čísel a tím zlepšit optimalizační proces. Nyní zde navržený postup je možné aplikovat i na jiné optimalizační problémy, což bude předmětem dalšího výzkumu. Navíc se ukázalo, že distribuční funkce HRNG může ovlivňovat směr a rychlost optimalizačního procesu, takže dalším předmětem výzkumu bude vliv distribuční funkce náhodného generátoru na kvalitu optimalizace.

Acknowledgements

My sincerest thanks are extended to my project supervisor, associate professor Dr. Karel Richta, for his guidance. My warmest thanks go to my colleague, associate professor Dr. Josef Buchtele from Czech Academy of Sciences. He has been a constant source of assistance and inspiration during my research and helped me with numerous problems and professional advancements. I shall not forget to mention Dr. Božena Mannová whose support and encouragement was crucial for the success of this thesis. This dissertation would not have been possible without the financial support of the Czech Technical University in Prague. Last but definitively not least, I want to thank Barbora Pilařová for proofreading. Finally, my greatest thanks go to my family for their infinite patience and care and to friends for support during the whole period of my PhD study.

Thesis Supervisor:

Karel Richta

Department of Computer Science and Engineering
Faculty of Electrical Engineering
Czech Technical University in Prague

Karlovo náměstí 13
121 35 Prague 2
Czech Republic

Contents

List of Figures

List of Tables

Preface

Motto:

Water *prerequisite for live*
*In tourism trio: sun – **water** – air*
*In global climate program: energy – **water** – food*

Modelling of rainfall-runoff models: parameter optimisation and ascertainment of evapotranspiration

The actual aim of the rainfall-runoff modelling is to use the right tools for the evaluation of various changes of water regime. In this context, the desired missing information concerning the vegetation cover is compensated by optimal monthly values of expected evapotranspiration. The intention is to decrease the uncertainties in the water regime that were caused by different oscillations. It requires the evaluation of the appearing natural fluctuations and also the seemingly abrupt random changes in the basin. This sequential variability of water regime is usually influenced by changes of vegetation cover (not only in the annual cycle), see Appendix B.

The long time series of *precipitation* and air *temperature* have been used for modelling the rainfall-runoff process and mainly for the precise assessment of the evapotranspiration demand, in our case for the Czech Labe River catchment. The occasional fluctuations and random changes of vegetation cover are to be followed as an indication of oscillations in the development of evaporation. The intention is to appraise such complicated time series as a relatively long process.

The modified version of the conceptual SAC-SMA model enables a prompt simulation that creates the conditions for automatic calibration of this rainfall-runoff model. The prompt simulation is applicable primarily to partial time intervals with diverse expected evapotranspiration. So, the resulting evapotranspiration is represented by the model outputs; such values could be hardly measured or computed.

The SAC-SMA model calibration is a complex issue. However, a well-calibrated model provides the best model output, such as ascertained evapotranspiration. The optimisation techniques can make the calibration process easier since it speeds up the whole process of rainfall-runoff modelling.

1

Introduction

Conceptual rainfall-runoff models are standard tools that can be used to predict the outflow or other hydrological characteristics in interest basins. A number of conceptual rainfall-runoff models has been developed over the last few decades. These models have a simpler structure than their physically based spatially distributed alternatives and generally have fewer input data, Wagener *et al.* (2004). The models need to be correctly configured by model parameters – this process is called the model calibration. One primary modelling task is validation of the model calibration which verifies that the model is able to return realistic results. It logically follows that useful hydrological information can be collected only if the model is calibrated in the most suitable way. Dozens of model parameters calibrate the rainfall-runoff models. However, combinations of model parameter values increase with the number of model parameters. Moreover, the vast majority of the model parameters are in the field of real numbers; therefore, the search space is infinite. The best way to calibrate the rainfall-runoff models is by using the global optimisation techniques that can find optimal model calibration, Gandomi *et al.* (2015). Successfully calibrated rainfall-runoff model provides practical and profitable information for a lot of sectors. Unfortunately, the optimisation techniques are not omnipotent and there is still no way how to efficiently calibrate the model parameters automatically by optimisation techniques. Furthermore, there are several instances of hydrological simulations where the optimisation of the model calibrations fails in defiance of the high quality of the model validation, Buchtele *et al.* (2009).

This dissertation focuses on the optimisation of the rainfall-runoff model and simulation cases where the current optimisation techniques fail and do not provide satisfactory results. Long time series with a lot of important hydrological events (e.g. floods, vegetation and agricultural changes, insect's disasters, etc.) that are not stable across the whole series bring the most significant problem during the model calibration. Observed catchments of this study are Malá Ráztoka, Liz, and

the Elbe River located in the Czech Republic. Ráztoka and Liz are small experimental basins (approx. 2 km^2) with many hydrological events that affect the model calibration because the events are monitored in the small area. In contrast, the Elbe River is a vast watershed with a hundred-year time series. A hydrological modeller must perform several model calibrations in order to achieve the required results. Additionally, the manual model calibration is a lengthy process and the quality is dependent on the experience and intuition of the modeller. The optimisation of the rainfall-runoff models is still a current topic according to Vrugt *et al.* (2006), Wang *et al.* (2010). Global search algorithms searching the infinite search space can provide the best results if applied to the rainfall-runoff calibration, Gandomi *et al.* (2015). The *genetic algorithms* (GAs) are the most common group of optimisation algorithms for rainfall-runoff models and are based on the principles of evolution, Holland (1992).

Further, this thesis describes the concept of a newly designed generator of random numbers which is key for optimisation algorithms, Storn and Price (1997). Randomness and independence of the random number generators (RNG) significantly affect quality and speed of the optimisation, Tigkas *et al.* (2016), Abdulla *et al.* (1999). Therefore, the structure of the RNGs is one objective of this proposition. Rainfall-runoff models specify the properties of modelled basins using discrete values which mirror certain natural phenomena that are, of course, continuous. However, the optimisation of the discrete definition does not take into account the continuity of optimised parameters, so results of these optimisations may be inapplicable. Lastly, we introduce an approach which defines discrete model parameters by applying continuous functions.

1.1 Problem Statement and Research Objectives

The model calibration of the rainfall-runoff models is a complicated process. It comprises many pieces of knowledge, like hydrology, statistics and combinatorics, optimisation, data mining, and computer science in general. The hydrological modeller must master mentioned science fields with different levels of knowledge. The calibration process can never be wholly automated since the modeller's experience and sense of modelling are always needed. Therefore, we categorise the problem statement into several separate issues. The first class is the model calibration itself. The manual calibration is a lengthy process, and the GA is a powerful tool to improve quality of the model calibration. However, the optimisation also has its own pitfalls which are another category of the problem statement. Finally, the model validation verifies the result of the model calibration

obtained from the optimisation process. Nonetheless, there are several cases of rainfall-run simulation whose model validations show a high level of model verification but parameter values of the verified model calibration are unusable for real application. The model validation issue is the last category of the problem statement.

Each category of the problem statement brings specific problems which we strive to avoid because they prevent a successful model calibration.

1.1.1 Model Calibration

Specific rainfall-runoff processes and their mutual interactions are observed in each basin and they are objectives of the rainfall-runoff modelling. The goal of the rainfall-runoff models is to understand the interactions between the processes. There are many rainfall-runoff models with different structures and concepts. We focus on the Sacramento Soil Moisture Accounting Model (SAC-SMA) which is a conceptual water balance physical model based on the physical principles of water movement in a watershed. The SAC-SMA model provides excellent results for long time series. However, there is still room to improve the model calibration quality.

The model input is a time series of *precipitation* and air *temperature* which are transformed into actual simulated runoff. The model is configured via approx. 30 parameters whose values affect the simulated runoff. The model calibration intends to approximate the simulated and observed runoff as close as possible. The SAC-SMA parameter values also produce information about the character of the modelled basin; e.g. groundwater capacity, water infiltration, water consumption of the vegetation, etc. Therefore, the more accurate the model calibration, the more precise the information about the observed basin, Burnash (1995). The SAC-SMA model has been designed for use in a warm climate. The studied watersheds of this thesis are located in a mild climate where meteorological conditions delay *precipitations* and thereby affect the simulated runoff. Hence, a snow model must be connected to the SAC-SMA model. The snow model simulates the accumulation and melting of snow cover and transforms *precipitations* into the snow cover and the snow cover into *emulated precipitation*, Anderson (2006). In short, the snow model influences total precipitations falling to a basin area. Finally, the last supporting model is a unit hydrograph describing a hypothetical response of a catchment caused by jaggedness of the watershed terrain (e.g. mountains, retention tanks, etc.) which delay *precipitation* and thereby delay the simulated runoff. Each supporting model brings other parameters to the model calibration.

So, there are dozens of model parameters, and estimation of their values is a complicated issue. Moreover, certain parameters are in correlation and affect each other. The whole problem is hindered by the fact that the correlation is different for each modelled watershed and even modelled period, Abdulla *et al.* (1999). The modeller must have a good knowledge of the SAC-SMA model and the modelled basin. The quality of input data can also influence the success of the model calibration since the input data are usually loaded with noise; especially for a long time series which are the focus of this study. We focus on the long time series in the range of 50-100 years. Unfortunately, there is a high probability of data noise brought about by certain factors, e.g. exchanging the measuring instruments. Furthermore, character and behaviour of the basin environment change during longer periods of time; especially the water consumption of the vegetation cover, Hejzlar *et al.* (2003).

It is sometimes assumed that 5-10 years time period is sufficient for an accurate simulation because there are significant hydrological events contained, e.g. floods and low-flow periods caused by dry seasons. At the same time, it is expected that the time period has not been artificially changed, e.g. deforestation, water buildings, dams, retention tanks, etc. Further, changes of vegetation cover play a serious role in water consumption since it brings about an alteration of evapotranspiration demand, so there is a change of water regime. This is another instance of long time series simulations which need to use the optimisation techniques since it is more complicated to calibrate the model manually. Moreover, the modeller has to analyse this long period to do a successful manual calibration, and therefore the optimisation fundamentally simplifies the estimation of model parameters. An example is the Elbe River catchment which was observed for a period of approx. 100 years. Specifically, high water consumption required for filling the new water reservoirs and dams in 1955-1970 has caused a loss in observed runoff although the model does not react to this situation, Buchtele and Košková (2008). Therefore, it is necessary to perform many auxiliary simulations and calibrations to obtain the best information about the monitored watershed. The quality model output is for example useful for assessment of water storage variability. Thus, the optimisation approach can accelerate this calibration problem.

It is clear from the above that the model calibration is necessary to be performed for each catchment for the modelled period. The same must be done if the source of the input data is changed since the model calibration and input data are closely interlinked. The modeller must accomplish several manual calibrations during which the model parameters are tuned to make the output match the modelled

reality. In some cases, the manual calibration is often limited to trial and error method even for advanced modellers. This also applies to the model calibration of the same basin but for various time periods, Buchtele and Tesar (2013).

It is evident that manual calibration is a very time-consuming process with many hitches. The optimisation techniques are used for successful model calibration, and they can speed up the calibration process significantly.

1.1.2 Genetic Algorithm and Random Number Generator

The *genetic algorithm* (GA) is a heuristic process which attempts to apply the principles of evolutionary biology to find solutions to complex problems for which there is no appropriate exact algorithm. The GAs use techniques imitating the evolutionary processes known from biology (e.g. inheritance, mutation, natural selection, and crossing). The modeller defines the GA parameters which affect the optimisation course and the success rate. The *population size* and *generation limit* are parameters influencing the computation time. The mutation, selection, and crossing rate impact the optimisation quality so the modeller should be informed about the parameter relevance, Holland (1992).

The random number generator (RNG) is a tool which generates series of random numbers. The most important applications of the RNGs are in the fields of computer simulation and modelling. Bastos-Filho *et al.* (2010) prove that quality of the RNGs is critical for the optimisation quality. Another facet of the optimisation success is the distribution function of the RNG and the range for each optimised parameter which specifies in which interval these values of the model parameters are estimated. The range setting is crucial for optimisation quality, and this issue is introduced in Section 1.1.3. However, the distribution of generated numbers affects the method of how the GA explores the search space since generated numbers have different probabilities that will be generated. Thus, the GA with appropriate settings of the parameter ranges may scout the search space in the right direction.

Software RNGs are generators of pseudo-random numbers (PRNG) with certain limitations. One of the limitations is periodicity caused by the final memory of computers. The result of the periodicity is that the generated numbers eventually begin to repeat as soon as more numbers are needed. It follows that the number of the SAC-SMA parameters increases the probability of the periodicity since the optimisation requires hundreds of thousands of random numbers. Therefore, we will investigate a hypothesis whether hydrological data (*precipitation*, *temperature*,

runoff, etc.) which are an excellent source of random numbers can be used to improve the PRNG.

1.1.3 Optimisation of Model Calibration

The optimisation of the rainfall-runoff models is the NP-complete problem whose solution is searched in a search space of real numbers that is infinite. It follows that we cannot find the optimal solution – the best model calibration. We can only approach the optimum solution. A large number of model parameters makes the optimisation problem more difficult; moreover, the supporting models (snow and unit hydrograph) increase the number of optimised parameter. All parameters are real numbers with different orders of magnitude of model parameter values which extends the scope of the search space.

Another barrier to a successful optimisation is the correlation between the model parameters, as we mentioned in previous subsection 1.1.1. The correlation is ambiguous, and there is no way how to find and determine which parameters are in the correlation, Abdulla *et al.* (1999). The GA uses a so-called chromosome that keeps information about estimated model parameters. However, the GA optimises each chromosome item one by one, so the GA cannot take the correlation between individual items of the chromosome into account. Moreover, the correlation between model parameters is diverse for each basin and modelled period; therefore, implementation of the GA would have to be different for each simulation instance which is unusable in practice. One of the issues that emerge from these findings is determining the direction of the optimisation according to the parameter correlation would require a great deal of effort to implement. Consequently, it is necessary to seek a broader part of the search space which can easily cause that the GA gets lost in the search space or gets stuck in local minima. This means that there are instances of the model calibrations which were optimised by current optimisation techniques that can be easily improved by the manual calibration. Hence, these techniques do not contribute to efficient model calibration.

Another important fact is that the modeller must define ranges for each optimised parameter since the search space is infinite and it is necessary to exclude parts of the search space where the optimal solution is probably not present. The inputs of the GA are the ranges for each optimised parameter value which guide the GA to what extent to explore the search space. The GA user can restrict an area of the search space which the GA explores and where it finds the optimal calibration. Due to this, the GA user might steer the optimisation way in the right direction but he/she can also restrict the search space, so the optimal model calibration

is outside this border, and thus make it impossible to find the best solution. One solution to this problem is to use wide intervals for values of estimated parameters, but there is a high probability that the GA will not scan the entire designated area of the search space. Moreover, the longer the algorithm is looking for the optimal solution, the higher the probability of the GA degeneration which devalues found solutions, Holland (1992).

At first glance, it is not clear that the modeller's knowledge of the computer sciences plays an important role in the quality of the optimisation. That is because the right configuration of the GA parameters affects the optimisation quality directly. Most modellers are primarily hydrologists with basic computer skills, but detailed knowledge of the GA architecture requires more advanced proficiency. Users of the GA must have experience and should become acquainted with the GA parameters, their values and relevance. The GA can be configured by several parameters which significantly influence the performance and optimisation results; typically, parameters determine the computation time and optimisation direction. The smaller the number of GA parameters which the user must configure, the lesser the tendency to the GA degeneration, Holland (1992). Current solutions do not allow the number of the GA parameters which the user can configure to decrease. Therefore, one of the goals of this thesis is not to add other parameters which would burden the modellers. Ideally, reduction of the GA parameters would be a step forward.

1.1.4 Model Validation

The model validation verifies the model calibration by comparing the simulated and observed discharges using statistical methods. If the differences between the discharges are relatively small, then the model calibration and model output are valid. The product of each statistical method is an indicator expressing the degree of calibration quality, Anderson and Bates (2001). The basic indicators are the Root Mean Square Error (RMSE), Coefficient of Efficiency (Nash–Sutcliffe), and Correlation Coefficient (R).

The indicators do not allow the verification of the model calibration whether it really is applicable despite the best value of the statistical indicators. In practice, this means that the optimisation result must be inspected by a hydrologist who assesses the relevance of the model calibration. The optimisation process determines the solution quality using these indicators, and therefore the GA also cannot evaluate the relevance of the model calibration. Aspects assessing the calibration relevance are different for each basin and modelled period so there is no general procedure to implement these aspects into the GA directly, Duan *et*

al. (2006). A user intervention to the optimisation progress is not possible since the GA generates thousands of simulations and the user cannot inspect each simulation and determine their quality. As a consequence of the calibration relevance it is evident that the GA can find the best solution (model calibration) based on the statistical indicators as validation tools, but values of the model calibration are inapplicable for real use. Unusable model calibrations do not reflect the modelled reality since the model parameters show abnormal values; which means that it is a false positive result. Typically, these are the parameters which are in correlation.

The occurrences of false positive results cannot be eliminated completely. The modeller can only define a range of parameter values which limit the abnormal values. Unfortunately, some parameters are in correlation and it is time-consuming to specify which parameters might cause the false positive results. Moreover, problematic parameters are again different for each basin and time period. The issue about the range settings is described in the Section 1.1.2.

However, there is a group of model parameters whose correlation is the same across the modelled basins and even time periods. Parameters specifying the evapotranspiration (ET) and unit hydrograph (UNIT-HG) are defined as sets of discrete values without mutual relations. Nonetheless, ET and UNIT-HG are continuous functions but they are defined as sets of discrete coordinates. These discrete values are optimised by the GA separately; hence the GA can disrupt the shape of these continuous functions since information about the correlation cannot generally be implemented into the SAC-SMA model and the GA.

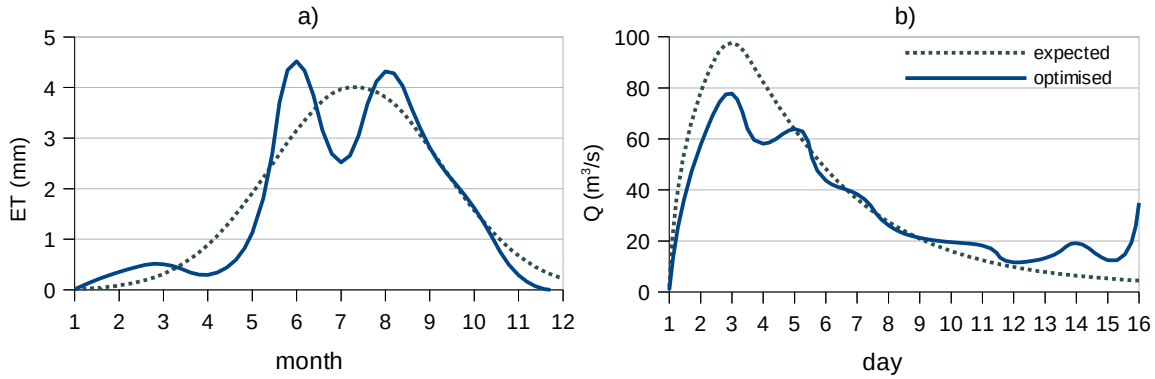

Figure 1.1: Distortion of curve shapes after optimisation: (a) evapotranspiration, (b) unit hydrograph

Figure 1.1 illustrates the shape distortion of ET and UNIT-HG parameters. The ET shape is expected to look like the Gaussian curve, but the optimised shape is approximately Gaussian only on the margins of the curve, as Figure 1.1a illustrates. Although, the model validation looks good because RMSE and R have satisfying values (see Table 1.1), the decrease of ET in the 7^{th} month does not mirror the modelled reality. This decrease in water consumption is not possible since there was not a significant change of vegetation cover on Ráztoka watershed in 1999. Similar case is the optimisation of the UNIT-HG where a 70 years long time series of the Elbe River is modelled. Figure 1.1b shows a decrease in the 4^{th} day and a significant increase in 13^{th} to 16^{th} day. However, these deviations are impossible in spite of the model validation (see Table 1.1), because such a fluctuating course of discharge has not been found on this long time series, Buchtele and Košková (2008).

Table 1.1: Model validation of false positive results

Indicator	**ET**	**UNIT-HG**
RMSE	0.0230	23.733
Nash-Sutcliffe	0.8179	0.7320
Correlation Coefficient	0.9111	0.8560

The examples described above are typical cases of the correlation between model parameters and their unsuccessful optimisation. Therefore, another aim of this dissertation is to adapt the SAC-SMA model so that the optimisation will take the parameter correlation into account.

1.2 Hypotheses of the Thesis

We have summarised two objectives based on related works from fields of hydrology and informatics.

The SAC-SMA model defines continuous properties of a watershed using discrete parameters which are independent of each other from the point of view of the optimisation. However, the parameters are dependent on each other from the point of view of the model simulation which the GA cannot take into account.

Objective 1: There is a hypothesis that if the continuous property of the rainfall-runoff model is defined using a continuous function instead of discrete parameters, then the GA will respect the correlation between these parameters.

The PRNG affects the quality of the optimisation. Hydrological data could provide the information useful for generating the random numbers whose randomness could be genuinely independent.

Objective 2: If the statement that hydrological data improve the quality of the PRNG is valid, then this enhanced PRNG should make the optimisation of the model calibration more reliable.

1.3 Motivation

The primary motivation of this work is to design a new concept of optimisation framework using the *genetic algorithm* with a newly constructed random number generator working on the principle of hydrological data.

The purpose of this framework is to find the best model calibration which reflects the reality of the modelled basin in the best way. It means that curves of simulated and observed discharges are identical to each other. The best model calibration and thus model output provide useful information about monitored catchment and can estimate model parameters which cannot be measured directly. Further, we expect that if the hypotheses of this thesis will be verified, these results should be applied to similar optimisation issues even in other scientific fields.

1.4 Structure of the Thesis

This thesis is organised as follows:

Chapter 1 introduces this work and the problem statement as well as the goals and contributions.

Chapter 2 provides an overview of the state of the art in model calibration, model optimisation, quality of input data, and previous researched results. In this chapter, we also describe several existing approaches to model optimisation using the global search algorithm.

Chapter 3 introduces theoretical background of hydrology, the rainfall-runoff model and its modelling. Further, the use of the SAC-SMA model is described which is the aim of this thesis. The second part of this chapter is dedicated to the *genetic algorithm* (GA) and the generators of random numbers (RNGs).

Chapters 4 to 6 present the approaches and novel contributions of the thesis. More precisely, Chapter 4 introduces a framework for the SAC-SMA simulation and its optimisation using the GA. In Chapter 5, we describe a newly designed random number generator based on hydrological data (HRNG), and its application to the GA. Finally, Chapter 6 is dedicated to the design and application of the continuous functions for optimisation of discrete model parameters.

Chapter 7 introduces basic information about study areas. We summarise the following basins: Mala Ráztoka, Liz, and the Elbe River. All monitored watersheds are located in the Czech Republic.

Chapter 8 summarises main optimisation results obtained from the newly designed optimisation framework which uses the GA with the HRNG.

Chapter 9 concludes the thesis and the possibilities of further future work.

2

State of the Art

A considerable amount of literature has been published regarding the usage and development of the rainfall-runoff model. These studies are focused mainly on the model calibration and its optimisation. However, a disadvantage of these studies is the fact that objectives are only observed and pursued on certain catchments. Therefore, the results are not often generally applicable since used methods have been adjusted to the particular basin and environment, even though these results still have been a valuable step forward. In this chapter, we summarise related works concerning calibration, optimisation of hydrological models and facts which prevent the application of these results in the dissertation objectives.

Section 2.1 discusses the research regarding a general *model calibration* which is the core of our effort. Section 2.2 is the most extensive part of this chapter because the *optimisation* is a significant part of this thesis. The most used global search algorithms for rainfall-runoff optimisation and diverse catchments are summarised there. The next chapters 2.3 and 2.4 analyse aspects that directly influence the *model calibration*. The first is quality of calibration data, especially for long time series. The second aspect is the uncertainty of model parameters which can change their values over time. The sections sometimes overlap since model calibration, optimisation, and data quality are very closely related. In the last chapter 2.5 we discuss which methods and algorithms can be applied to our case study and why we cannot directly use the current state of the art.

2.1 Model Calibration

Numerous studies have attempted to explain and demonstrate how to efficiently calibrate rainfall-runoff models and present general instructions to make the models useful.

STATSGO Soils Database

A recent study by Oudin *et al.* (2008) focuses on the fact that similar watersheds can quickly and efficiently estimate model parameters which represent behaviour of an observed/monitored catchment in the vicinity of the modelled basin.

The first step is to create a combination of model parameters from neighbouring river basins. The parameters are derived and based on their physical similarity and spatial proximity. The physical aspect provides better results compared to simple averaging of estimated parameters. However, this method is advantageous only in certain cases. There is still room for improvement of this regionalisation approach which is intuitively attractive. The success of this method depends on the density of the basin network.

In our case, this approach is inapplicable since the Czech basin network is not homogeneous and combining parameters from neighbouring catchments is not reliable; moreover, there are no data available for certain basins. Anderson *et al.* (2006) use a similar approach which estimates model parameters based on STATSGO soils database. Initial parameter values, obtained from the database, avoid data quality problems of rainfall–discharge, Koren *et al.* (2003).

The STATSGO approach provides quality results even for manual calibration for large catchments (100–200 km^2). Quality data for the Czech basins are not available as we only observe small catchments; therefore, this method is not applicable to our case.

Distribution functions describing basin changes

The aim of our study is calibration of long time series, where the model parameters had been changed across longer periods of time. Therefore, the model calibration is difficult. A similar issue has been resolved by Hartmann *et al.* (2012) since near-surface dissolution of carbonate rock affects a spatial and time variability of groundwater recharge in karst systems. A reliable calibrated model represents the dominating recharge process between each zone of the calibrated model. The changes in the karst systems are similar to changes in the majority of other basins but occur in different time periods. The changes are taking place within a few months. Meanwhile, in the typical catchment, the changes are taking place during several decades.

The authors developed simple distribution functions which represent the changes in the system. The functions determine total baseflow of the calibrated system. The Shuffled Complex Evolution Metropolis algorithm (SCEM) developed by Vrugt *et al.* (2003) was selected to identify parameter values. The results indicate

that this approach is able to realistically calibrate the model but only if the quality information about the calibrated system is included into the model. It is not possible to prepare and verify the quality information for our case study since the series information from 100 years ago is not available because the certain measuring instruments were not available back then.

2.2 Optimisation

In this chapter, we summarise the related works aimed at the optimisation focused on global search algorithms which provide the best results, Gandomi *et al.* (2015). Some of the past researches that deal with the optimisation problem of the rainfall-runoff models by search algorithms have been focussed on various multi-step procedures which calibrate the model parameters sequentially in a precisely defined sequence, Westerberg *et al.* (2011), Moriasi *et al.* (2007).

ADM model

Although Franchini *et al.* (1998) can be understood as outdated, we think that it is beneficial to introduce his conclusions. This study compares three global search algorithms that are applied to the ADM model, which is similar to many other rainfall-runoff models. Therefore, these results can be relatively generalised, Franchini (1996).

The selected objective function uses the sum of the squared errors between observed and simulated discharges. The described analysis was applied to single and complex basins with areas of 822 and 340 km^2. For a single basin, performed optimisations were more consistent, i.e. the optimal parameter settings were always the same in spite of the fact that initial population was different. The more errors are present in a used dataset, the more unstable the parameter settings are and the easier the algorithm gets trapped in local a minimum. For a complex basin, the algorithms always stop with the smallest number of algorithm iterations and get stuck in a local minimum which then causes the relatively big value of the objective function. The more errors are present in the used dataset, the more amounts of local minima are present.

The results can indicate that complex basins are a bit affected by the local minima; however, a modelled basin is only one factor which affects the automatic calibration of the rainfall-runoff models. Franchini *et al.* (1998) summarise aspects affecting the quality of the final model parameters:

1) a structure and conceptual base of used rainfall-runoff model,

2) error rate and information quality of data used for calibration,

3) selection of the objective function, and

4) the definition of parameter space which ranges of the feasible space and is defined with subjective criteria.

In fact, the mentioned aspects are slightly dependent on each other. For instance, the aspect no. 4, if a parameter range is not reduced enough, the algorithm can get stuck in a local minimum. On the other hand, if a parameter range is too wide, the algorithm may not find the optimum calibration. To decrease uncertainty in the identification of the optimal model parameters, it is necessary to create and tune up a calibration strategy which includes the aspects mentioned above. This is a starting point for the optimisation in our case.

Stochastic optimisation methods

Arsenault *et al.* (2013) compared ten stochastic optimisation methods. The performance of an optimisation algorithm was compared for each used basin-model combination. For each combination, 40 calibration runs with the 10 optimisation algorithms were used. The studied basin Saguenay-Lac-St-Jean is located in Canada, with the area of 45,432 km^2 and with mean annual flow of 850 m^3/sec. Results of these experiments were evaluated using a multi-comparison procedure based on Friedman and Kruskal-Wallis tests, Friedman (1937).

This paper investigates several performances of the observed algorithms. The first aspect of this paper is that all algorithms are able to find a credible result. The second aspect is the complexity of the model. Model parameters can be interdependent, that is a generally known problem, which complicates the performance of many optimisation algorithms. Next aspect is the fact that the selected basins do not affect the performance of the optimisation. This is true if the basins are in a similar environment (temperate climate, the presence of snow, etc.).

One of the most critical aspects of the optimisation is the convergence speed to the optimum as well as its ability to find the minimum of the objective function. The convergence speed is crucial in any field. The speed is dependent on the length of simulated periods. The methods used for optimisation are: Adaptive Simulated Annealing (ASA), Ingber *et al.* (2012); Covariance Matrix Adaptation Evolution Strategy (CMAES), Hansen and Ostermeier (2012); Dynamically Dimensioned Search (DDS), Tolson and Shoemaker (2007); Genetic Algorithm (GA),

Holland (2007); Pattern Search (PS), Abramson *et al.* (2004); and Shuffled Complex Evolution (SCEUA), Duan *et al.* (2006).

The results indicate that ASA, CMAES, and DDS are obviously the best methods for optimising large parameter space and SCEUA is best used for small space, but only if the calibrated watershed has a homogeneous structure from the environmental point of view. The size and location of a modelled basin affect the algorithm performance very little. On the other hand, the complexity of a used model is crucial for optimisation quality and especially if model parameters are dependent. Because of all that, the ASA method requires a careful setup of the algorithm parameters and the ASE has many parameters.

We had selected six best methods and we evaluated these approaches from the point of view of our problem instance. Even though our experiments do not correspond with the results mentioned above, there are several possible explanations for this outcome. The first explanation could be that a different observed basin and period can influence the optimised model calibration. Another fact is the correlation between the calibrated parameters since we use supporting models that are increasing the total amount of calibrated parameters. Therefore, our aim is focused on the GA.

SCEM-UA algorithm

Vrugt *et al.* (2006) use the Shuffled Complex Evolution Metropolis (SCEM-UA) algorithm. The SCEM-UA algorithm is a general global search optimisation technique that provides an estimate of parameters as a set of most likely values and its probability distribution within a single optimisation run. The method is most efficient using parallel computing cluster where the set is subsequently partitioned into a number of complexes and launched in separate threads. This method was applied on the Leaf River watershed with the area of 1,950 km^2 and SAC-SMA model. This study optimises only 13 model parameters; however, we need more than 20 parameters since the snow model must be used. Furthermore, commutating time despite parallel running is still big for our objectives. This approach returns reliable results for relatively short and thermally stable period. However, it is not designed for long periods of fluctuating temperatures and precipitations.

Efficiency criteria

Krause *et al.* (2005) research another important part of optimisations. The selection of the optimised criterion is crucial for quality results. The opti-

misation criteria evaluate simulated and measured streamflow at the catchment's outlet and determine the quality of model output.

This study describes basic statistical functions determining differences between observed and simulated discharges of the rainfall-runoff model. It includes correlation functions which Legates (1999) excluded as inappropriate optimisation criteria. The main efficiency criteria are the following characteristics: coefficient of determination, Nash-Sutcliffe efficiency and Nash-Sutcliffe efficiency with logarithmic values. The observed area and period are 13 km^2 and period of 6 months.

Our observed basins and periods contain several significant floods and a dry season in which the mentioned efficiency criteria react poorly. Extreme fluctuations during the short seasons influence the optimisation run, and the optimisation algorithm deviates from the optimal path. Therefore, we need to specify the efficiency criteria for our objectives.

ARNO model

Many rainfall-runoff models and their implementation have been limited because of a dearth of calibration and initialisation data in some cases on a large scale, Dumenil and Todini (1992). For this reason, Abdulla *et al.* (1999) aim for the ARNO model or more precisely the soil drainage (baseflow) model. This part of the model can complement the calibration and initialisation data but only for the deep soil. Therefore, the evapotranspiration is not modelled.

Evaluating of the baseflow using the ARNO model depends on the initial soil moisture content which must be known at the beginning. This approach completes the missing observed initial value of the baseflow estimate which is determined from the sequence that is known. Several optimisation techniques were used there, among these were the Simplex method of Nelder and Mead (1965), the Newton–Raphson method of Gupta and Sorooshian (1985), the pattern search method of Hooke and Jeeves (1961), and the SCE genetic method of Wang (1991) which is the focus of this thesis.

Abdulla *et al.* (1999) state that some problems occur due to the existence of multiple optimal model calibration, week objective functions in the multi-parameter space, and a correlation between some of the model parameters. This approach uses four objective functions: least squares, maximum likelihood, pseudo-maximum likelihood, and Bayesian methods. The sum of the squares of the difference between the observed and the simulated baseflow is used.

For our objectives, the sum of the square poorly responds to fluctuations in long time series. The SCE method starts with a population which is randomly

distributed in the solution space. This population is divided into several units while each is optimised as the simplex local search optimisation. This procedure relies on one important factor – the effect of the seed random number generator. This fact was checked and verified so the seed value together with objective function selection and bounds of modelled parameters influence the optimisation quality. Abdulla *et al.* (1999) develop a few schemes that include a suitable combination of the seed value, the bounds of the model parameters, and objective function. Each scheme was applied to a different time period and the results indicate that the schemas converge to the same values of the objective functions.

The sensitivity of this approach is different for each optimisation technique. Therefore, this method cannot generally be used. Despite all the benefits and achievements, Abdulla *et al.* (1999)'s approaches do not produce satisfactory results for our objective since the resulting calibration was possible to be improved after the SCE optimisation.

Prescreened Heuristic Sampling Method

Issues of large dimension optimisation have been researched by Bi *et al.* (2015). This study analyses large instances of realistic problems which are related to the objectives of this thesis.

The first one is low computational efficiency which limits the use of the practical problem. The reason behind this is that the global optimal calibration is unlikely to be found within usable computing time. One of the solutions is an enhancement of computing power, such as distributed computing or parallel processing, Roshani and Filion (2012). The second analysed problem is a sophisticated production of the initial population of the genetic algorithm (GA) which can provide suitable solutions using a variety of analytical techniques.

The main achievement of Bi *et al.* (2015) is the utilisation of engineering experience of the modelled watershed. This paper introduces a new heuristic sampling method for determining the initial population of the GA that is based on engineering experiences or domain knowledge, called the Prescreened Heuristic Sampling Method (PHSM). This method maps the watershed network to a network graph where the edge represents a pipe, its value determines the baseflow velocity, and the node of the graph represents the groundwater confluence. Naturally, the pipe diameters get smaller, the further they are from the source. This model, based on the domain knowledge of the given watershed, is divided into several areas corresponding with the main runoff.

The PHSM uses a three-step procedure:

1) for each area a realistic path of groundwater is selected based on the domain knowledge,

2) it dynamically adjusts the velocity threshold to take account of the reality,

3) the diversity of the initial population is controlled by sampling from distributions using the heuristic procedures in steps 1 and 2.

The advantage of this approach is to find a better initial population which is crucial for GA success. The PHSM is independent of optimisation algorithm; therefore, it can be used with other optimisation techniques. However, this is not the domain knowledge for all catchments, especially small watersheds. Therefore, we cannot use the PHSM in our case.

Standardised Regression Equation

An attractive approach which studies the model calibration of the conceptual rainfall-runoff model using a sensitivity analysis is introduced by Wu *et al.* (2012). These authors have described the application of the standardised regression equation with use of a real-value coding in the genetic algorithm. The method estimates and optimises model parameters by a multinomial trial process, where values of the GA operations (selection, mutation and crossover) are based on the sensitivity analysis of the runoff estimation. The method optimises 19 parameters of the SAC-SMA model during seven rainstorm records in Taiwan watersheds.

Most of the model parameters are sensitive to high baseflow no matter which time scale and watershed is used. Tang *et al.* (2006) analyse this dependency on the SAC-SMA model and its evaluation of characteristic baseflow, i.e. the runoff volume, and the peak discharge. This analysis can be distinguished into these two types:

1) the regression method based on the linear regression of the model input on the output vector using regression coefficient (RC);

2) the second method is variance-based, where an observed variance is sorted into components induced by variance-based variables.

Wu *et al.* (2012) combine these two types together so that the greater RC coefficient has more significant effect on the model output. The positive value of RC indicates that the model input is directly connected to the model output and the sensitive parameters can be pontificated using the variance-based equation.

The following methods are used for the model validation: the efficiency coefficient, the error of peak discharge, and root mean square error. What is interesting about these results is that the correct settings of the GA operators, i.e. generation and population size, crossover, mutation, etc., can prove optimal model parameters and thereby the quality model outputs.

The study also shows that their approach can provide the optimal model parameter which can capture the change in the runoff, especially for the peak discharge. The method uses a single objective method that can ignore the effect of low and high rainfall. However, some correlations should exist among standardised values of model parameters, which were manifested in this study (see Section 1.1.1).

Therefore, we are not able to obtain suitable results with this method. Moreover, the study optimises the peak discharge events in a separate period; these are not precisely known for our long-time series.

Medbasin-D model

A calibration of Medbasin-D model is the aim of Tigkas *et al.* (2016)'s research which compares two global search algorithms: Shuffled Complex Evolution (SCE) and Genetic algorithms (GA). Medbasin-D model is a daily conceptual hydrological model developed for conditions of the Mediterranean. A successful calibration of 14 model parameters is required for a reliable prediction of streamflow. The calibration is also based on measured streamflow data.

Both optimisation algorithms are embedded into the Medbasin-D model and the model user selects an objective function which the algorithms try to minimise. The selection of the objective function is a subjective decision of the model user so the quality calibration result is not guaranteed since a wrong objective function causes an inefficient exploring of the optimal search space.

The optimisation process is semi-automatic so the user selects a set of calibrated model parameters and defines a range for each parameter. However, this subjective decision requires the user to have advanced knowledge to achieve the best calibration. An incorrect decision such as unnecessary extension of the optimisation procedure or inefficient exploring of the optimal search space can cause problems. On the other hand, an experienced model user can actively set the simulation for specific needs of the study.

Gupta *et al.* (1998) demonstrate that a single objective function does not usually extract the maximum information included in the calibrated time series. Therefore, there had to be several objection functions used, namely: the Root

Mean Square Error, the Nash-Sutcliffe efficiency (NSE), and the Mean Absolute Error (MAE). These functions are more sensitive to peak flow. Therefore, modified versions of NSE and MAE had to be used, providing an even sensitivity, Krause *et al.* (2005). The workflow of the GA and SCE are comparable to the general genetic algorithm.

The objective of the Medbasin-D model is Koutsoulidis river, located in the southern part of the island of Crete in Greece. The area of the watershed is 96 km^2. What is interesting about this basin is the fact that the upper part consists of karstic limestone; therefore, the effective area is only 39 km^2.

Ten independent simulations were performed for each optimisation criteria because of the probability character of the SCE and GA. The results showed that the GA is computationally more efficient but the calibration results are worse. We have deduced several conclusions for our work. The GA is robust and computationally efficient. We assume that the worse result can be improved by using another objective function and a suitable range of calibrated parameters.

Micro-Genetic Algorithm

A similar comparison, as Tigkas *et al.* (2016) performed for Medbasin-D model, was performed by Wang *et al.* (2010) for the grid-based distributed rainfall-runoff model (GBDM) published by Yu and Jeng (1997).

Authors of this study investigated the SCE algorithm with the same results as Tigkas *et al.* (2016). This study makes several noteworthy contributions while using the Simple Genetic Algorithm (SGA) and the Micro-Genetic Algorithm (μGA) which despite their simplicity provide interesting results but only on short time series and storm events.

The SGA uses simple genetic operation, e.g. mutation, selection, crossover, and does not apply sophisticated methods which increase the computing time but provide better calibrations. The μGA is a light version of the SGA because it only uses selection and crossover operation. Moreover, the population size is significantly lower than the one of the SGA. The study has shown that the SGA and μGA have similar quality of calibration results and neither one of them is better in relation to performance indicator, i.e. computation time, calibration quality, etc. What is interesting about these results is that the seed value for random number generator, which generates an initial population, can significantly influence calibration quality. Respectively, it affects time necessary to achieve the optimum calibration.

It is difficult to interpret this result generally since it was only used in one objective function, but it might be related to the conclusion of Tigkas *et al.* (2016) since the selection of optimisation algorithm is not the main criterion.

Another optimisation approaches

Gupta *et al.* (2003) use a vector of the estimated model output generated by using model parameters. The goal is to find a vector with the best estimate parameters in the sense that observed and modelled outputs are as close as possible. The entries of the vector are various statistical functions which represent the quality of the calibrated model. Gupta *et al.* (2003) also define different optimisation criteria which are then merged together into a single optimisation criterion, called the multiple-criterion fitness function, which indicates the quality of the model calibration.

Further, Wang *et al.* (2012) expound a technique which combines elements of chaos and simulated annealing methods. The aim is to improve the calibration by using various hybrid GA techniques. Le *et al.* (2016) define three objective functions investigating the performance of the rainfall-runoff model. An optimised period is divided into sets according to the weather; a different objective function is applied to each set. This season-dependent strategy can improve the calibration quality in some cases.

Another approach is based on two nested optimisation loops transferring their results by a transfer function which changes its attributes during the optimisation. This decreases the number of model evaluations in the initial stage, Klotz *et al.* (2016).

2.3 Data Quality and Parameter Uncertainly

The quality of model input data significantly affects the condition of model output. Therefore, if input data are low quality, the calibration of rainfall-runoff models is another important task.

Goodness and BALANCE indexes

Poor quality of rainfall data, mainly for long time series, decreases the accuracy of calibrated models. Andréassian *et al.* (2001) deduce two indexes which determine the quality of precipitations via computing the square roots of the actual and reference precipitation input.

The first index, the Goodness of Rainfall Estimation (GORE), uses the Nash and Sutcliffe coefficient as a transformation criterion. The GORE can take a value

between minus infinity and 1. When the estimated precipitation equals the reference precipitation, the GORE index is 1; otherwise, the value is smaller than 1 and decreases as the estimates become poorer. The second index called BALANCE classifies whether the actual precipitation is an overestimation or an underestimation of the reference precipitation.

These two indexes describe the quality of rainfall time distribution as this study indicates. However, we cannot use this approach on such a small watershed as Ráztoka and Liz because their size is only approximately 2 km^2. Moreover, the reference precipitation value cannot be assessed precisely for long-time periods since there are environmental events taking place which distort this value and it would have to be recalculated for each separate period. However, determining of these periods is not an easy task.

Hydrological uncertainty

The analysis of hydrological uncertainty is an integral part and is closely related to data quality. Hughes *et al.* (2010) include the uncertainty estimation into a procedure of water resources assessment in the regions of southern Africa. This result can generally be applied on our case study. The analysed area is a typical representative of low precision data.

Naturally, the primary source of uncertainty is the parameter estimation of hydrological models. This study designs a framework for determination of parameter values by investigation of the interdependence of parameters and determination of uncertainty parameter bounds.

The Pitman model is widely used in these regions, Pitman (1973). The model is based on principles of sensitivity and uncertainty analysis which are well documented, but some limitations are decreasing the model performance, e.g. data scarcity and accuracy, model user knowledge, etc. This framework defines bounds of parameter uncertainty, but no experiments have analysed a probability distribution of the uncertainty bounds yet. The initial estimation of model parameters is regarded as the most probable, while lower and upper bounds are least probable. At this stage, it is not clear whether a more quantitative adaptation could resolve the bound problems.

The results also indicate that the bounds of the uncertainty could be too wide for the effective water resources assessment. The parameter bounds and its uncertainty are very important for the quality parameter optimisation from our point of view.

Shuffled Complex Evolution

A strong relationship between data quality and optimised period has been reported in Zhang *et al.* (2015). In short, we describe secondary methodology. The Shuffled Complex Evolution (SCE) was applied on the Xinanjiang (XAJ) model (Zhao *et al.* (1980)) for Yandu River watershed located in the Three Gorges Region of Yangtze River. The area of catchment is 601 km^2 and the elevation drop is 2,800 m.

The selection of a fitting objective function is crucial for a successful model calibration. However, the choice is very subjective and can result in getting stuck in local minimum. Unfortunately, some model parameters can be in correlation and therefore there are more calibration sets which can be optimal solutions. Accordingly, the optimisation results are ambiguous. To achieve the best calibration combination, it is necessary to use more objective functions at the same time. This study shows that the objective function influences the parameter optimisation and results vary according to different objective functions. To avoid the influence of errors in model input data, ideal data series were created.

Zhang *et al.* (2015) use a multiobjective function which converts and combines several specific qualitative functions together. One of the most commonly used functions is the total runoff error and the water balance. The second part of the multiobjective function is the relative error of the calculated discharge. The last function is the Nash-Sutcliffe efficiency coefficient that reflects exactness of the simulated baseflow.

The XAJ model is used for daily rainfall-runoff simulation and flood simulation. Different simulations call for appropriate multiobjective functions. Nevertheless, the primary objective of Zhang *et al.* (2015) is comparison of the optimisation effect on various time series that are of different lengths, namely for ideal data and observed data burdened by error.

The ideal data was created for the observed basin as follows. XAJ model parameters were randomly generated within the parameter search intervals. These parameters are taken as a set of "real" parameter values under which they have been generated as sequence of streamflows. It is evident that this ideal data is without error and does not influence the optimisation processes.

As expected, the results are obvious. The ideal data does not affect the parameter optimisation for arbitrary lengths of time series. In case of the observed data, different lengths of time were used, specifically 1, 2 and 3 years. When observed data are stimulated, errors in data structure cause significant uncertainties in the

parameter optimisation. All these results are conditioned by the use of an appropriate objective function.

In summary, errors contained in data structure lead to uncertainties of optimised parameters. Moreover, the objective function cannot be determined unambiguously since the selection is always depended on a calibrated basin and used time series. The main advantage of a multiobjective approach is focusing on the performance of the optimisation process. However, the selection of the multiobjective function is still impacted by a subjective sense, user's experience and knowledge.

Dynamic Identity Analysis

In short, we discuss the research performed by Abebe *et al.* (2010) which analyses individual sensitivity of model parameters during automatic optimisation. The Multi-Objective Shuffled Complex Evolution (MOSCEM) and the Monte-Carlo algorithms are used for the optimisation of the HVB model, Bergstrom (1976). The case study is the Leaf River catchment near Collins in Mississippi with the area of 1,924 km^2. Dynamic behaviour of calibrated parameters is analysed using DYNIA (Dynamic Identity Analysis), Wagener and Kollat (2007). The DYNIA is an approach for identification of the optimal parameters and which values are changed over time. A probabilistic scale estimates the time changes of parameter values and their uncertain distribution. This approach helps to identify the parameter values and the model structure by improving the amount of information that can be obtained from the observed river basin variables. The optimisation algorithms with two objective functions (BIAS and RMSE) show that there are disjointed groups of parameters which affect the total runoff volume errors and errors from the high-flow periods. The DYNIA analysis presents that parameters have specific periods where they have higher identifiability of the parameter values. All in all, the uncertain distribution is variable and the optimisation algorithm should adapt accordingly.

2.4 Impact of Natural Influences

It is worth mentioning that the diverse water changes caused by natural variability and abrupt events are significant in measuring the runoff and it requires meaningful attention.

The historical changes in the land use (water reservoirs as fishing ponds, rivers regulations, etc.) should be re-considered. In current conditions, the potential evapotranspiration and soil water content influence each other. This matter should be reconsidered precisely during the model calibration. It could be recognized

during the simulation when long-term hydrological data series are to be analysed. It is necessary to ascertain the evapotranspiration when the information to provide geographic data for evaluation of the role of vegetation covers is missing.

The natural variability of water regime is primarily influenced by solar radiation, which is a critical phenomenon for terrestrial precipitation and evapotranspiration. The regular oscillation of solar activity is usually mentioned as a sunspot cycle which is repeated every 11 years, Beer (2005). It is worth mentioning, that this process occurs regularly in a period of approximately 9-13 years, Hathaway and Rightmire (2010).

Various random events arise during the rainfall-runoff process and diverse tools are usually required for the long-term runoff evaluation. In this context, the long-term persistence and oscillations in long time series have been followed by different spheres and periods, Hurst (1951), Beer (2005). Three natural phenomena require evaluation of the input values to clarify the influences on the variability of runoff:

1) The periodic and more or less regular climatic oscillation and certain phenomena are the precipitation and evapotranspiration determining the water consumption, while Beer (2005) clearly shows the correlation between solar activity and climate variability, and some similar fluctuations have also been pursued quite recently, Buchtele *et al.* (2009).

2) Long-term evolution of the vegetation covers, including its possible abrupt changes, i.e. the extraordinary wind disasters and even devastations by insects; those were the events in central Europe during the second half of 19. century, Vicente-Serrano *et al.* (2010).

3) Significant and flexible geomorphological conditions, or the seemingly random diverse events; those were caused by the growing agricultural production, Brown (1997).

Those are the primary processes for the efficient appraisals of the active evapotranspiration. The deterministic conceptual water balance model is frequently viewed as a convenient approach for the simulation of the rainfall-runoff process. Such tool provides the outputs which can be helpful in the analysis of this complicated and long-term process. This modelling approach provides the runoff simulation without requiring geographic data for its calibration. The priority of long time series is supported by two circumstances: the uncertainty and complexity of evapotranspiration behaviour in the actually available hydro time series, and the possible automatic parameters optimisation, Kundzewicz (2002), Merz *et al.* (2006).

2.5 Related Work Summary

At first glance, it is evident that the optimisation of the rainfall-runoff models is still a current topic. There is no universal optimisation algorithm or approach which would successfully calibrate any catchment and period yet. We could find the parallels in physics since the theory of everything is a universal approach which is still waiting for its discovery.

The data quality is a great aspect of calibration quality which cannot be eliminated entirely. Therefore, we have to assume that model calibration cannot be perfect, especially for long time series where model parameters are changing. The selection of a proper optimisation technique cannot be determined definitely. The main consensus is that the global search algorithms must be used for a successful model calibration since the optimisation problem is NP-complete, Arsenault *et al.* (2013). However, individual parameter settings of the used algorithm are dependent on the modelled watershed or the period. Naturally, the settings are crucial for a successful model calibration. The bounds of the model parameter values are crucial when delimitating the search space. However, it can unreasonably prolong the computation time without other noticeable effects. The global search algorithm may not find a calibration optimum otherwise, therefore suitable settings of the parameter bounds are essential aspects as well. Another crucial aspect of a successful calibration is selecting the objective function which depends on a modelled basin and even on modelled time series. In terms of the inner structure of global search algorithms, quality of used random number generator plays an important role in the value estimation of model parameters as well.

In brief, we focus on aspects following from the related works. Particularly, we concentrate on used global search algorithm, parameter bounds, parameter uncertainty, objective function selection, and random number generator.

3

Theoretical Background and Terminology

This extensive chapter overviews the theoretical background of the methods, materials and data used in this thesis. The goal of this chapter is a conjunction of the hydrological and computer technology terms and approaches. After reading the chapter, readers will get a comprehensive overview of the subject and fundamental terms of hydrology and informatics.

Sections 3.1 and 3.2 introduce basic terms of hydrology, hydrological models and foundations use of computer sciences in hydrological modelling. Sections 3.3 and 3.4 describe rainfall-runoff models, their calibration and modelling. Sacramento Soil Moisture Accounting Model (SAC-SMA), its model structure and used hydrological sub-models, are described in Section 3.5 in detail. Section 3.6 illustrates the structure of the Sacramento model, which is a union of all necessary hydrological sub-models, including SAC-SMA, together for the purpose of realistic simulations on a real catchment area. Further in Section 3.7, the validation methods of the hydrological simulation are defined.

The most extensive Section 3.8 focuses on global search algorithms, namely the *genetic algorithm* (GA). This section introduces basic terms of optimisation, GA structure, and its workflow in the context of the Sacramento model. In addition, the section defines key features of the GA as a fitness function, Monte Carlo Simulation, etc. The Section 3.9 is purely informative since it deals with the random number generator (RNG) and statistical methods for its validation, which determines quality of randomness.

3.1 Basic Terminology in Hydrology

In this chapter, we summarise the key terminology of hydrology. We focus on terminology concerning rainfall-runoff models. The primary sources of information in this chapter are Diersch (1990), Jandora *et al.* (2011), Kemel (1994), Říha (1999), and Sommer (1973).

Humankind understood the meaning of water for our lives a long time ago. Observations of water movement and fluctuations have been related to agricultural and economic activity of man. The hydrology is a science which systematically discovers the law of occurrence and circulation of water in nature. Obtained knowledge and information about water resources, creation, and distribution of runoff on the surface and under the surface can be used to improve the living conditions on Earth. Hydrological data that contain essential water regime characteristics are the basis for a design of conceptually correct, rational, and well-functioning hydraulic structure. Additionally, hydrology utilises methods and resources of theoretical sciences like mathematics, statistics, the theory of probability, physics, chemistry, and last but not least, computer sciences.

3.1.1 Fundamental Terminology

Basin

Basin (watershed, catchment) is a fundamental work unit in hydrology. It is an area from which all water flows to a certain point – so-called closure profile. The closure profile is a collection area of the surface and underground baseflow, where groundwater slightly deviates from the surface baseflow. The boundary of basin area is determined from topographic maps.

Precipitation

The precipitation is production of atmospheric water condensation that falls to the ground due to gravity. If the atmosphere is cooled, the air saturation with water vapour increases. If air *temperature* falls below the dew point, a part of contained steam is precipitated around the condensation cores. There are slight droplets of water or snowflakes which create clouds and fog. Under certain conditions they grow and fall as airborne precipitation. Another kind of rainfall is precipitation, which arises directly on the Earth's surface; e.g. dew, frost, and ice. These phenomena are called the horizontal precipitations whose yield is relatively small. Generally, the rainfall is divided into liquid (rain, mist) and solid (snow, hail, ice, and frozen rain).

Runoff

The baseflow from a basin can be characterised as the volume of water flowing out from the basin per unit of time. It includes several types of partial runoffs:

1) *Surface runoff* is part of the total baseflow which flows directly over the terrain into the river network.

2) *Subsurface* or hypodermic *runoff* is the amount of water that infiltrates the subsoil and flows through the soil profile. However, the water flows just below the surface and it is not in contact with groundwater.

3) *Underground runoff* is formed by the water that got infiltrated and flows underground. It is significantly slowed down compared to the hypodermic and surface runoff.

The surface runoff and the hypodermic runoff, which occur during or after precipitation, create so-called *direct runoff*. It results in a temporary increase of the water-level. The underground runoff together with the delayed hypodermic runoff then forms the so-called *basic runoff*. It is the runoff that supplies water to the streams and rivers during periods without precipitation.

Evaporation

A constant movement of water molecules causes evaporation which is escalated by temperature rises. Evaporation is a process where some molecules overcome the attractive force of neighbouring atoms and pass into the atmosphere. The evaporation from a water surface is relatively simple and it is the most important component of water loss. It is dependent on meteorological conditions and soil properties. A rough and wavy surface contributes to the evaporation more than a flat and smooth surface. Another aspect is the darkness of soils which affects the evaporation level. The influence of location is also crucial since the enlarged slope increases the evaporation on southern and eastern slopes while it reduces the evaporation on western and northern slopes.

Transpiration

Transpiration is a manifestation of plant life processes. The groundwater in which nutrients are dissolved is absorbed by plant roots. The nutrients and part of the absorbed water create the plant tissue. The amount of water in grams necessary to make 1 g of dry tissues is so-called *transpiration factor*.

Evapotranspiration

Evapotranspiration is the total vapour of physical vapour (evaporation) and physiological vapour (transpiration), which relates to a particular territory. In other words, it is the current evapotranspiration (ET_{act}) from a certain catchment area which takes into account the current conditions of water status and energy supply. In addition to the actual evapotranspiration, we also define the potential or demand evapotranspiration (ET_{dem}), which is the maximum possible evapotranspiration that can be achieved in particular climates and certain climatic conditions. The actual evaporation is much lower in the dry months than the potential evaporation. ET_{act} and ET_{dem} are equal only during precipitation periods. Evapotranspiration presents 70-80 % of the total water movement in many Czech catchments. Knowledge of evapotranspiration dynamic is therefore essential to a simulation of rainfall-runoff processes.

The evapotranspiration, as one of the components of water balance, is one of the most important hydrological phenomena. It is one of the meaningful constituents of water regime, namely in basins with vegetation cover. The modelling of rainfall-runoff process is extensively used for the evaluation of that regime, Hanson (1991). However, the measurement of the evapotranspiration requires relatively precise measuring devices and extensive network. Unfortunately, these measuring devices and networks are scarcely realistic for large river basins. If older and longer time series are analysed, then there are no values of evapotranspiration at all, Kuczera (1997). Therefore, the simulation of rainfall-runoff process has to be used to obtain the values of evapotranspiration.

The evapotranspiration is usually part of the rainfall-runoff simulation. It needs substantial efforts to reach its realistic values in the framework of runoff modelling. In this context, it might be expected that the actual evapotranspiration, as a complicated process, is more uncertain phenomenon in comparison with the monitored precipitation and runoff, Buchtele and Tesař (2009).

Rainfall-Runoff Process

A rainfall-runoff process is a subsequent transformation of precipitation falling to a basin to the total baseflow of the closure profile. It is evident that this is a very complicated process which is influenced by many factors. Above all, it is a group of climatic aspects. This includes time and space course of falling precipitation, atmospheric humidity, vapour, air *temperature*, speed, and direction of the wind, atmospheric pressure, etc. For this group, meteorological variables mainly affect the total water evaporation from a catchment area. Another group are geographic factors of a river basin; particularly area, size, mean altitude, shape, relief, river

network, hydro-geological conditions, vegetation cover, etc. This group describes environment in which the rainfall-runoff process is taking place. It determines dynamic (transmission) properties of a catchment area which are crucial for the way how the time course of the *precipitation* is transformed into runoff time at the closure profile.

The rainfall-runoff process consists of two partial transformations. The first one is a hydrological transformation. It represents hydrological losses which are gradually subtracted from the *precipitation* falling on a basin. Major losses consist of evapotranspiration (total evaporation from a surface of vegetation cover, plant pore, water retention on a surface of vegetation, and soil), loss by moistening, water infiltration into a soil, loss of surface retention, and surface runoff occurs only after filling an uneven terrain with water. Sequential separation of the hydrological losses from the time series of the precipitation results in an effective rainfall intensity. The amount of water that fell onto the basin surface then flows out as flat surface runoff. This is the start of the second phase of the transformation.

The hydraulic transformation is the second stage of the runoff transformation. The flat surface runoff is gradually concentrated in the erosion grooves, river network, and the closure profile. This is not the total runoff which flows through the closure profile. One part of the total runoff is the underground runoff, which is absorbed underground mainly by the rainfall infiltration. Thus infiltrated *precipitation* leaks from the underground either from unsaturated zones to the groundwater level or from saturated zones into the river network in the form of an underground flow. In unsaturated zones of an agricultural-cultivated watershed, the soil is very loosened up, therefore it has a much higher permeability than the soil that has not been cultivated. Water may leak out on the surface of the soil via this boundary; this effect is called hypodermic runoff. Water flows in saturated zones on a relatively impervious bedrock.

Occasionally, water seeps through the cracks from impermeable zones to considerable depths and then it can spring to the surface of another basin than where the *precipitation* fell. This penetration is called the percolation. The total runoff from the basin underground is called flat underground runoff and it is analogous to the flat surface runoff.

The total runoff for a watershed is the sum of the flat surface runoff and flat underground runoff, including the evapotranspiration. All these elements are part of the basic equilibrium equation describing the total catchment runoff.

3.2 Hydrology and Informatics

In hydrology, the expansion of mathematical models is closely related to information technology; namely simulations and optimisations. Development and research of hydrological models was a domain 10 years ago. Currently, the models are used operationally in actual case studies.

Nowadays, the use of the hydrological models has broad scope of application. Although the majority of the professional public associates the models with the field of hydrological forecasts, the present need of a water management is focused on solving other hydrological problems. There are certain possibilities, needs, and areas of application, as follows. One of the applications can be replenishment and extrapolation (or as the case may be generation) of runoff time series based on another hydrometeorological data; e.g. *precipitation* and air *temperatures*. Another application is the evaluation of changes in runoff caused by human activities; i.e. climate changes, vegetation or land changes of basin cover (deforestation, urbanisation, agricultural activity), and other interventions within the observed watershed. The additional application is the evaluation of resources and water supplies based on the relationship between surface/underground runoff, evapotranspiration, and infiltration; Bronstert *et al.* (2002), Clark *et al.* (2015), Shahin (2002), Vörösmarty *et al.* (2000), Wallace and McJannet (2012).

However, several assumptions need to be ensured to achieve an efficient and routine use of the models. It is necessary to have an overview of existing approaches to modelling of hydrological processes. It is related to a realistic idea of used models, their possibilities, strengths, and limitations. And finally, it is necessary to adopt a software for model calibration, Bergström (1991), Donigian and Huber (1991), Singh and Woolhiser (2002).

3.3 Rainfall-runoff Models

The hydrological model of a watershed is an ambiguous term. Within our scope, the hydrological model is used for simulation of the rainfall-runoff process. More precisely, the simulation of the conceptual, primarily balance, hydrological model with more or less detailed realistic structure. The structure of the conceptual rainfall-runoff model is vertically organised into several hypothetical zones, Liu *et al.* (2017). This model can be found in: Stanford Sacramento model (SAC-SMA), Japanese Tank model, and Swedish HBV model.

A conceptual rainfall-runoff model is a theoretical physical model based on principles of water movement in a watershed and describes simplified hydrological processes using a mathematical apparatus. The model describes the relation between rainfall-runoff and observed watershed area or drainage basins. This relationship represents surface runoff hydrograph reflecting a response of catchment according to rainfall events. A model output is total runoff calculated from the rainfall. The most common use of a rainfall-runoff model is to estimate parameters which are not readily measured, or to predict the future behaviour of the modelled catchment based on historical data. If the model is calibrated well, the model will provide quality results, Jayawardena (2014).

Unfortunately, using the rainfall-runoff models is not an easy task, especially for large catchments and surface topography of basin terrain. Moreover, an imbalance of *precipitation*, evapotranspiration, and other model inputs induces the division of the area of interest into a number of sub-basins. Subsequently, the rainfall-runoff simulations of the sub-basins are performed separately and the final closing profile of the baseflow is composed of outflows from inter-catchments. So, the overall algorithm for the rainfall-runoff simulation includes the following steps. The first step is quantifying the water balance including the feedback between evapotranspiration and soil moisture. The second step is using a sub-model for a simulation of the creation of snow cover and its melting. The last important component of the algorithm is a model of water movement in flow channels, i.e. translational and transformational processes, and eventually procedures simulating wave retention and accumulation of water in tanks or lakes. The method of the division of an observed watershed into the sub-basins and river sections depend on a configuration of a basin terrain, river network, variability of runoff, purpose of simulations, etc. A location and number of measuring stations often decide the method of the basin division; Buchtele and Tesar (2013), Dubrovský *et al.* (2004), Hejzlar *et al.* (2003). This thesis focuses on already created sub-basins, so we will not discuss the issue of the division any further; for more information, see Berga *et al.* (2006), Hamed (2008), Pykh *et al.* (2000).

3.4 Hydrological Modelling

In sub-chapters 3.1 and 3.3, we introduced basic hydrology terms and the static and dynamic structure of the rainfall-runoff models. In this sub-chapter we describe the hydrological modelling, and we also discuss modelling difficulty from the perspective of the users.

Mathematical modelling of the rainfall-runoff process is a very complex problem. There are models predominantly aimed at simulating the rainfall-runoff process in a catchment area; however, it is not always possible to deal with this issue in detail. Therefore, it is not possible to provide all required information, and input data must be estimated. These facts reduce model quality and usability. Moreover, these problems significantly influence the modelling of the rainfall-runoff process in large basins. However, significantly simplified models provide only very rough estimates of the runoff rate at the closure profile. It is always necessary to seek an acceptable form of simplification, Diersch (1990).

The rainfall-runoff model can also be understood as a tool for organisation or transformation of existing information into other forms for specific tasks. Useful information can be extracted from historical and current data about an observed catchment via the rainfall-runoff model. Therefore, the hydrological models are always potentially more reliable means for an evaluation of future development of water movement and balance. These models provide better results than sometimes more preferred intuitive and empirical approaches based on subjective knowledge and experience. On the other hand, less experienced users expect an auto-efficiency of the models, and it is also expected that just use of the models can radically improve the interpretation of information which are and will be available. This may be a source of misinterpretation of modelling results. Therefore, preconditions upon which information is created or processed should always be taken into account. An example of such misunderstanding can be found in a situation where a model input is a time series of the average rainfall that fell in the basin. However, the simulated baseflow as a model output is significantly smaller than real baseflow. It is rather trivial example but it illustrates the necessity of evaluating the simulation results.

Knowledge and experience of model users play a non-negligible role in the modelling process. It is true that the models provide more reliable simulation only if the model is in the hands of an expert. Experienced modellers declare that the ability to work efficiently with the hydrological models is a long-term issue based on practical knowledge and skills, just like playing a musical instrument, Bergström (1991), Montanari and Toth (2007), Pianosi *et al.* (2016). However, the statement that the hydrological modelling is an art rather than science is still applicable, Savenije (2009).

Another goal of the rainfall-runoff modelling is mining information about the possibility to discover the diverse changes in the flow simulation which influence the evapotranspiration demands and consequently the complex water regime. The intention to decrease uncertainties in the water regime due to different

oscillations requires the evaluation of occasional natural fluctuations and the abrupt seeming random changes in the basins. These consecutive variabilities of water regime are usually influenced by changes of vegetation cover during the annual cycle and also by its development in the span of decades during which other natural events occur as well; e.g. winds. The changes of vegetation cover and the desirable appraisals of the existing interaction between evapotranspiration demand and sub-surface water storage seem to be significant processes, this whole matter may appear significant, both at the local as well as at the regional scales. This is the motive for the rainfall-runoff modelling carried out in small and large catchments. The conceptual SAC-SMA model enables the prompt simulation that creates the conditions for automatic calibration of this model, and simulations for individual partial time intervals with diverse expected evapotranspiration. The resulting evapotranspiration is represented as the outputs of the modelling. Hence, the values could be hardly gained as measured data or computed values, e.g. from other meteo-observations.

3.4.1 General Modelling Process of Hydrological Models

The modelling process is composed of several procedures following the exact order.

The first step is selecting the right rainfall-runoff model since each situation and case study requires a different approach and thereby a different hydrological model. Subsequently, the modeller must prepare all available information about the observed catchment; e.g. size of the basin area, forestation, elevation, etc.

The second step is the composition of supporting models. In some cases, certain sub-models are required for the most accurate results, such as snow model or transformation of the total runoff depending on the terrain. In this step, the modeller must also estimate the parameters of all used sub-models. It is an initial estimate of the model parameters and it strongly depends on experiences of the modeller.

Another step is running the simulation calculations. The resulting simulation is further validated using a specific set of statistical indicators comparing observed and simulated runoff. This step is repeated several times even by experienced modellers since the initial calibration is important for achieving reliable results. In this manner, the modeller adjusts the model calibration several times interactively until the simulation results have satisfactory quality.

All mentioned steps depend on experience, knowledge, and to some extent also on the sense and talent of the modeller.

3.5 Sacramento Soil Moisture Accounting Model

The Sacramento Soil Moisture Accounting Model (SAC-SMA) is among the most widely used rainfall-runoff models. It is a conceptual water balance physical model based on the physical principles of water movement in a watershed. The SAC-SMA model simulates runoff within the catchment using spatially-focused parameters. The model provides excellent results for large drainage basins and long time calibration series. The model has been prepared as part of a library, the Modelling techniques of National Weather Service River Forecast System (NWSRFS), developed since the 1970s in the US, Burnash (1995). The NWSRFS uses the SAC-SMA model as a key rainfall-runoff model to forecast the properties of watersheds across the country.

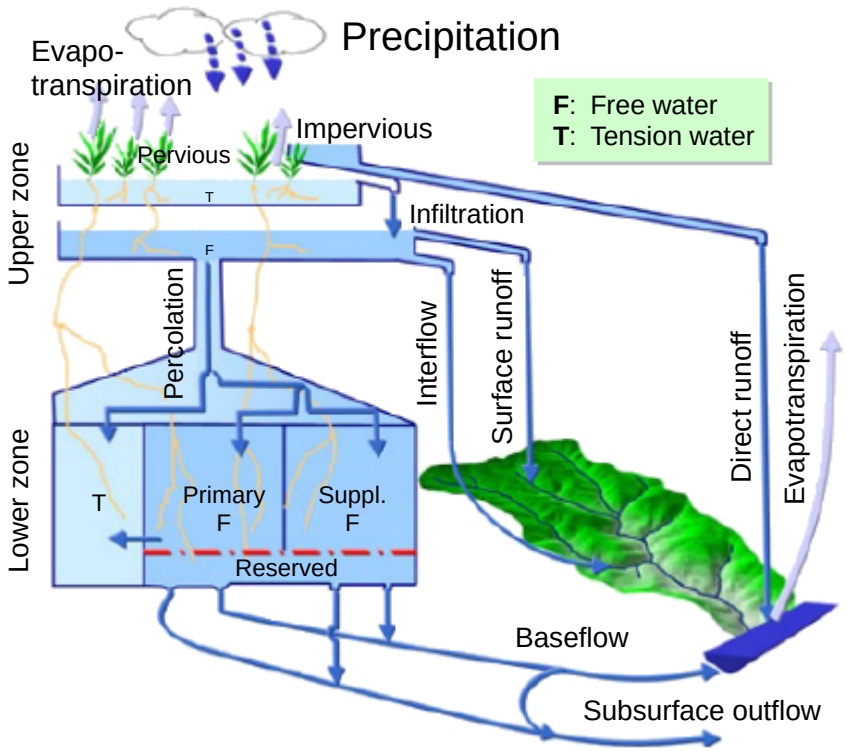

Figure 3.1: Static structure of the SAC-SMA model, Model Primer (2017)

Figure 3.1 illustrates the static structure of the SAC-SMA model. The model operates with a system of hypothetical water reservoirs (tanks). The model input is water in the form of *precipitation*. In particular tanks, the water is:

1) retained,
2) consumed by vegetation during evapotranspiration,
3) infiltrated into low-lying system tanks,
4) flows into a river network.

The total runoff is the sum of all partial runoffs of the tanks. The model distinguishes and divides the tanks according to the capacity of basin components into lower and upper zones located in different depths and defines conditions for the moisture distribution. There are two types: tension water (controlled by evapotranspiration) and free water (controlled by gravitational forces). The model generates a total of 6 runoff components, see Figure 3.1:

DIR *direct runoff*, i.e. outflow from areas that are temporarily impervious due to the saturation of soil zones

IMP *impervious runoff*, i.e. outflow from impermeable surfaces

SUR *surface runoff* is meant as a flat phenomenon

INT *interflow*, i.e. runoff created by excess water in zones connected with a vegetation cover

SUP *supplementary underground runoff*, i.e. seasonal component of the total underground runoff, it is a relatively variable component formed from shallow groundwater collectors

PRM *primary underground runoff*, which is generated from stocks with long delays in the catchment area, i.e. runoff mainly from deep-seated collectors

The model uses *temperature* and *precipitation* records to estimate the amount of water which enters and leaves a watershed. Additionally, the model takes the state of soil moisture and relative permeability of basin terrain into account. The model processes the input records at several time intervals (1, 2, 3, 4, 6, 8, 12 and 24 hours). Small intervals are used to estimate the runoff during flood events and large intervals to estimate long-term processes, e.g. vegetation cover or evapotranspiration development.

The SAC-SMA model estimates diverse hydrological processes, such as evapotranspiration, interflow, percolation, and different forms of basin runoff. The usability of the model varies, mainly the runoff forecasting, basin hydrological hazard estimation, climate change assessment, and water supply forecasting.

The success of the SAC-SMA depends on the quality of the input data and a proper model calibration. The model usually needs to be calibrated by up to 20 parameters, grouped according to zones. The evapotranspiration (ET)

phenomenon is separately defined by twelve discrete values. These values determine the expected evapotranspiration for each month, which is the total evaporation including the vegetation's consumption of water (transpiration) and the physical vapours (evaporation).

Model inputs

The SAC-SMA model first requires a mandatory parameter, *precipitation*, in the form of rain plus melt. Another optional parameter is a *potential* ET in the form of a 24-hour long time series. Last optional input is an *areal extent of snow* in the form of time series representing relative snow coverage of a simulated basin.

Model parameters

The SAC-SMA model can be calibrated by parameters summarised in Table 3.1. The following circumstances should be taken into account for a correct interpretation of the parameters.

The sizes of the model zones (UZTWM, LZFPM, LZFSM) are given in the water column equivalent of water supply (in millimetres). The LZPK, LZSK, and UZK parameters are coefficients determining the exhaust of the model zones. PCTIM is a percentage of the catchment area that produces runoff from impermeable surfaces. The PCTIM value can be assessed from obvious precipitation episodes that occurred after a dry period. Due to these episodes, the zones are empty enough that the runoff is produced only by impermeable surfaces (urbanised areas, roads, water areas, etc.). ADIMP is a percentage of the catchment area, which becomes temporarily impervious after a zone saturation. The ADIMP value can be based on the *precipitation* and runoff which occurred after the preceding heavy rainfall since the runoff is in temporarily impervious zones (clayey or swampy land). The parameters ZPERC and REXP influence the intensity of infiltration. The group of model parameters listed above represent quantity which can be ascertained by historical records.

Special mention requires data on evapotranspiration. Actual or potential evapotranspiration is exceptionally available in the format of daily series for a given basin; especially for long time series where measuring instruments were not available. The model enables us to define the evapotranspiration in two ways. The first way how to define the evapotranspiration is the time series of daily evapotranspiration whose values can be adjusted using the adjustment coefficient for each month. The second manner is defining the evapotranspiration by 12 values that are an estimation of long-term monthly totals (given in *mm/day*) and daily values of assumed evapotranspiration computed by linear interpolation.

Table 3.1: SAC-SMA model parameters

Parameter	Description	Units
UZTWM	Upper layer tension water capacity	mm
UZFWM	Upper layer free water capacity	mm
UZK	Upper Zone Free Water storage coefficient	-
ZPERC	Maximum and minimum percolation rates	mm
REXP	Shape parameter of the percolation curve	-
LZTWM	The lower layer tension water capacity	mm
LZFSM	The lower layer supplemental free water capacity	mm
LZFPM	The lower layer primary free water capacity	mm
LZSK	Lower zone supplementary depletion rate	mm
LZPK	Lower zone primary depletion rate	mm
PFREE	Percentage percolating directly to lower zone of free water	%
PCTIM	Percentage of permanent impervious area	%
ADIMP	Percentage of additional impervious area	%
SIDE	Ratio of deep recharge water going to base-flow	%
RSERV	Fraction of lower layer free water not transferable to lower layer tension water	-
ET	ET-demand for the 16th of each month (January - December)	mm/day

Model outputs

The model outputs contain 4 groups. The first main output is a channel outflow (runoff) given in *mm*. It is the total runoff at the closure profile of a basin. The second group represents runoff components (DIR, IMP, SUR, INT, SUP, PRM) given in *mm*. The third group is 5 soil moisture storages for each simulated time interval; namely upper zone tension water deficit (UZTWM-UZTWC), upper zone free water contents (UZFWC), lower zone tension water deficit (LZTWM-LZTWC), lower zone free supplemental contents (LZFSC), lower zone free primary contents (LZFPC). The last output group provides information about the actual and potential evapotranspiration.

3.5.1 Snow Accumulation and Ablation Model

The SAC-SMA model was originally developed for modelling the Sacramento catchment, which is located in warm climate in California. Therefore, some supporting sub-models must be connected to the SAC-SMA model because other parts of USA and Europe, the Czech Republic in particular, are located in a mild climate.

In this study, we use the *Snow Accumulation and Ablation Model* (SNOW-17), which simulates the accumulation and melting of snow cover using a simple energy equation. The number of major calibrated parameters is 12. The SNOW-17 sub-model can be divided into several height zones, where the amount of water accumulated in the snow cover is simulated separately as it better reflects the distribution of snow reserves in a catchment, Anderson (2006).

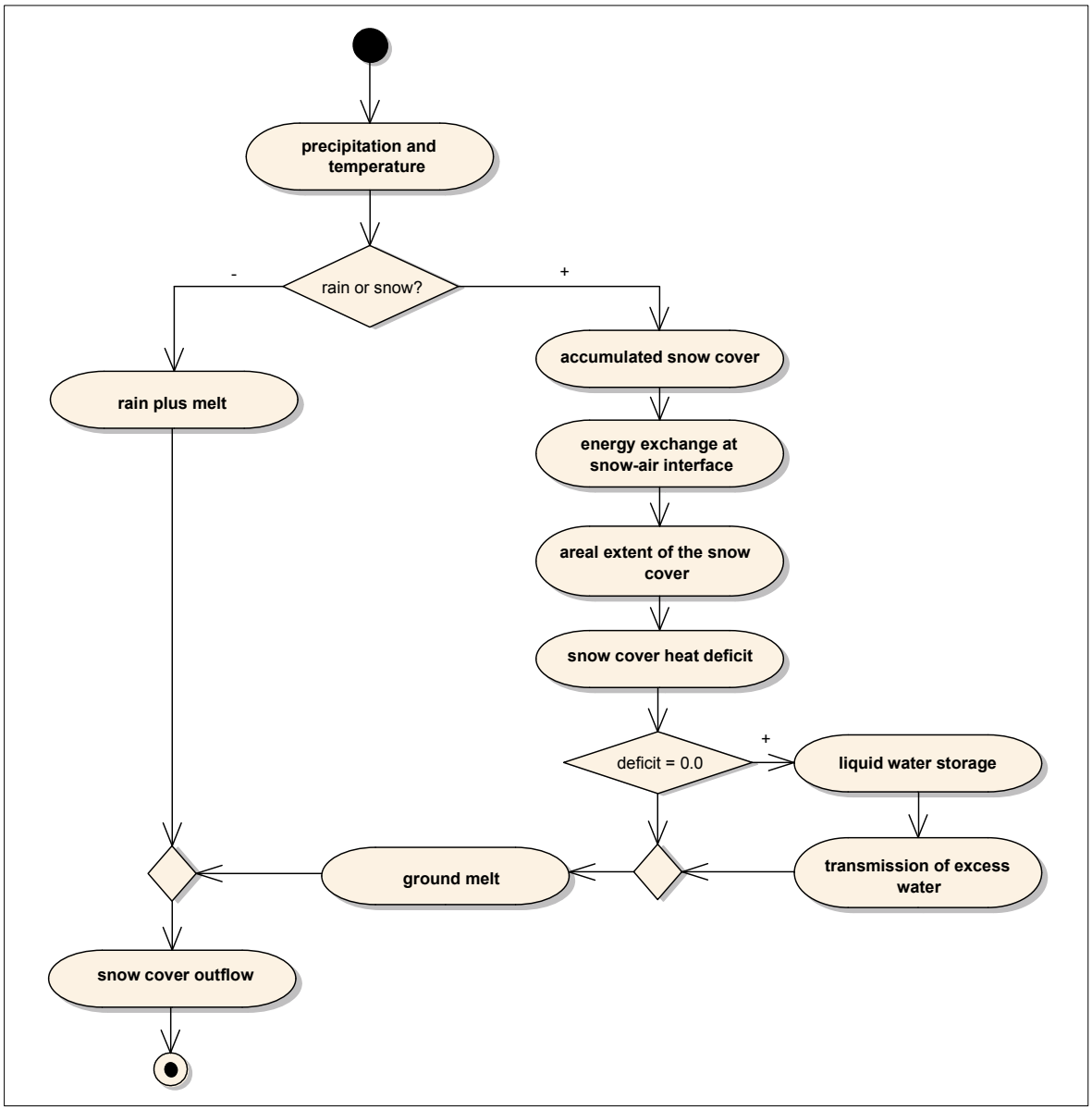

Figure 3.2: Flowchart of the SNOW-17 model

Figure 3.2 illustrates the calculation of SNOW-17 model. In short, if the form of *precipitation* is determined as rain (from a record of *precipitation* and *temperature*), the *precipitation* falls directly to a basin area. If the *precipitation* is in the form of snow, a complicated process of snow accumulation calculates the snow cover using the energy equations, taking into account energy exchanging of air, incoming solar, snow cover, and soil energy.

Model input

The model simulates the meltdown and creation of snow cover based on records of *precipitation* and air *temperature*. The model does not require additional terrain information about the basin and therefore the number of input information required for quality results is not overwhelmingly demanding, and the snow simulation has favourable quality.

Model parameters

It is frequently convenient to distinguish main and additional kinds of parameters; those are sorted in Table 3.2 which summarises SNOW-17 model parameters.

PXTEMP parameter represents snow accumulation since it separates rain from snow. If the *temperature* is less than PXTEMP, the *precipitation* is expected in the form of snow and vice versa.

The *precipitation* classified as snow is adjusted by the SCF parameter which equalises losses occurring during accumulation periods. The SCF balances sublimation and redistribution of snow cover, caused by blowing snow, and corrects transfers of *precipitation* fallen outside a basin district.

The *temperature melting factors* MFmax and MFmin are the most important parameters of the snow sub-model. Those determine maximum/minimum melt factor during non-rain periods. The melt variability in an annual cycle takes different duration of sunshine and total solar radiation into account, e.g. in January and May. Values of the MFmax and MFmin parameters depend on what kind of catchment the terrain is modelled on; e.g. for open area MFmax = 8.0 $mm.day^{-1}/1°C$, or MFmax = 2.0 $mm.day^{-1}/1°C$ for forest.

Different terrains and uneven winter conditions in mountains and lowlands, including various wind conditions, are modelled by another model parameter. SI parameter is a value which determines the mean areal water equivalent above which there always is 100 percent areal snow cover (mm).

Table 3.2: SNOW-17 model parameters

Parameter	Description	Units
MFmax	Maximum of the melt factor	$mm.day^{-1}$
MFmin	Minimum of the melt factor	$mm.day^{-1}$
SCF	Snow coefficient correction factor	$mm.day^{-1}$
UADJ	Wind function for the given region	$mm.day^{-1}$
SI	The mean areal water-equivalent	mm
ADC	Areal depletion curve of the snow cover	-
NMF	The maximum negative melt factor	$mm.day^{-1}$
TIMP	Antecedent temperature index parameter	-
PXTEMP	The temperature which delineates rain from snow	°C
MBASE	Base temperature for snowmelt computations	°C
PLWHC	Percent liquid water holding capacity	%
DAYGM	Melt rate of the snow-soil interface	$mm.day^{-1}$

Areal Depletion Curve (ADC) defines the areal extent of the snow cover as a function determining how much of the original snow cover remains after a significant area of bare ground appears, Anderson (2006). The ADC also reflects a reduction in the mean areal melt rate, which occurs because fewer areas are covered with snow.

The Areal depletion curve (ADC) regulates the process of how the areal extent of the snow cover is changed during the melt seasons. The ADC curve shows the correlation of the snow areal extent and the mean areal water equivalent. In other words, the ADC chart is a non-dimensional plot of the snow-covered area against water equivalent. ADC is used when the snow depth is less than the snow depth for 100% cove, see parameter SI. The final snow-covered area is computed using ADC.

The shape of the ADC depends on the physiographic factors in a given area. The model user specifies the areal extent of the snow cover for W/A_i ratios; where W is the water equivalent, A_i is the area index of the areal extent of the snow cover. There are 11 ratios where $W/A_i = 0.0$ the snow coverage is 0.05, since a small amount of snow remains after the melting. It is typical for mountainous regions that small spots of dense snow remain throughout the summer but these are hydrologically insignificant.

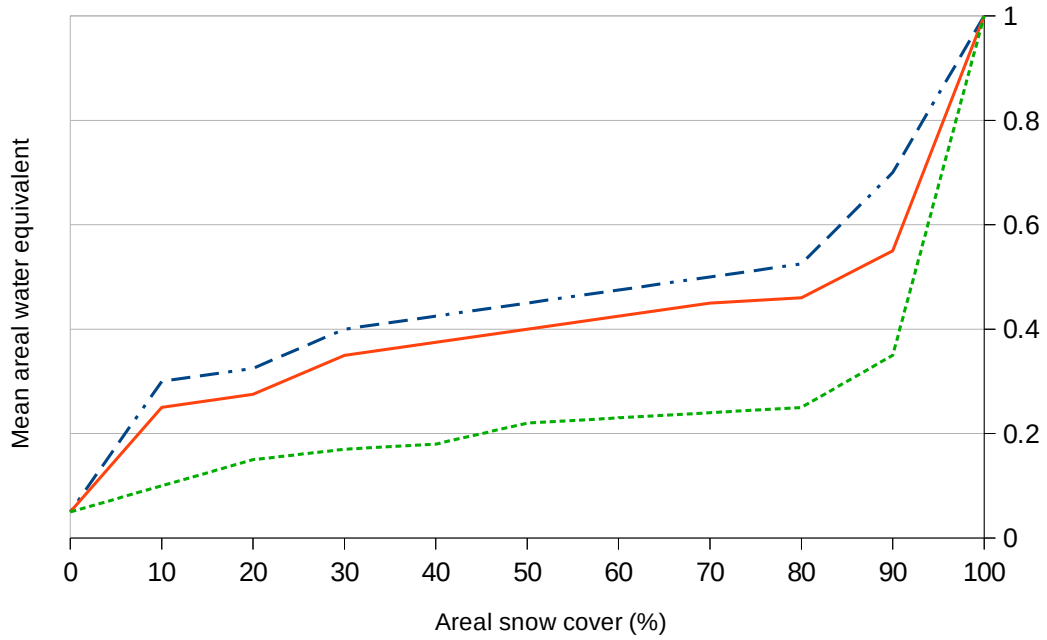

Figure 3.3: Areal depletion curves for different years

Figure 3.3 represents the shapes of three ADC curves. The courses of all three ADC curves are becoming more similar as the quantity of bare ground begins to grow.

Model output

The main output is the total outflow from simulated snow cover. It is composed of the rain fallen on bare ground and the melted snow cover, given in *mm*. The value is also referred to as rain+melt and is inputted into subsequent rainfall-runoff models, like the SAC-SMA in our case.

Another output group provides information about the areal snow cover in *percentage*, the snow depth (*cm*), and the simulated water equivalent of the ice portion of the snow cover (*mm*).

3.5.2 Unit Hydrograph

Another supporting model that we use is a Unit Hydrograph (UNIT-HG), which describes the hypothetical response of a catchment. The UNIT-HG is a useful hydrology tool because it simplifies the algorithm for the runoff distribution. In technical terms, the UNIT-HG represents a linear and time-invariant system.

The UNIT-HG specifies the values of runoff according to the height of the *precipitation* and characteristics of the basin. In other words, UNIT-HG characterises the transformative effects of a watershed. These effects take influences such as the size, slope, basin cover, and other geomorphological features into account, Sherman (1932). UNIT-HG is used as constant transportation of runoff in most rainfall-runoff models. The transformation defines how the actual runoff is distributed in the catchment in the form of several sub-runoffs in time. In other words, the transformation is a continuous function, of which the first derivative with respect to t defines the runoff at time t. The model calibration defines the UNIT-HG as a set of points, where each point determines the ordinates of the UNIT-HG.

Model input

The only input is the runoff obtained from a rainfall-runoff model, the SAC-SMA in our case. The runoff is given in mm.

Model parameters

The BASE parameter adds constant baseflow to computed instantaneous discharges. It is usually used for instances when runoff is not from a simulated basin but it is from a strange watershed.

The AREA parameter defines the drainage area to be represented by a unit hydrograph, given in km^2.

The essential parameter is the definition of the unit hydrograph. The first sub-parameter is the number of ordinates in the unit hydrograph. The second sub-parameter is an ordered set of unit hydrograph ordinates, given in m^3s^{-1}/mm. Figure 3.4 illustrates an example of a simple unit hydrograph of the Elbe catchment. It is evident that the most significant runoff occurs 2 days after the *precipitation* falls. The curve shape of the unit hydrograph usually corresponds to the Poisson distribution function which can be described by the diffusion equation.

Model output

The only output is instantaneous discharge measured in m^3/s which is the final outflow at the closure profile.

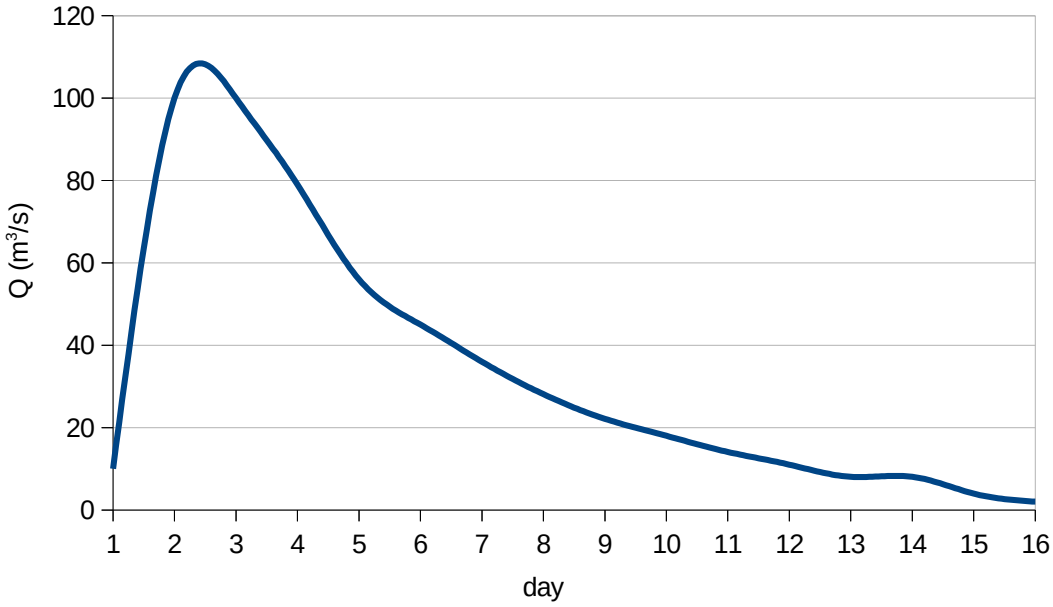

Figure 3.4: Unit hydrograph of the Elbe basin

3.6 Sacramento Model

At this point, we have defined the rainfall-runoff (SAC-SMA) model and the supporting models (SNOW-17 and UNIT-HG). This subchapter describes the SAC-SMA model in overall view including the dynamic structure of the rainfall-runoff simulation.

Records about air *temperature* and *precipitation* together with the model calibration (parameters) constitute the inputs into the Sacramento model, as is illustrated in Figure 3.5. The Sacramento model is a working name for the SAC-SMA rainfall-runoff model containing the SNOW-17 and the UNIT-HG supporting models. The model calibrations include all required model parameters as listed in the previous chapter (Section 3.5) in concerning sections.

The workflow of the simulation process, captured in Figure 3.5, starts with the SNOW-17 model. Rain+melt and snow cover, which are input for the SAC-SMA model, are based on the *temperature* and *precipitation* as inputs of the SNOW-17 model. The SAC-SMA computes the actual runoff which is the input for the UNIT-HG model. The instantaneous discharge is the final runoff from a basin and is used for the model validation. In this form, the Sacramento model provides complex information about a simulated catchment if the model is well calibrated.

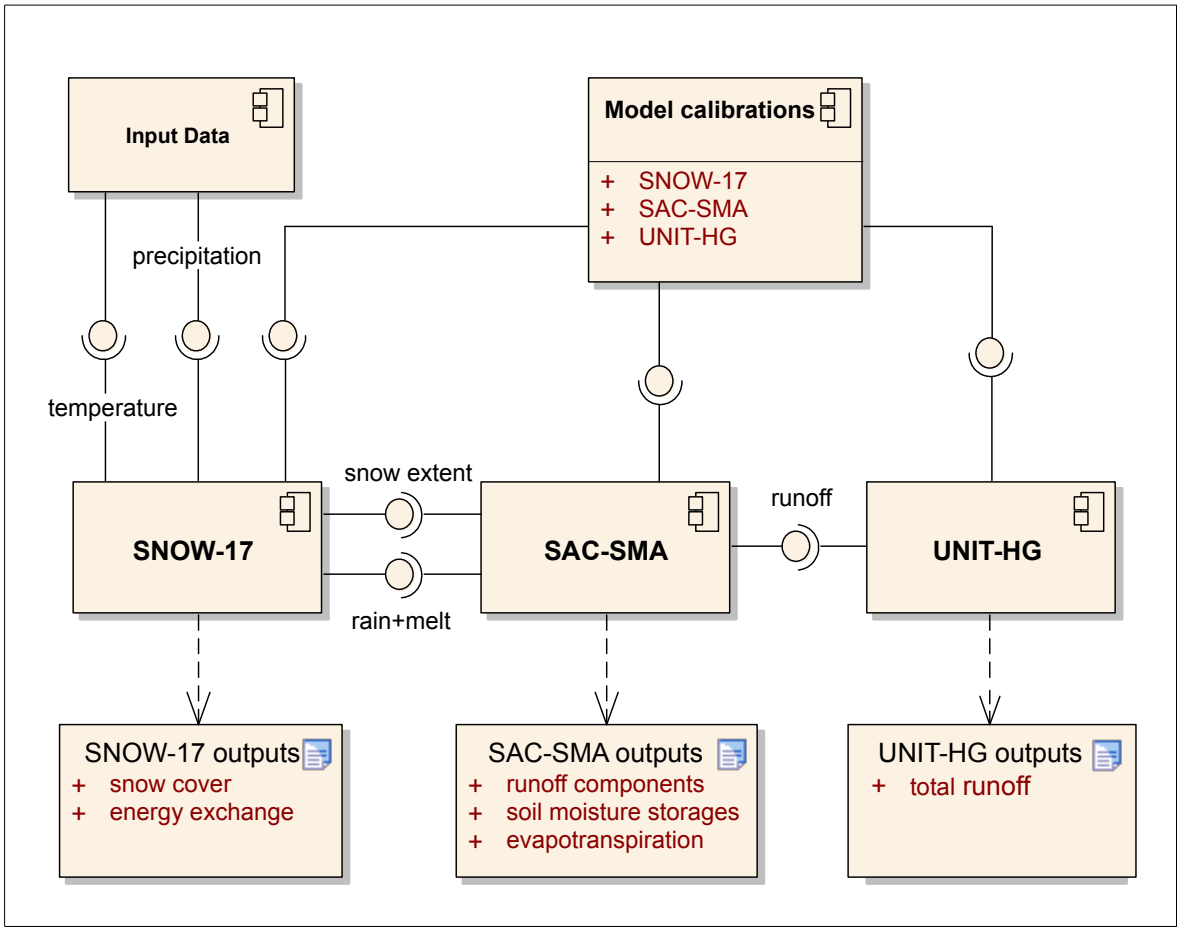

Figure 3.5: Sacramento model structure

3.7 Validation of Hydrological models

The differences between the observed and simulated discharge determine the calibration success of the rainfall-runoff models. In the context of the Sacramento model (Section 3.6), the simulated discharge is the output of the UNIT-HG, the observed discharge is obtained by a measurement at a closure profile of a simulated catchment. If the differences between observed and simulated discharges are relatively small, the model is valid and all sub-model outputs (SNOW-17, SAC-SMA, UNIT-HG) of the Sacramento model are realistic and usable in practice.

There are diverse methods for model validation. However, the evaluation of the estimated runoff is usually performed using one of these two ways: one uses a statistical indicator, and the other is a graphical comparison. If the statistical indicators cannot be evaluated, the second method can be used but only for a subjective review, Sargent (2013).

This thesis primarily focusses on the statistical method and uses 4 of the most fundamental indicators in basic form, as summarised below, Moriasi *et al.* (2007):

1. Root Mean Square Error (RMSE)

$$RMSE=\sqrt{\frac{1}{n}\sum_{i=1}^{n}(Q_i-S_i)^2} \tag{3.1}$$

2. Bias

$$Bias=\frac{\sum_{i=1}^{n}(S_i-Q_i)}{\sum_{i=1}^{n}Q_i} \tag{3.2}$$

3. Coefficient of Efficiency (Nash–Sutcliffe model efficiency coefficient)

$$E=\frac{\sum_{i=1}^{n}(Q_i-S_i)^2}{\sum_{i=1}^{n}(Q_i-\overline{Q})^2} \tag{3.3}$$

4. Correlation Coefficient

$$R=\frac{n\sum_{i=1}^{n}S_iQ_i-\sum_{i=1}^{n}S_i\sum_{i=1}^{n}Q_i}{\sqrt{\left(n\sum_{i=1}^{n}S_i^2-\left(\sum_{i=1}^{n}S_i\right)^2\right)\left(n\sum_{i=1}^{n}Q_i^2-\left(\sum_{i=1}^{n}Q_i\right)^2\right)}} \tag{3.4}$$

where, S is the simulated discharge, $\overline{Q}$ is the mean of the observed discharge, Q is the observed discharge, and n is the number of events. Modified forms of these equations can be useful for a different time scale (e.g. a monthly or daily).

Each statistical indicator expresses the degree of calibration quality. Each indicator is prone to a different set of model parameter values. Therefore, the model validation must be evaluated using more indicators and overall evaluation of model calibration quality is a complicated issue. Like the model calibration, the model validation is dependent on the user's knowledge and experience; since there are instances of simulations where statistical indicators show satisfactory values, but the model calibration is not possible.

3.8 Global Search Algorithms

Optimising such a complex problem as the Sacramento model (Section 3.6) requires the use of a global search algorithm because there is no deterministic algorithm for resolving this issue. Therefore, the stochastic approach needs to be applied.

This sub-chapter overviews heuristic methods which look for an approximately optimal solution. The main used algorithm is the *genetic algorithm* (GA) together with the Monte Carlo Simulation. Special attention is paid to the GA terminology, operations, and parameter representation of the optimised model; all regarding the Sacramento model. Another part focuses on the fitness function (or objective function) which determines optimisation quality of found solution; this is closely related to the model validation (Section 3.7). The next topic targets the delineation of optimisation framework for the Sacramento model and optimisation workflow. The final part of this subchapter aims at the random number generator (RNG) which is the core of the stochastic and global search algorithms.

3.8.1 Monte Carlo Simulation

The *Monte Carlo simulation* (MCS) is a numerical method that uses random variables and the theory of probability. One of its points is to simulate the possible outputs based on acceptable inputs using statistics, Mooney (1997). Its advantage is its simple implementation, as is illustrated in Algorithm 3.1. This occurs at the expense of relatively low accuracy, which can be increased by other stochastic techniques (e.g. the *genetic algorithm*). One of its weaknesses is a weak random number generator leading to systemic errors in the MCS, Resende and Costa (1998).

Algorithm 3.1: Monte Carlo Simulation

Input: n, number of simulation
Output: $\boldsymbol{x}$, vector of the best model calibration
begin
1 Let $f(\boldsymbol{x})$ be a definition of a model validation, where $\boldsymbol{x}$ is a vector of the model's parameters
2 **Repeat** n times, where n is a parameter of MCS
3 Randomly generate values of the vector $\boldsymbol{x_n}$
4 Let $y_n = f(\boldsymbol{x_n})$, where y_n is the result of the model validation
5 **end repeat**
6 Let $\boldsymbol{z} = \max(y_1, \ldots, y_n)$ be the best model validation
7 **return** $\boldsymbol{x}_z$
end

In the context of the Sacramento simulation and Algorithm 3.1, line 1 is the definition of the Sacramento model and its validation; line 3 randomly generates values of the Sacramento model parameters mentioned in Tables 3.1, 3.2, and the unit hydrograph coordinates; line 4 performs the Sacramento simulation followed by the model validation with the parameters from line 3; the outputs of the MCS are those values of the Sacramento parameters that have the best value of the model validation.

The initial manual model calibration (i.e. mostly iterative) is the starting point. The MCS then estimates the values of the vector $\mathbf{x}$ (see Algorithm 3.1) based on the initial values of the manual calibration. A range of the estimated parameters is defined as an input parameter of the MCS. We use a percentage range for each optimised parameter, which determines the absolute range for the model parameter. The parameter value is calculated accordingly: Let v be the initial value of parameter p, let r be the range of p, then a new p is generated by the random number generator in the range $(v - r.v,\ v + r.v)$. However, the chosen range is crucial for the quality of the optimisation: if the interval is too small, the MCS can get stuck at a local minimum. On the other hand, the MCS may not be able to find the best model configuration in reasonable computing time if the interval is too large.

3.8.2 Genetic Algorithm

The *genetic algorithms* (GAs) represent one of the evolutionary techniques which are inspired by processes in nature. The structure of the GA is based on Darwin's theory of natural selection. Each individual is a candidate for a solution to a given problem. The fitness function quantitatively expresses the quality of a candidate. The task of the algorithm is to "breed" an individual with the best fitness function value. The GA evaluates the population composed of chromosomes containing data in a similar way to a biological chromosome, Gallagher and Sambridge (1994). Each chromosome in the population is a set of genes, which are coded by binary or real values. The GA tries to discover a combination of the genes which maximises or minimises the fitness function. To achieve this, it uses equivalents of natural genetic operators, for instance: selection, crossover, and mutation, Holland (1992).

New sets of chromosomes are appraised with each generation. The fitness value is calculated and assigned to each newly estimated chromosome. The fitness value provides information about a chromosome's quality, which is used for probabilistic selection of a chromosome to pass on to the next generation. This selection is analogous to natural selection. The GA is terminated if predetermined criteria

are met. Each new chromosome is the result of the genetic operations. The most significant genetic operations are *crossover* and *mutation*, both of these operations are random processes with defined probabilities. Crossover takes two chromosomes as parents and produces a new chromosome by exchanging their genes with each other. Parts of the exchanged chromosomes are randomly selected and can be determined using one or multiple points. The GA can get stuck in a local minimum despite the crossover operation. The mutation operation can avoid this disadvantage because it randomly changes the gene value. This change can discover a solution in another part of the search space. In other words, mutation prevents getting stuck in a local minimum, Holland (1992). The GA can be scaled by algorithm parameters summarised in Table 3.3. We introduce these parameters in the following paragraphs, which describe the GA operations in the context of the Sacramento model in more detail.

Table 3.3: Description of GA parameters and selected optimal values

Parameter	**Field value**	**Description**	**Optimal value**
Generation limit	integer	Generations upper bound	400
Population size	integer	Dimension of population	175
Crossover	One-point(p) Two-point(p)	Crossover type; where p is crossover probability	One-point(0.8)
Mutation	<0.0-1.0>	Mutation probability	0.03
Selection	TournamentSelector RouletteWheelSelector	Selection method	TournamentSelector
Elitism	integer	Number of individuals selected to next generation	7 (4% of population size)

Parameter Representation

Each individual represents one model calibration of the SAC-SMA model, including the sub-models. The individual stores information about the model calibration in a chromosome, which is defined as an array of real values, and each model parameter has a specified position in this array. One element of the array is called a gene.

The Sacramento model is not just a state model; the model parameters are represented via real values. It follows the chromosome mirroring these real value parameters, so each gene of the chromosome retains one real-value parameter of the Sacramento model. Figure 3.6 demonstrates an example of the individual chromosome characterising the parameter calibration of the Sacramento model.

The first part of the chromosome codes parameters of the SNOW-17 model. The second part stores the SAC-SMA model parameters. Finally, the last section contains information about the UNIT-HG parameters. The last chromosome part is variable since the unit hydrograph is various according to a modelled basin. However, the number of unit hydrograph points is constants across the population, so all individuals have the same chromosome cardinality.

Individual, Population and Generation

In the context of the GA and the Sacramento model, an individual represents one model calibration of the Sacramento model. Values of the calibration are collected in the chromosome where one parameter value is stored in one gene.

Population and generation look very similar at first glance, but there seemingly is a slight difference. Population is a set of individuals across generations, which means that generation is time-dependent. Normally, a generation defines a subset of a population at specific time since population is always evolving. Therefore, generation is actually a timestamp of a population.

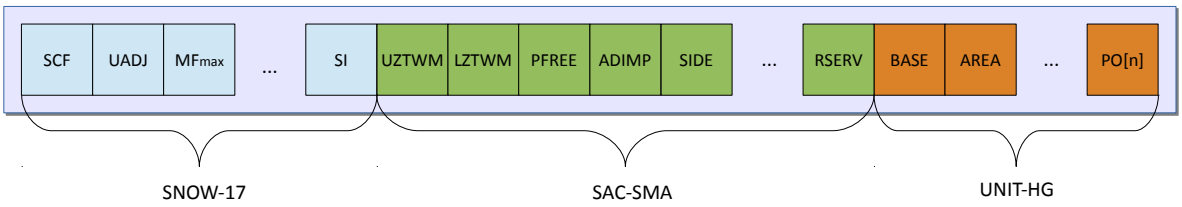

Figure 3.6: Sacramento chromosome

Figure 3.7 illustrates the differences between population and generation. A population is composed of every individual that is still active and can be used for reproduction. In this case, the population consists of all individuals in the previous, current and next generation. So, individuals from the previous and current generation can be selected for the GA operations and a newly created individual is added into the next generation. While population is a set of all potential individuals, generation is a subset of the population which is processed by one GA iteration. In this case, the current generation has been evolved and the next generation is prepared for the next GA iteration. After evolving the next generation, the previous and current generations are shifted so that the current generation becomes the previous one, the next generation becomes the current one, and so on. The grey individuals represent inactive individuals which are not used in the next GA iteration. They are the ones with a low fitness function or with invalid model calibration.

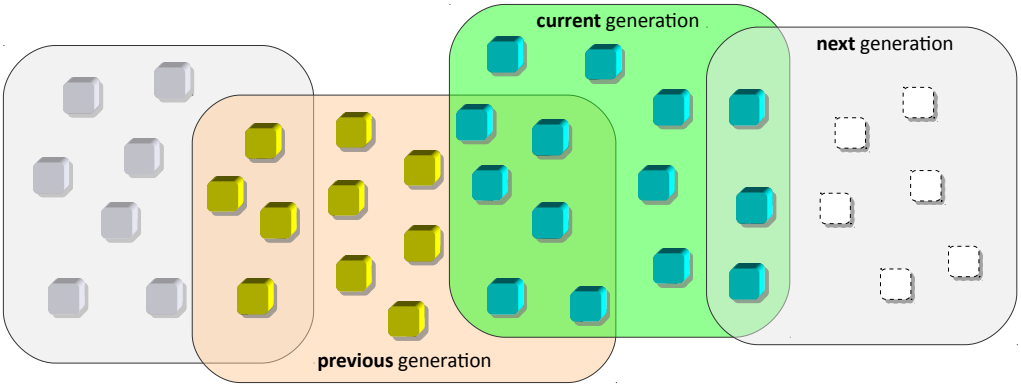

Figure 3.7: Illustration of individuals in generation and population

Crossover, Mutation, and Elitism

Crossover is a GA operation which crosses two individuals (model calibrations) of a current population in a defined manner. The output is a new individual of the next generation whose chromosome is composed of both input chromosomes in a particular ratio. The manner and random probability of the ratio are the given input parameters. The ratio is usually a higher value. In other words, the ratio defines the probability that the individuals will be crossed and a new individual will be created.

There are two ways a new individual can be created by the crossover operation:

1) One-point crossover: Let p be a real number generated at random. The pointer p divides input chromosomes into two equal parts as follows: $\mathrm{x} = x_{1\ldots\mathrm{p}}x_{p+1\ldots n}$ and $\mathrm{y} = y_{1\ldots p}y_{p+1\ldots n}$, where n is the chromosome length (number of genes). The new individual is $n = x_{1\ldots\mathrm{p}}|y_{p+1\ldots n}$; where $|$ is a concatenation operation.

2) Two-point crossover: Let o and p be real numbers generated at random. These pointers divide the input chromosome of each input individual into three parts: $x = x_{1\ldots o}x_{o+1\ldots p}x_{p+1\ldots n}$, $y = y_{1\ldots o}y_{o+1\ldots p}y_{p+1\ldots n}$. The new individual is $n = x_{1\ldots o}y_{o+1\ldots p}x_{p+1\ldots n}$.

See Figure 3.8 for the illustration of the crossover operation.

Mutation is another GA operation, it is a unary operation applied to a single individual. Each gene of the individual chromosome is mutated with the probability p, which is the parameter of this operation. The MCS generates a new value of the mutated gene which prevents getting stuck in a local minimum, Holland (1992).

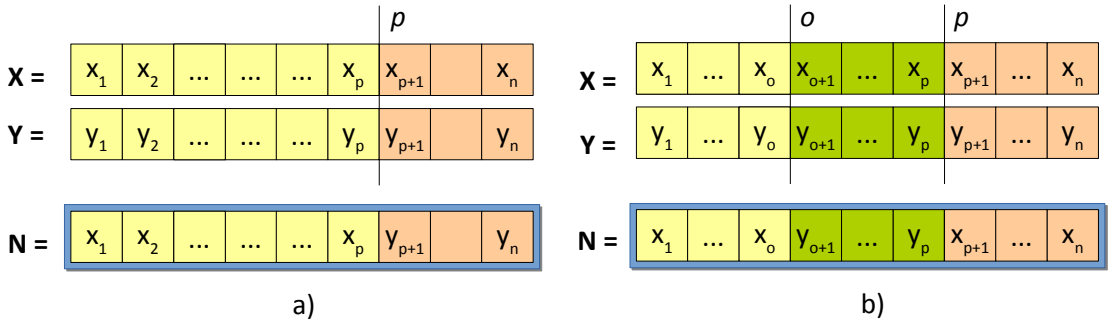

Figure 3.8: Crossover operations, a) one-point, b) two-point

The last GA operation that works with individuals is Elitism. The best individual (model calibration) from each generation should always be transferred to the next generation to preserve the best configuration across all generations. Thus, the Elitism guarantees that a certain number of the best individuals are preserved for the next generation, i.e. the individuals with the best fitness function value.

Reproduction and Selection

The task of the *Reproduction* and *Selection* operations is to generate a set of individuals called a generation whose cardinality is defined by the GA parameter *Population size*. The MCS creates new individuals usually with a small parameter n of Algorithm 3.1. One generation corresponds to one iteration of GA in which the following steps form the population.

1) Certain number of individuals with the best model calibration is transferred from the current to the next generation. The GA parameter *Elitism* determines the number of the best individuals.

2) The crossover operation complements the rest of the individuals to the capacity of the new population. The capacity is defined by the GA parameter *Population size*.

The following two methods select a pair of individuals from the previous and current generation for the crossover operation. The probability of the selection ensures that an individual with a low fitness value can transfer a part of its chromosome to the next generation, where the new individual can improve its fitness value.

The first selection method is the *roulette wheel* selection: it resembles a roulette wheel in a casino, where the selection probability is defined by Equation 3.5.

$$p_i = \frac{f_i}{\sum_{j=1}^{N} f_i} \tag{3.5}$$

Here f_i is the fitness of an individual i and N is the cardinality of the population.

The second selection method is the *tournament* selection: the tournament takes the fitness values of all individuals into account and generates a random number in the interval (0,1). If the random number is smaller than the probability selection, the fitter individuals are chosen; otherwise the worse individuals are selected. This step selects n individuals with diverse values of the fitness function while the best individual of this choice is the winner of the tournament, Ghanea-Hercock (2013). It again ensures that an individual with worse fitness value can get a chance to improve itself or its part of a chromosome can improve other individuals' fitness value.

3.8.3 Fitness Function

As discussed above, the value of the fitness function is a scalar quantity determining the condition of an individual. In the context of the Sacramento model, the fitness function defines the quality of the model calibration. The fitness function uses statistical indicators, such as the RMSE or the Correlation Coefficient to determine the fitness value. In general, the fitness function uses mathematical functions which inspect differences between observed and simulated flows. Mathematically the fitness function is function f mapping individual to R.

The fitness value determines the condition of each individual, which is necessary to be interpreted differently for each fitness function since the smallest value of the fitness function does not always mean the best individual condition. For example, smaller RMSE means higher quality of the individual, but smaller Nash–Sutcliffe efficiency coefficient means lower individual quality. Therefore, the GA minimises/maximises the value of the fitness functions. The GA can only reduce the fitness value, even for effective coefficients (Nash–Sutcliffe or Correlation Coefficient), since the functions representing the effective coefficients are converted to a reverse value.

In the context of the Sacramento optimisation, choosing the right fitness function is crucial for the optimisation of the model calibration. However, the proper fitness function can be different for each catchment, period, or input data, so the fitness function cannot be determined conclusively. Therefore, the fitness function will be represented by Equations 3.1-3.4, which will be used for the optimisation of the study areas (see Section 7).

3.8.4 Model Optimisation Framework

The foundation of Sacramento optimisation is the GA, as is illustrated in Figure 3.9. The initial model calibration and percentage ranges for each initial model parameter are the inputs for the GA component. The algorithm evaluates newly improved model calibration, which is input for the Sacramento model. The model sets the model parameters according to the new model calibration, and the simulation is performed using the input data (*precipitation*, *temperature*, runoff, etc.). The simulated runoff, being the output of the Sacramento simulation, put together with the observed runoff are the inputs for the model validation. The model validation generates statistical information describing the quality of the simulation. Evaluation of each individual (model calibration) means that the Sacramento simulation is performed. When all individuals of the current generation are evolved, the GA compiles the ranking of the individuals based on the statistical information and creates the next generation.

In this section, we describe the GA optimisation in detail. The optimisation workflow is composed of 7 steps, which use the GA operations mentioned above (Table 3.3 in Section 3.8.2). The workflow consists of the following steps:

Step 1 (initiation): encode the initial model calibration of the Sacramento model into the genes and the chromosome. The MCS generates an initial population. The number of individuals is determined by the GA parameter *Population size*.

Step 2 (evaluation): calculate the fitness value for each individual of the population and sort the individuals by their fitness values, from best to worst.

Step 3 (selection into a new population): transfer the x individuals from the current generation into the next generation, where x is the GA parameter *Elitism*.

Step 4 (crossover): the selection operation selects two individuals from the population. The GA parameter *Crossover* determines the crossover operation which creates a new individual of the next generation. Step 4 is repeated until new generation is filled.

Step 5 (mutation): apply the mutation operation to each individual of the next generation with probability p set by the GA parameter *Mutation*.

Step 6 (continuation): if the current generation number is smaller than the GA parameter *Generation limit*, then increment the generation number and go to Step 2, otherwise continue to the next step.

Step 7 (completion): perform Step 2 and select the first individual from the last generation. This individual is the best individual among all generations.

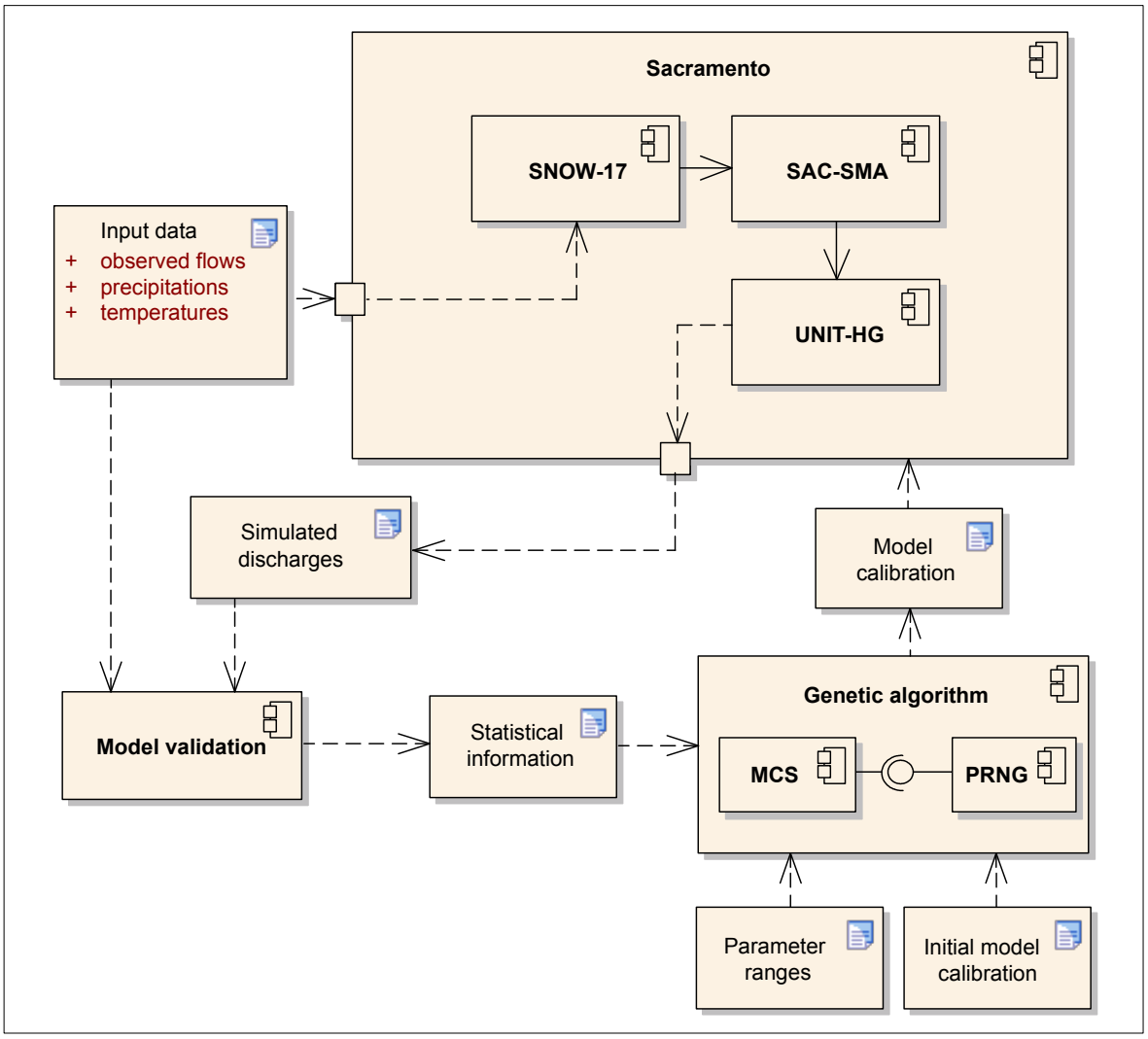

Figure 3.9: Optimisation framework of the Sacramento model

3.9 Random Number Generator

Although it may not be apparent at first glance, the random number generator (RNG) is the core of the *genetic algorithm* and the Monte Carlo simulation, since the quality of generated random number affects how the GA searches the solution space. In other words, it influences whether the GA gets stuck at a local minimum. Most of the available optimisation software frameworks contain a pseudo-random number generator (PRNG) with a uniform distribution.

Unfortunately, PRNGs are not sufficiently random because the ideal randomness is in conflict with the determinants of the PRNG algorithms. The ideal RNG is infinite, non-periodical, with a uniform distribution and efficient calculation. Primarily, the non-periodicity is the most fundamental problem of the PRNG. The periodicity is a consequence of bit generation in the finite space of the computer memory. For this reason, random number sequences begin to repeat after a while. The periodicity is evident in the second part of Figure 3.10.

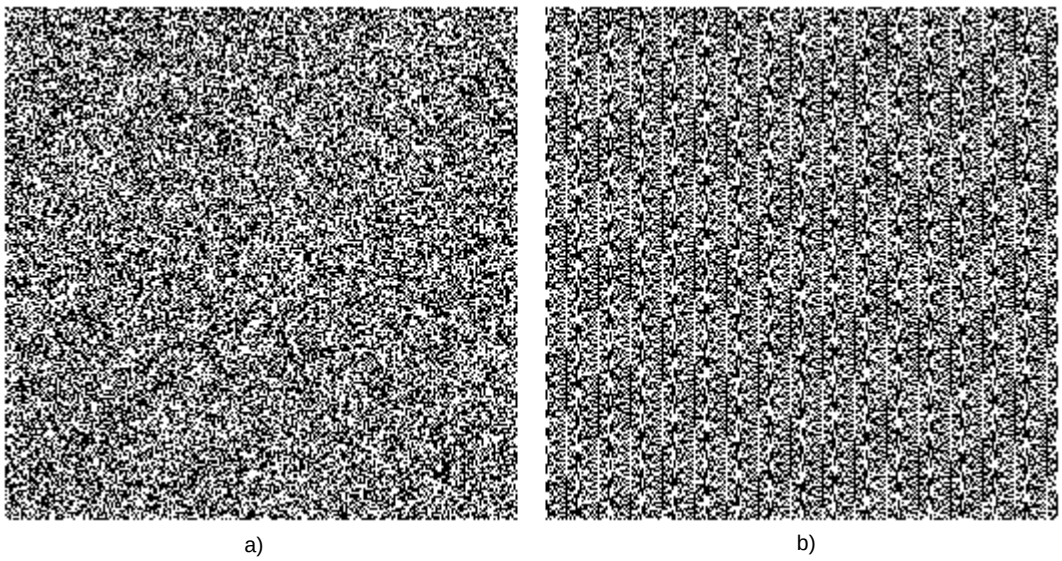

Figure 3.10: Visualisation of randomness, a) TRNG b) PRNG, Haahr (2017)

The periodicity only arises with a small probability in small simulations (a small number of optimised parameters), L'Ecuyer (2012). However, the number of calibrated parameters is a significant factor influencing the periodicity; since the more pseudo-random numbers are needed, the higher the probability of the periodicity increases, Persohn and Povinelli (2012). There are many True Random Number Generators (TRNGs) which eliminate the deficiencies of the PRNG. Persohn and Povinelli (2012) prove that the periodicity is an integral part of the

PRNG. The TRNG eradicates the imperfection of the PRNG entirely because they are based on processes like noise, measurement of photon motions, and other physical processes, and these TRNGs usually have the Gaussian distribution. A few basic principles of the TRNG based on physical processes are the following:

1) Johnson's effect generates a random voltage at terminals of resistances with temperature higher than absolute zero.

2) Measurements of a physical system in chaos. Currently, chaos systems like optical, electrical or optoelectrical are mostly used.

3) Repeating the same measurement of the same quantity and random values are a consequence of the quantum theory.

All examples mentioned above require expensive hardware equipment, but a significant advantage is that they provide trueness and significant speed of generating, Stipčević and Koç (2014).

3.9.1 Pseudo-Random Number Generator

The Pseudo-random number generator (PRNG), as the name suggests, is the only artificial number generator. Therefore, the PRNG is represented as a deterministic algorithm. We use the Mersenne Twister generator developed by Resende and Costa (1998) that is based on the Linear Congruential Generators described by the following Equation 3.6:

$$X_n = (aX_{n-1} + c) \, mod \, m \tag{3.6}$$

Here, $m > 1$ is the modulus, a $\in \{1, 2, ..., m-1\}$ is the multiplier, $c \in \{0, 1, ..., m-1\}$ is a constant, $X_0 \in \{0, 1, ..., m-1\}$ is the initial value called a seed. Equation 3.6 represents the PRNG which is a partial differential equation in principle.

The seed variable introduces an element of randomness into the PRNG and its value is usually derived from the PC's system clock. A disadvantage of this PRNG is periodicity, which is a consequence of the bit generation in the finite space of computer memory. So, the more pseudo-random numbers are needed, the more the probability of the periodicity increases, Persohn and Povinelli (2012). Barker and Kelsey (2007) have proved that the periodicity comes much sooner before a number of m requests for a random number. The optimisation of the Sacramento model requires hundreds of thousands of requests for a random number. The number of requests for a random number depends on the number of optimised parameters.

The following example illustrates how the PRNG described by Equation 3.6 works. Let $m = 11$, a $= 3$, $c = 4$, $X_0 = 8$. Equation 3.6 starts at seed $X_0 = 8$ and generates the following sequence of random numbers: 6, 0, 4, 5, 8, 6, 0, 4, 5, 8, 6, 0, 4, 5, 8, 6, ... At first glance, the sequence is not random since the selection of the PRNG variables determines a periodicity of the PRNG as Persohn and Povinelli (2012) proved. They have shown that periodicity is an integral part of the PRNGs.

Mersenne Twister Generator

Practically usable PRNG like the Mersenne Twister Generator (MTG) involves a sophisticated mathematical apparatus. The MTG has several advantages, such as long periodicity, so random numbers begin to repeat in many requests for a random number. Furthermore, the MTG has good distribution properties and efficient use of computer memory.

The power of the MTG is that the generator only uses bit operations (and, or, xor, shifts) and avoids arithmetic operations (multiplication, division, addition, subtraction). Although the generator algorithm is deterministic, all states of the MTG are defined by the seed variable which creates a buffer of random numbers that are used for a final random number generation. The seed variable initiates the whole process of generation. Each request for a random number pulls an integer number from the buffer. The pulled element is so-called *tempered* by using the bit operations to improve the randomness of the element. If the buffer is empty, new elements are created by applying the bit operations, seed variable, and constants for bit masking. The embedded constants and the algorithm are regulated by the permutation and the tempering operations. Therefore, the period of the MTG is longer than any other PRNGs, which is one of the reasons for its popularity.

Function 3.2: RandomBuffer(S)

Input: value of seed variable S
Output: initial buffer B
begin
1 B[1] ← S
2 **for** i ← 2 **to** |B| **do**
3 B[i] ← 0×6C078965 * B[i-1]
4 **end**
5 **return** B
end

Function 3.3: UpdateBuffer(B)

Input: used buffer of random numbers B
Output: new unused buffer B
begin

```
1       for i ← 1 to |B|-1 do
2               y ← (B[i] & UPPER_MASK) | (B[i+1] & LOWER_MASK)
3               B[i] ← B[(i+|B|/2) mod |B|] ^ (y >> 1) ^ MATRIX_A
4       end
5       y ← (B[|B|] & UPPER_MASK) | (B[1] & LOWER_MASK)
6       B[|B|] ← B[|B|/2)] ^ (y >> 1) ^ MATRIX_A
7       return B
```

end

UPPER_MASK = 0×80000000
LOWER_MASK = 0×7FFFFFFF
MATRIX_A = 0×9908B0DF

Function 3.4: nextInteger()

Output: integer random number
begin

```
1       if all items of B used? then B ← UpdateBuffer(B)
2       y ← pull(B)
        // tempering
3       y ← y ^ (y >>1)
4       y ← y ^ (y << 7) & 0×9D2C5680
5       y ← y ^ (y << 15) & 0×EFC60000
6       y ← y ^ (y >>> 18)
7       return y
```

end

Function 3.5: nextDouble()

Output: double random number in the interval [0, 1)
begin

```
1       y ← nextInteger()
2       z ← nextInteger()
3       return ((y >> 6) << 27) + (z >> 5) / (1 << 53)
```

end

The workflow of random number generating is defined by Functions 3.2 - 3.5, those functions specify the core of the MTG. The initialisation of the MTG calls, among other things, Function 3.2, which prepares the buffer of random numbers determined from the seed value. The size of the buffer is 624 items. Request for a random number invokes Function 3.4 which tempers one buffer item using bit operations and constant masking. Function 3.3 updates the buffer when this one is empty. For more information, see Resende and Costa (1998). The Function 3.5

returns a real number in the interval *[0,1)*. This algorithm uses tempering of two integers and their bit shifting which is divided by a real constant. This division then returns a double value that is in the proper interval using the shifting operation (see line 3 of Function 3.5), Oracle (2017).

3.9.2 Validation of the Random Number Generator

Computer simulations, computational number theory, and cryptography need good RNGs and the interest in the RNGs' quality and suitability evaluation is still increasing.

No artificial generator is ideal and has all attributes of the TRNG. For these reasons, validation of the PRNGs must be done so that the PRNGs are usable in practice. Deciding whether generated random data are high-quality is undoubtedly a complex statistical issue. Several analytical approaches can validate properties of the PRNG, like the periodicity, probability distribution of generated numbers, etc.

Diehard tests and statistical methods facilitate how to decide which RNGs are good.

Diehard tests

The Diehard tests are suites which form criteria and requirements for proper RNGs in the form of statistical tests. If these tests fail, the RNG does not have suitable properties for use in practice. If the tests pass, the RNG has pseud-ideal properties and can be used in practice. Individual tests differ in their complexity, so some tests may be easier to pass, Marsaglia (1995).

The following points introduce the primary Diehard tests.

1) Birthday Spacings Test

This test is based on the birthday paradox, Flajolet *et al.* (1992), where random points are chosen on a large interval. The distance between these points should have an asymptotically exponential distribution. The random points are obtained using a tested RNG.

2) Overlapping Permutations Test

The test generates five consecutive random numbers. 120 possible permutations should appear with the same probability. The test analyses 10^6 integers of tested RNG.

3) Binary Rank Test

Diehard tests use three variations of the Binary Rank Test applying the following general procedure. The test selects a defined number of bits from random numbers of tested RNG. The bits are arranged into a matrix over {0,1} and the test determines the matrix rank (number of independent rows or columns). The value of the rank determines the RNG quantity. The variations are: 31×31, 32×32, and the 6×8 matrix.

4) Minimum Distance Test

The test operates with a unit square of 10,000×10,000. The test randomly places 8,000 points into the square and then evaluates the minimal distance between the pairs of the placed points. The resulting square of the distance should have an exponential distribution.

5) DNA Test

DNA test is computationally the most demanding. DNA test defines 4 characters: C, G, A, T; similar to fragments in the biological DNA. Randomly generated integers determine a sequence of these characters (string) based on two designated bits from the random integers. The test presupposes 10-character strings so there are 2^{20} possible words, the mean number of the missing words is 141909. DNA test analyses the overlapping of these strings which determines the RNG quality.

6) Overlapping Sums Test

The Overlapping Sums test is very simple. It generates a long sequence of random float numbers in the interval (0, 1), then adds another sequence of 100 consecutive float numbers. This sequence should not disrupt a normal distribution with characteristic mean and variance.

Each Diehard test returns a *p-value* in the interval [0, 1) which determines whether the RNG generates genuinely independent numbers. Hence, if the RNG generates a number that is considerably far from the acceptable standard, the Diehard tests declare that the RNG fails; it usually results from a comparison of *p-value* in used tests.

Let *f(X)*, where *f* is a function with an expected distribution of a random variable *X* with usually normal distribution. The predicted distribution is merely an asymptotic approximation. Therefore, if the *p-value* is on tails, randomness of the RNG is worse. In other words, the *p-value* near 0 or 1 indicates that the RNG encountered a big fail, Marsaglia and Tsang (2002).

Chi-squared Test

Another property which we investigate for the RNG is its distribution function of generated numbers. Chi-squared test (χ^2) is used for this purpose.

The χ^2 test sorts out a random variable of the tested RNG to k non-overlapping bins determining the expected and actual number of samples. For each bin a probability that the random variable gets a value of *k-th* bin is assessed. It performs N experiments and it determines how many values of the experiments originate from the defined bins. The frequencies of these bins are marked as X_1, X_2, ... X_k. After that, the expected frequencies in individual bin parts are compared with the frequencies obtained from the tested RNG. χ^2 value is computed by Equation 3.7.

$$\chi^2 = \sum_{i=1}^{k} \frac{(X_i - N_{p_i})^2}{N_{p_i}} \tag{3.7}$$

If a random tested variable X generated by the RNG has a predicted distribution, χ^2 has approximately chi-square distribution. Then, the value of χ^2 is compared with the critical value of the appropriate chi-quadrate distribution on the required significance level. Thus, χ^2 test derives a single number representing a correspondence of the expected and actual distribution, Zvára and Štěpán (2006).

3.10 Used Software

This chapter introduces used software, frameworks, and libraries. History of the SAC-SMA development and implementation is described in Section 3.10.1. The legacy software was reimplemented to Java platform since it was attached to an optimisation framework, also written in Java. The optimisation framework Jenes is introduced in Section 3.10.2.

3.10.1 Hydrological Software

Currently, software for hydrological models such as SAC-SMA, SNOW-17, and UNIT-HG are managed and developed by the Hydrologic Research Laboratory, National Weather Service (NWS), National Oceanic Atmospheric Administration (NOAA). The rainfall-runoff models have gone through long and interesting development. The first version of the SAC-SMA model was developed at Stanford University in the USA under the name Stanford Watershed Model. The model was a product of professional needs of Ray Linsley and Norman Crawford.

NOAA had taken over the legacy model including its software and they have started their own development with the guidance of professor R.J.C. Burnash. However, several developers from Stanford University were in professor Burnash's development team. The first use of the upgraded model was applied at the catchment of the Sacramento River; hence the name of the current model is **Sac**ramento **S**oil **M**oisture **A**ccounting. Burnash *et al.* created a model structure for solving tasks in the rainfall-runoff evaluation processes that is more flexible and more generally applicable than the previous version. In NOAA, the lead developer is Eric Anderson who updated the legacy software for newly designed model structures. The software was written in FORTRAN language. The SAC-SMA model has also become a full-fledged alternative to the Japanese TANK model which is simpler, Crawford and Burges (2004).

The NOAA conference in 1983 convinced the Czech representatives of the Institute of Hydrodynamics AS CR that the SAC-SMA model can be implemented at Czech watersheds and geographic conditions. Documentation including software of the SAC-SMA model was provided to the institute. The software was revived on the EC1030 mainframe, made in the USSR at that time. With the onset of personal competitors the software was converted to PC format in 1986. The benefits of the PC version need not be mentioned explicitly. In the subsequent years, the SAC-SMA model was integrated into Aqualog system used by the Czech Hydrometeorological Institute (CHI). The Aqualog applies the SAC-SMA to various simulations of water regime and simulations of the impact of expected climate changes on water resources.

Reimplementation to modern platforms

The legacy software of the SAC-SMA model written in FORTRAN was reimplemented to Java platform using reverse-engineering. The main reason for the reimplementation is easier maintenance and the possibility of software expanding. Moreover, model platforms can be connected with other supporting frameworks as optimisation, parallel processing, graphic representation, etc.

3.10.2 Genetic Algorithm Framework

Jenes 2.0 is an open source library for problem optimisation using *genetic algorithms* in Java. The library has been developed by the Intelligent Systems Engineering Lab (CISELab) at University of Sannio. According toTroiano *et al.* (2013), the main features of the library are the following:

Modular and highly reconfigurable

The framework is a component designed tool with stages. The GA population passes through the components and stages. The population is input for each component, which transforms it into the next population. All parts of the framework are compatible, so the structure of the optimisation workflow can be arranged accordingly to meet the problem characteristic and user needs. Framework user can design and assemble his own walk-through and structure of the algorithm; e.g. GA operators, crossover method, reproduction, etc.

Architecture and memory

Population evolution requires a lot of objects to be present in computer memory. Jenes framework recycles already created objects continuously. This approach prevents the overhead of the garbage collection in Java virtual machine, which is crucial for algorithm efficiency. It follows that all necessary objects are created at the start of the algorithm, when the memory occupation increases and no object is created during the GA evaluation. The framework works on a level of single bits if the bitwise chromosome is used, which accelerates the computation.

Strong type checking

Data types of the Jenes framework are strongly typed so that all used data structures, e.g. chromosome, fitness function, genes, etc., can only work with the compatible types. It reduces runtime checks because parametric or generic classes are checked during compilation time which uses only the right data types. Hence, the runtime casting of the used objects is not needed. Therefore, the framework has better speed and accuracy.

4

Sacramento Optimisation Framework

In previous Chapter 3, we introduced the used hydrological models and the software framework. This chapter describes the implementation details of the Sacramento model including the optimisation framework. We focus on input and output data of the *Sacramento* and *genetic algorithm* components, as Figure 3.9 illustrates. This chapter summarises our approaches.

4.1 Implementation of the Sacramento model

In this chapter, we introduce the components of the Sacramento model illustrated in Figure 3.9. The workflow of the Sacramento model is described in Section 3.6.

Input data

The input data of the Sacramento model are *date*, *precipitation*, *temperature*, observed *flow*, and *evapotranspiration* in the following form:

```
dd.mm.yyyy      F.4     F.4     F.4    [F.4]
dd.mm.yyyy      F.4     F.4     F.4    [F.4]
                        …
dd.mm.yyyy      F.4     F.4     F.4    [F.4]
```

where F.4 is a real number with an accuracy of 4 decimal places. The last column is applicable only if evapotranspiration data are available. Otherwise, evapotranspiration is specified by 12 values (see Section 3.5).

Input parameters

Input parameters are in the form of INI file[1)] in the following structure:

```
[sacramento]
tile = Raztoka 1953-2011
from = 1.1.1953
to = 31.12.2011

[snow17]
card1 = ELEV; ALAT
card2 = ITPX; PXADJ
card3 = IDT;  TAELEV; TALMAX; TALMIN
card4 = SCF;  MFMAX;  MFMIN;  UADJ;   SI
card5 = NMF;  TIPM;   MBASE;  PXTEMP; PLWHC;  DAYGM
adc = ADC01; ADC02; ADC03; ADC04; ADC05; ADC06; ADC07; ADC08; ADC09

[sacsma]
card1 = PXADJ; PEADJ; UZTWM; UZFWM; UZK;   PCTIM; ADIMP; RIVA;  IOPTET; EFC
card2 = ZPERC; REXP;  LZTWM; LZFSM; LZFPM; LZSK;  LZPK;  PFREE; RSERV;  SIDE
card3 = UZTWC; UZFWC; LZTWC; LZFSC; LZFPC; ADIMC
et = etTs | et12
etTs = 12 values as adjustment coefficient for each month
et12 = 12 values as estimation of monthly evapotranspiration
etGauss = σ; μ; m; a

[unithg]
card1 = BASE; AREA
uhg = ordinates of unit hydrograph
```

The `[sacramento]` section defines information about modelled basin; it characterises the title of the project, especially date interval which delimits the time period of the simulation. This enables the setting of the simulated period within one input data file without modification. Sections `[snow17]`, `[sacsma]`, and `[unithg]` determine the relevant model parameters described in Tables 3.1 and 3.2.

Properties *et, etTS, and et12* in section `[sacsma]` describe the manner how evapotranspiration values are processed. *etTS* (ET time series) specifies that evapotranspiration data are available for each day in the form of time series (last column of *Input data*). *et12* means that 12 discrete values define the values determining the expected evapotranspiration for each month, see Section 3.5. Model user can set the manner of ET definition via *et* property in the section `[sacsma]`.

Output data

There are two kinds of model output. The first form is a simple text file containing the data of all used models, see sections of model output in Section 3.5. The file can be easily imported into a Spreadsheet. The second one is a graphical output illustrating differences between observed and simulated discharges.

1) The INI file format is a standard form for configuration files. INI file is simple text file contains a structure composed of defined sections, properties, and values.

The graphical output is in HTML form which can be opened in almost all web browsers. Among other things, the HTML form illustrates monthly and yearly evapotranspiration sums. Figure 4.1 shows an example of HTML output. The advantage of HTML output is a user-friendly interface since it easily enables to zoom to a specific area of a simulated period which allows a quick and efficient interactive modelling. The interactive chart supports logarithmic and linear scale. Logarithmic scale is a powerful tool for depth investigation of the differences.

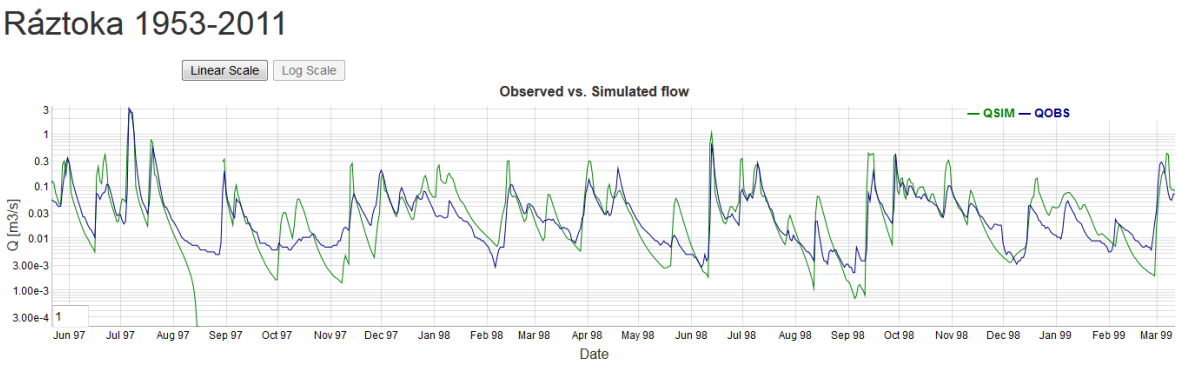

Figure 4.1: HTML output of the Sacramento model

Another output is statistical information about the simulation. The first part includes statistical data on the whole simulated period. Values of statistical indicators are computed using the Equations 3.1-3.4. Table 4.1 introduces all used indicators which are based on Equations 3.1-3.4 and their values determine the simulation quality.

Table 4.1: Statistical indicators of the Sacramento model

Global indicator		**Monthly indicator**
acronym	***description***	
drmse	Daily RMS error	Simulated mean runoff
dabe	Daily AVG ABS error	Observed mean runoff
aamve	AVG ABS Monthly vol error	Percentage bias
mvrmse	Monthly volume RMS error	Monthly bias
correlation	Correlation Coefficient	Percentage average absolute error
nash	Nash-Sutcliffe coefficient	
mbae	Monthly ABS volume error	

The second part of the statistical output is statistical information about monthly sums in column 3 of Table 4.1. The indicators applied to the whole simulated period are mentioned in column 2 of Table 4.1.

Appendix A illustrates the examples of input data, model parameters, and statistical information.

4.2 Implementation of the GA Optimisation Framework

This chapter describes the genetic algorithm component of Figure 3.9.

The workflow of the GA is described in Chapter 3.8.4. The GA parameters are defined in `[optimisation]` section in the INI file with the following structure:

```
[optimisation]
OptimCriterion = mvrmse
Generator = hrng | prng
PopulationSize = 175
GenerationLimit = 400
```

OptimCriterion defines which fitness function is used as the optimisation criterion. *OptimCriterion* property can take values listed in the *acronym* column of Table 4.1. *Generator* property specifies the type of the RNG used in the GA. It can take two values: *hrng* (see Section 5) and *prng* (Mersenne Twister Generator, see Section 3.9.1). *PopulationSize* and *GenerationLimit* are properties that represent the main GA parameters (see Section 3.8.2).

The rest of the GA parameters (see Table 3.3) are embedded into the software. Therefore, the framework user cannot change their values. The user is shielded from the GA parameters, which have minor impact on optimisation quality. It should simplify the usability of the framework.

Optimisation input

Initial model calibration is one of the GA inputs whose form is the same as the input parameter of the Sacramento model. This initial model calibration is the baseline for estimate model parameters using the MCS. This estimation requires percentage ranges for each model parameter which is next to the optimisation input. This input has the same form as the Sacramento parameter input except that instead of parameter values there are peregrinate ranges for each model parameter (see Appendix A).

Optimisation output

The main GA output is an optimal model calibration in the same form as the input model calibration mentioned in Section 4.1. The rest of the GA output is equal to the Sacramento model output where the simulation is performed with the optimal model calibration.

Statistical information about the simulation is expanded by a set of statistical information of the GA optimisation; e.g. total optimisation time, number of valid and invalid individuals. Another set of information is values of the highest, lowest, and deviations of the fitness function value.

5

Hydro-Random Number Generator

As was mentioned several times, the random number generator (RNG) is the core of the *genetic algorithm* (GA) and the quality of the RNG is crucial for a successful optimisation. This chapter brings a detailed overview of our approach on how to improve the Mersenne Twister Generator (MTR) to achieve the optimal model configuration of the Sacramento model. We summarise an architecture of a new PRNG operating on the principle of hydrological data with normal distribution of generated numbers. We call this new random number generator the Hydro-Random Number Generator (HRNG).

The periodicity and the influence of the seed variable are discussed in Section 5.1. It specifies the contribution of hydrological information as a good source of random data. Section 5.2 introduces a variability of an interval in which random numbers are generated. HRNG generates random numbers with a normal density of probability, see Section 5.3. The final Section 5.4 discusses the efficiency of the HRNG and its randomness validation.

5.1 Periodicity and Seed Variable

The periodicity is the only disadvantage of the PRNGs which is a consequence of the finite space of computer memory. Simulation of the Sacramento model requires up to hundreds of random numbers. Naturally, a probability of the periodicity increases with the number of optimised parameters. The Mersenne Twister Generator (MTG) is based on the Linear Congruential Generators, its principle is illustrated by Equation 3.6. The example in Section 3.9.1 demonstrates that this RNG has the periodicity. Logically, the example is very simple and

is only for periodicity demonstration but this fact is applicable even for real problem instances with bigger numbers.

Periodicity of PRNG

The TRNG makes use of natural processes which can be mapped to a numerical value. This value is usually used as the seed variable in the process of generating random numbers. So, we can say that numbers generated in this way are truly random. The randomness of the PRNGs is generally dependent on the seed variable. The PC system clock often initiates a value of the seed variable. However, the PC clock is not a good source of random numbers. Moreover, each HW manufacturer has a different architecture influencing the quality of the RNGs, Fischer and Drutarovsky (2002). In several applications, the seed value is determined by programmes and the value is often embedded into software, which is not the right way to increase the RNG effectiveness.

For reasons mentioned above, we want to use a new method that initiates and maintains the seed variable for the Sacramento optimisation.

Value of seed variable

Based on a theory by Lyon (2013), who defines randomness as a fundamental feature of nature that has a normal distribution, we find data with normal distribution in the hydrology field and we use them to generate random numbers based on natural events.

Hydrological input data of the Sacramento model are an excellent source of random numbers but not in its raw form. However, hydro data can inject interesting features of randomness into the PRNGs. We have found natural data which show normal distribution. Input data for the Sacramento model are *precipitation*, *temperature* and *observed runoff*. Figure 5.1 demonstrates courses of the input data. It is evident that *temperature* has approximately periodical normal distribution. Data were being collected from the Ráztoka basin for a period 1959-1965. Although the hydrological data show an asymptotic periodicity, there is no distinctive sequence of numbers being repeated. This fact has been tested in the 100-year long series on the Elbe catchment.

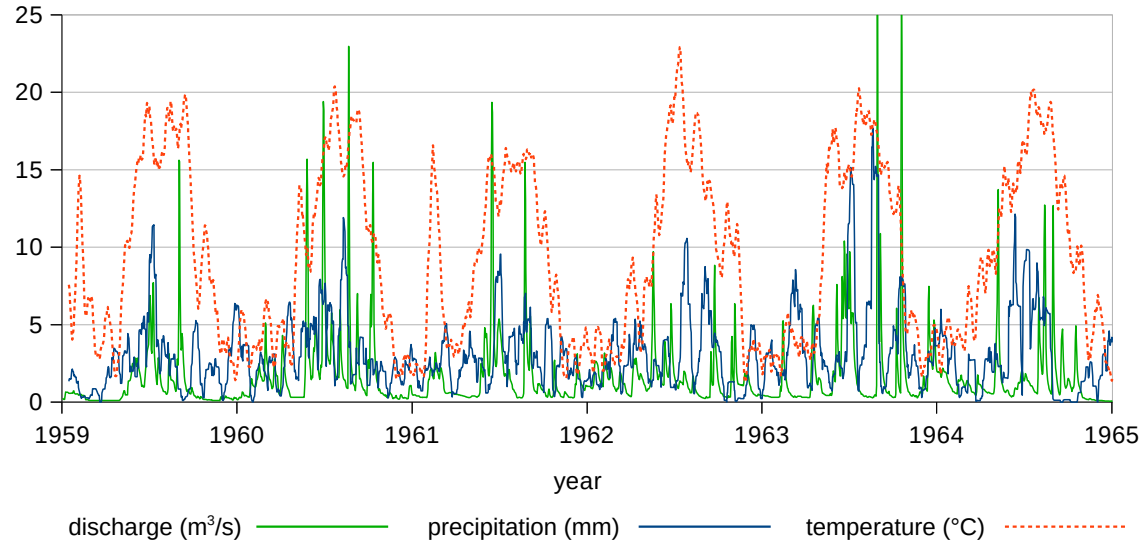

Figure 5.1: Six-year course of hydrological data of Ráztoka basin

The curve of *temperature* oscillates relatively dramatically. Therefore, we smooth it using a simple operation which adds *temperature* and *precipitation* values.

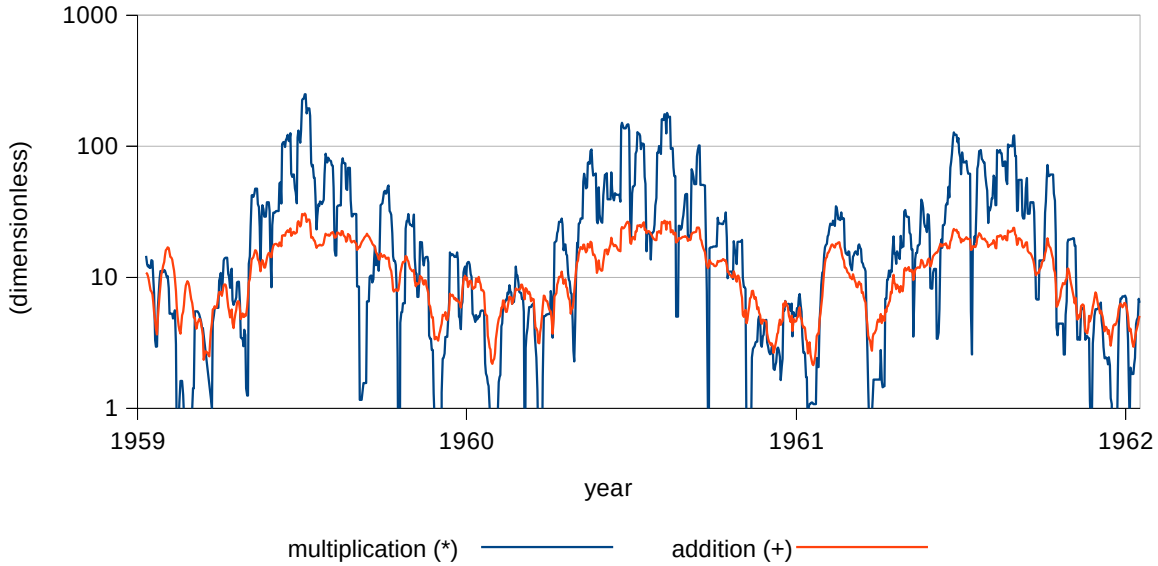

Figure 5.2: Course of the temperature and precipitation data while using addition and multiplication operations

Let function *f(t)* be defined accordingly:

$$f(t) = P_t + T_t \tag{5.1}$$

where t is the observed day and P_t/T_t is the observed *precipitation*/*temperature* of the day t.

If we use *f(t)* to add *precipitation* and *temperature*, the resulting course of *f(t)* is smoother than the individual curves of *precipitation* and *temperature*. Figure 5.2 illustrates that addition operation is more efficient than a multiplication operation, since it creates a smoother course.

As a result, we use the function *f(t)* for determining the seed variable because its functional values are based on natural events.

The following text deals with an integration of *f(t)* into the algorithm of the MTG. We have updated the MTG as follows. Each requirement for a random number updates the buffer B which means that each random number requires a buffer recalculation using the Functions 3.2 and 3.3. Although the buffer update prolongs the computation time, the randomness of generated numbers is increased. From the point of view of the implementation each request invokes Functions 3.2 and 3.3. However, the index determining which item of the buffer B will be pulled next is not reset. Therefore, the buffer B must always be updated.

We try to test the example mentioned in Section 3.9.1 again, where the Linear Congruential Generators (LCG) is described. This illustration is extended by *f(t)* and the results indicate that the function increases the randomness of generated numbers. We use the same variable values as in the previous example, so let $m = 11$, a $= 3$, $c = 4$, $X_0 = 8$. Further, let vector $S = (8, 7, 7, 6, 5, 4, 3, 3, 3, 2, 2, 2, 2, 2, 2, 3)$ be derived from the observed *temperature*, then *f(n)* returns the items of the vector S cyclically.

$$X_n = (a\, f(n)\, X_{n-1} + c) \mod m \tag{5.2}$$

The series obtained by using Equation 5.2 is as follows: 9, 6, 9, 1, 8, 1, 2, 0, 4, 6, 7, 2, 5, 1, 10, 6, ...

It is evident that this sequence has no periodicity, although the vector S is not random. Both examples are very simple illustrations of the LCG, which is a base for most PRNGs. However, the examples clarify the principle of complex PRNGs, like the MTG. Moreover, these examples support the view that additional natural based data can influence the randomness of the RNGs.

Values of p*recipitation* and *temperature* for function *f(t)* are loaded from the input data of the Sacramento model, see Figure 3.5. A number of required random numbers within one optimisation is in the order of hundreds of thousands. Input data does not contain too many records so it is cyclically retrieved from the input file. Nevertheless, the data cyclicality does not affect the quality of the RNG due to the "tempering" and inner states of the MTG. More specifically, when input values of p*recipitation* and *temperature* (as a seed value) are repeated and their sum is used to generate a random number, then the value of the generated random number is with very high probability different from the same combination of p*recipitation* and *temperature* values. The reason is that the seed value goes through the states of the RNG and the bit operations change the final value of the generated number. Therefore, the probability that the states, constants, and inner variables of the RNG are the same as in the previous state with the same seed value is very low. Moreover, it is unlikely that the same states and the same seed value are used for generating the same model parameter as in the previous GA generation.

5.2 Interval of Generated Random Numbers

The HRNG should generate real random numbers in the interval *[0, 1)* since the Sacramento model uses real-value coding of individual chromosomes. Function 3.5 returns numbers in this range. However, model parameters are not only in *[0, 1)* interval. If a different interval is needed, a simple mapping described by Equation 5.3 projects this interval into another one.

$$g(l,u) = X(u-l) + l \tag{5.3}$$

Where X is a random number of the HRNG in the interval *[0, 1)* and l/u is the upper/lower limit of the required range.

5.3 Distribution

The change of the MTG internal logic using *f(t)* (Equation 5.1) can influence a distribution function of generated numbers. The original architecture of the MTG has been designed with a uniform distribution whose random values have the same probability.

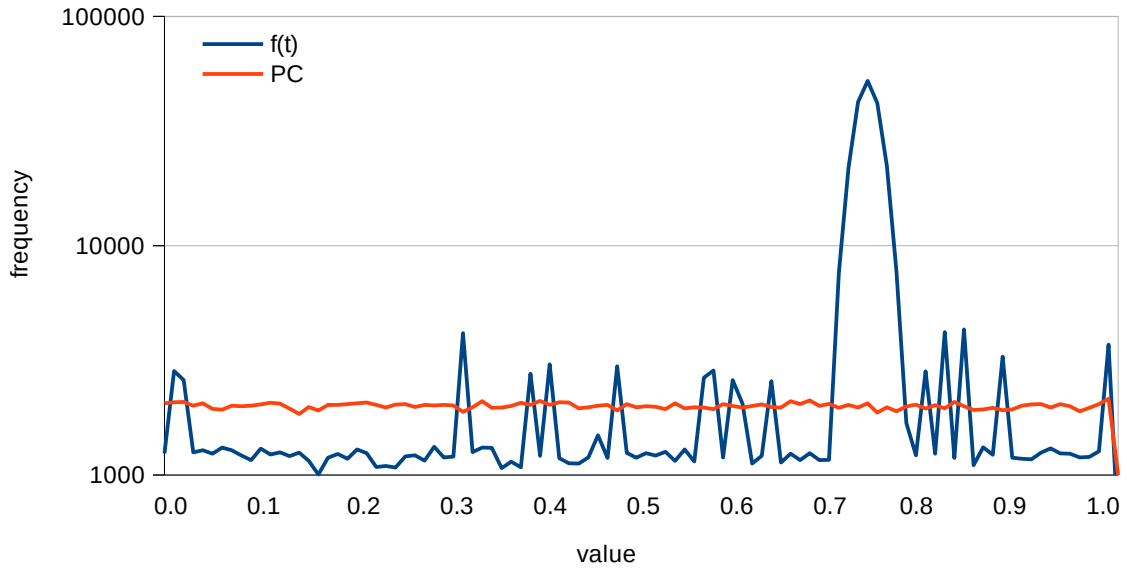

Figure 5.3: Probability distribution of the MTG when the system clock or Equation 5.1 initiates the seed variable

The change of the MTG distribution function is illustrated by Figure 5.3. The original design of the seed variable has shown that the distribution function is ideally uniform in interval *[0,1)*. If the seed variable is determined by *f(t)*, the distribution is only asymptotically uniform, except for interval *(0.7, 0.8)* where the significant peak occurs. The distribution of Equation 5.1 has an asymptotic Gaussian shape with variance σ^2=0.015 and mean μ=0.735.

We follow the Lyon's (2013) theory that natural processes have normal distribution. The HRNG will be used for simulation of the rainfall-runoff processes. Therefore, the HRNG should have normal distribution because the optimisation of the Sacramento model is an optimisation of natural systems. The parameters of normal distribution for the HRNG are derived from Lyon (2013); namely variance σ^2=1.3 and mean μ=0.5. The next step is to transform the distribution of *f(t)* into the required distribution.

The Box-Muller transformation is a method for number sampling which generates pairs of independent normally distributed numbers. The source of the numbers, which are transformed, is a uniformly distributed RNG. The method takes two random numbers form a uniformly distributed RNG and maps them into two numbers which are normally distributed. The method uses sinus and cosine functions, which derivate two coordinates of the new normally distributed number using the two-dimensional Cartesian system, Box and Muller (1958).

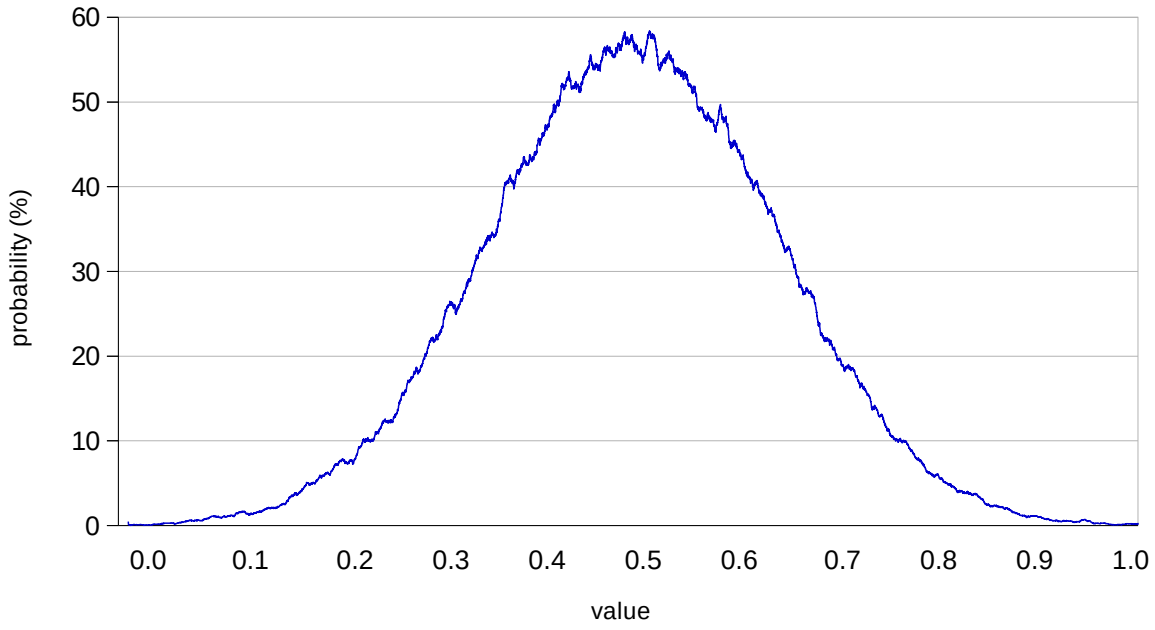

Figure 5.4: Final distribution of HRNG after the Box-Muller transformation

Figure 5.4 demonstrates the final result of the Box-Muller transformation where the distribution of *f(x)* is spread out; namely the interval *(0.7–0.8)* of Figure 5.3. The final distribution shows a slight fluctuation over the entire interval compared to the ideal Gaussian distribution. This phenomenon is caused by the HRNG which is not an ideal RNG but this is a consequence of using real random numbers as input data. However, the HRNG has a normal distribution with the required parameters.

5.4 Validation and Efficiency

The asymptotic complexity is *O(1)* because the HRNG is based on the Mersenne Twister Generator (MTG) and the Box-Muller transformation. Both methods are also *O(1)* but contain a large hidden constant. In absolute value, the speed of the MTG is approximately 25 Mreq/s and that of the HRNG is 7 Mreq/s, where req/s is the number of random numbers per second. The time ratio between the MTG and HRNG is approximately 3.5. However, the optimisation time using the HRNG is in minutes which is admissible.

The following results prove that the HRNG has a normal distribution with parameters $\sigma^2 = 1.3$ and mean $\mu = 0.5$. Figure 5.4 represents the probable density in the interval *(0, 1)* for 100,000 random numbers from the HRNG. It is clear that the HRNG has approximately normal distribution except mild fluctuations, mainly on the top of the curve. The results of a χ^2 test with the 95% significance level demonstrate that the parameters of a normal distribution correspond with the distribution of the HRNG. Let the hypothesis H be that the samples are normally distributed if the *p-value* is less than 0.05, Resende and Costa (1998). The *p-value* of the test was calculated for 10^8 samples and 100 bins in the interval *(0, 1)*. The *p-value* is 0.5486 which proves that the HRNG is indeed normally distributed.

The last validation tests are the Diehard tests (see Section 3.9.2), which were performed on a dataset containing 3.10^7 random numbers from the HRNG. Table 5.1 gives the performance evaluation of the Diehard tests. The table compares both RNGs and shows average *p-values* of these tests. It reveals that the HRNG meets the requirements for randomness because the average *p-value* of the HRNG is 0.51.

Table 5.1: Results of Diehard tests

RNG	**Birthdays**	**Permutations**	**Binary Rank**	**Minimum Distance**	**DNA**	**Average**
MTG	0.956	0.703	0.821	0.584	0.120	**0.64**
HRNG	0.182	0.406	0.868	0.930	0.182	**0.51**

6

Evapotranspiration and UNIT-HG using Continuous Function

Evapotranspiration (ET) and Unit Hydrograph (UNIT-HG) in the Sacramento model is defined by a set of coordinates specifying an appropriate mathematical function. The disadvantage of this approach is that functions are described by discrete values which are independent of each other. However, the functions of the ET and UNIT-HG are continuous, and their function values are in correlation. Typically, the course of the UNIT-HG is similar to the Poisson distribution so that the maximum value cannot be at the end of the distribution. Analogically, ET has an asymptotic Gaussian distribution.

The GA optimises the coordinates of the ET and UNIT-HG functions separately and does not take into account the correlation between the coordinates. Therefore, if the GA user sets ranges of the coordinates inappropriately, the optimisation result of the ET or UNIT-HG may have an unrealistic course with an acceptable model validation.

As a result, our approach takes into account the correlation between coordinates of discrete model parameters, which are represented via continuous functions. We have identified two continuous functions for defining the ET and UNIT-HG. The following sections introduce their application and optimisation in the Sacramento model.

6.1 Evapotranspiration

We estimate the shape of the evapotranspiration course by using the Gaussian curve and its parameter from long-term observations and principles of annual weather cycle. A real ET shape is not distributed that ideally. The real shape varies for each observed period, basin, water regime, weather, and vegetation

conditions (*temperature* influences water consumption and thereby ET). The typical shape of ET is illustrated in Figure 6.1. It is evident that ET is highest in warm months, compared to being at its lowest during winter months. This phenomenon is caused by the growing season (ca. April – September).

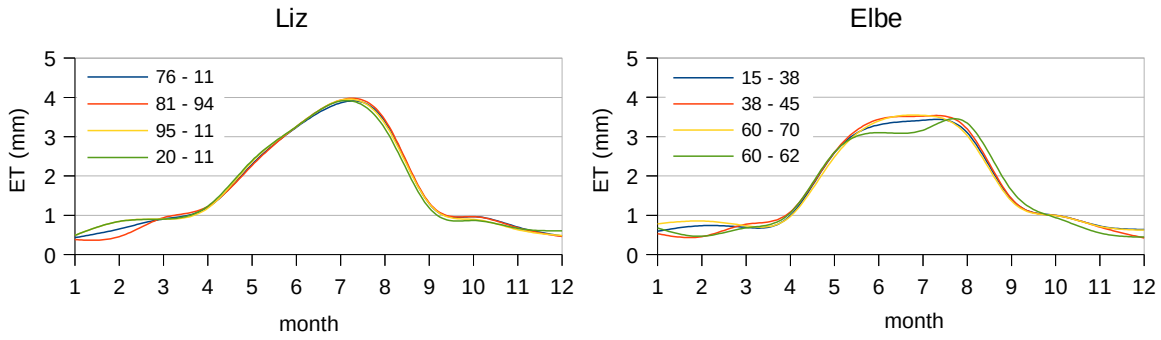

Figure 6.1: Evapotranspiration courses of Liz and Elbe catchments

Figure 6.1 also demonstrates the fact that each period has a slightly different shape; however, the shape is asymptotically Gaussian.

The Sacramento model defines ET using 12 discrete values. Each value specifies average ET value of a certain month, see Appendix A: section `[sacsma]` and key *et12*. The Sacramento model iterates in one day period, therefore the ET values for each day are computed using linear interpolation which interpolates the required value from the 12 discreet model parameters as follows:

$$ET(m,d) = ET_m + d\frac{ET_{m+1} - ET_m}{f(m)} \tag{6.1}$$

where m is month and d is a day for which the ET value is computed, $f(m)$ returns a number of days of the month m.

Figure 6.2 shows final interpolation of 12 discrete values using Equation 6.1. There are evident interpolation sections between individual months which are caused by the interpolation Equation 6.1. On the other hand, the Gaussian function has a smoother course.

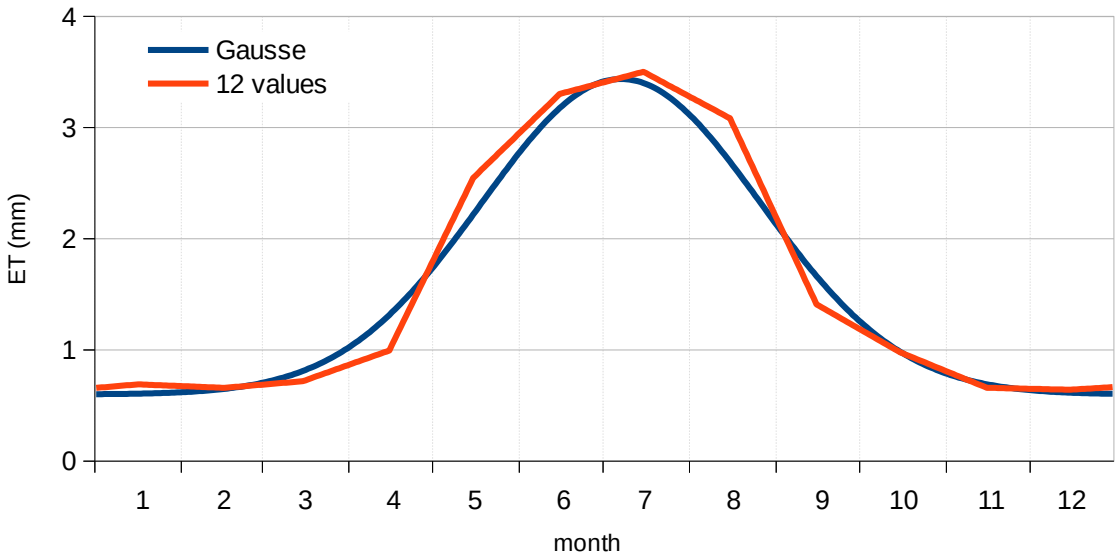

Figure 6.2: Evapotranspiration defined by Gaussian function and the 12 values

In Figure 6.2, it can be seen that the Gaussian function best copies the course of evapotranspiration. The function is defined as follows:

$$f_g(x) = \frac{1}{\sigma\sqrt{2\pi}} e^{\frac{-(x-\mu)^2}{2\sigma^2}} \tag{6.2}$$

where σ is a standard deviation with variance σ^2, μ is a mean value.

Function $f_g(x)$ is generally defined in interval $(-\infty, \infty)$, but for Sacramento objectives it is necessary to map the interval into interval (1, 2, ..., 365) as a range of x values; i.e. values 1...31 represent January, 32...60 represent February, etc. Therefore, this mapped function returns the ET values for each day of the year, more precisely the annual cycle. Function values of $f_g(x)$ must be adjusted for the purpose of the Sacramento model since ET values are in the order of units. Another variable m is an adjusting factor which multiples values of $f_g(x)$ using m values. It enables function values to shift into desired values. Another constant is an addition constant a which adds a constant value to the function values of $f_g(x)$. The addition constant implements phenomena that ET is not equal to zero in warm months; more precisely at the tails of $f_g(x)$.

Hence, the final function used in the Sacramento model for derivate ET value for each day is as follows:

$$f_{ET}(x) = a + m \frac{1}{\sigma\sqrt{2\pi}} e^{\frac{-(x-\mu)^2}{2\sigma^2}} \tag{6.3}$$

where a is addition constant, and m is multiplication constant. Model user can easily define ET using Equation 6.3.

Regarding the legacy implementation of the SAC-SMA model, we have replaced the code implementing Equation 6.1 by code which implements Equation 6.3. Therefore, the implementation process was very simple and with minimal impact on the whole model implementation. This process has a few advantages. Primarily, the ET parameter is now defined via 4 instead of 12 parameters, so the optimising problem is reduced by 8 parameters. It means that the optimisation time can be reduced as well. Another advantage is the continuity of the ET parameter, since the 4 ET parameters are in correlation and their individual optimisation estimates the ET curve as a whole and without significant deformation of the ET shape.

The new ET parameter definition is simply defined in the parameter file of the Sacramento model. The INI file has been extended by a further property of *etGauss* which contains variables from Equation 6.3, see the flowing structure:

```
[sacsma]
et = etTs | et12 | etGauss
etGauss = σ; μ; m; a
```

A model user can quickly convert the 4 parameters of *etGauss* into 12 original values using Equation 6.3.

6.2 UNIT-HG

The Unit hydrograph is very similar to the evapotranspiration from the optimisation point of view. It means that the UNIT-HG is defined as a set of real discrete values but the points of UNIT-HG are in correlation. For UNIT-HG, we have used the same principle of optimisation as in the previous Section 6.1.

In Section 3.5.2, we illustrated that the shape of UNIT-HG is approximately similarly distributed by Equation 6.4, like the *Poisson distribution:*

$$P(X=x)=\frac{\lambda^x}{x!}e^{-\lambda} \tag{6.4}$$

where x are all values of the random variable X, λ is a diffusion parameter.

The diffusion parameter λ describes a phenomenon of an observed event, which is represented by variable X. The UNIT-HG is characterized by the *Translation Diffusion Equation* (TDE) based on Equation 6.4. The TDE is applicable as a transformation procedure in the rainfall-runoff process as well as simulation of water movement in various catchments. TDE is defined as follows:

$$f_d(t)=\frac{1}{4\pi K}\frac{D}{\sqrt[3]{t}}\ e^{-\frac{(tC-D)^2}{t4K}} \tag{6.5}$$

where t is time (day), D is runoff length (km), C is velocity (km.h^{-1}), and K is diffusivity (km^{-2}h^{-1}).

Function $f_d(t)$ must also be adjusted to the purpose of the Sacramento model as well as $f_g(x)$. Therefore, the final function used in the Sacramento model for UNIT-HG is as follows:

$$f_{UH}(t)=a+m\frac{1}{4\pi K}\frac{D}{\sqrt[3]{t}}\ e^{-\frac{(tC-D)^2}{t4K}} \tag{6.6}$$

where a is addition constant and m is multiplication constant.

The UNIT-HG is defined by all parameters of the Equation 6.6; namely K, D, C, m, a. However, it is necessary that another parameter p specifies how many points from $f_{UH}(t)$ are derived. The parameter p determines for how many days the runoff is distributed to the river network (closure profile). Additionally, the p parameter defines the adjustment of the value range in the interval $[1..p]$. In short, p specifies how many functional values describe the UNIT-HG. In the context of the Sacramento model, p parameter is a cardinality of the set representing coordinates of the UNIT-HG, see Figure 3.4 for an example: $p=16$, codomain of $f_{UH}(t)$ is 1..p, and the set of coordinates $S = \{f_{UH}(1), f_{UH}(2), \ldots, f_{UH}(p)\}$ is used in this case. Figure 6.3 illustrates an example of two UNIT-HGs defined by $f_{UH}(t)$ for p parameter 16 and 5. There are two sets S_{16} and S_5 with the following items:

$S_{16}=\{10, 100, 97, 79, 56, 45, 36, 28, 22, 18, 14, 11, 8, 8, 4, 2\}$

$S_5=\{10, 63, 25, 10, 2\}$.

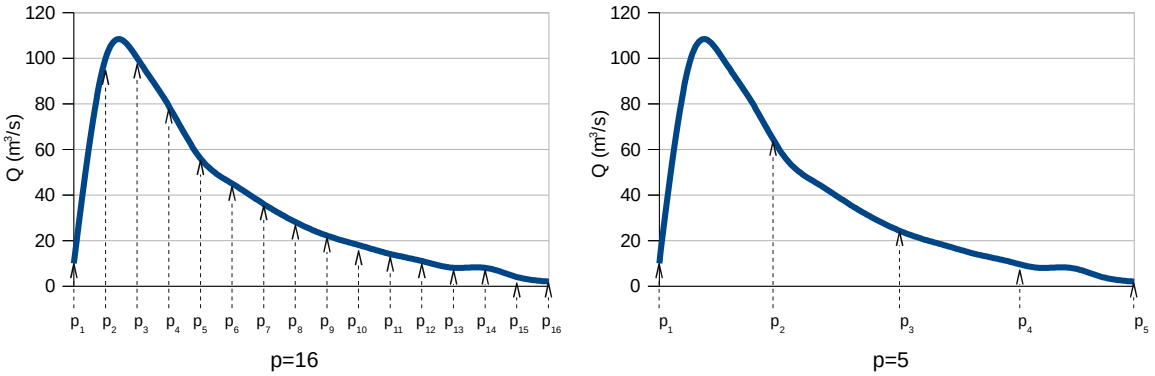

Figure 6.3: UNIT-HG defined by diffusion Equation 6.6 for p = 16 and 5

Generally, Sacramento modellers are able to properly define the shape of the UNIT-HG using the parameters of $f_{UH}(t)$ including p parameter. However, there are certain pitfalls that can be the reason for a legal model validation, but the shape of the UNIT-HG is utterly unrealistic. More precisely, $f_{UH}(t)$ does not mirror the real description of the modelled catchment in spite of a proper model validation. The implication of this possibility is that the human factor is still necessary.

Suitability for the use of $f_{UH}(t)$ is vindicated by several facts. Primarily, an initial estimation of $f_{UH}(t)$ parameters is relatively easy if background materials about a modelled watershed are available, like the topography of river sections, a measured speed of runoff, retention points, etc. Fortunately, this information is available for most modelled terrains.

The new UNIT-HG parameters are defined in the parameter file. New property *uhgDiff* extends the section *unithg* in the INI file as follows:

```
[unithg]
uhg = uhgDiff | uhgTs
uhgDiff = p, K; D; C; m; a
uhgTs = c₁; c₂; … ; c₃
```

The model user can select which method for the UNIT-HG definition will be used. The option *uhgDiff* defines UNIT-HG using Equation 6.6 and the option *uhgTS* defines UNIT-HG as a time series of instantaneous discharges for each day.

This approach has a significant advantage since the p parameter can be easily optimised. Therefore, the optimisation process is quicker because the framework tries many model calibrations with a various number of UNIT-HG coordinates. In other words, the optimisation estimates how long the response of a catchment for given runoff and instantaneous discharge for given day are. Moreover, the UNIT-HG for

large basins can have dozens of coordinates so that the optimisation can be limited only to the optimisation of few parameters instead of dozens.

Implementation of this approach is not overly complicated. The original Sacramento model uses a double array which represents the set of UNIT-HG coordinates. The new implementation creates the same data structure, whose dimension is set by p parameters and their values are computed by applying Equation 6.6. Hence, the new implementation influences the model minimally.

6.3 Areal Depletion Curve

The area depletion curve (ADC) corresponds to a change in the actual snow-covered area that occurs after the snowfall. The user determines 11 ratios of the water equivalent (W) and the areal extent of the snow cover (A). ADC can be described as a non-declining function, so each value of the ADC must be greater than or equal to the previous value.

The course of the ADC does not resemble any continuous function with proper parameters and variations of the course. Therefore, we cannot use the principle of continuous definition as in the ET and UNIT-HG cases.

Parameters of ADC are defined using 9 discrete values. The two remaining values (0.05 and 1.0) are fixed, see Section 3.5.1. The GA optimises the parameters one by one, and the correlation between the individual parameters is not taken into account. This optimisation often breaks the condition of each value being greater than the previous one.

Function 6.1 illustrates an algorithm that fixes the ADC parameters according to the ADC condition. Lines 3 and 4 are given by the SNOW-17 model. Lines 6 to 12 iterate the ADC array items one by one. If the condition is not met, the array items are adjusted using averaging and linear interpolation. The ADC parameters can be easily fixed by using this approach with *O(1)* of time complexity.

Function 6.1 just adjusts the ADC parameters which are generated randomly. Therefore, our approach does not change the model workflow. However, the shape (estimated ADC parameters) of the ADC still needs to be inspected by an experienced modeller.

Function 6.1: correctADC(adc)

Input: adc - double array of incorrect ADC
Output: double array of fixed ADC
begin

```
1       x ← adc
2       l ← lenght(x)
3       x[1] = 0.05
4       x[l] = 1.00
5       avgADC = average(x)
6       for i ← 2 to l-1 do
7               x[i] = average(x[i-1], x[i], x[i+1])
8               if x[i] < x[x-1] then
9                       maxADC = max(x)
10                      x[i] = average(x[i-1], maxADC, avgADC)
11              end if
12      end for
13      return x
```

end

7

Study Areas and Data

Sudden rainfall and resulting runoff are typical for small catchments and are also one of the objects of this study. We focus on experimental watersheds Malá Ráztoka, located in the Beskydy Mountains, and Liz catchment, located in the Bohemian Forest (Šumava Mountains), both in the Czech Republic. Another objective is the Elbe River which is the representative for a large catchment.

7.1 Ráztoka Catchment

In Malá Ráztoka area the north-west winds capture the most atmospheric precipitation, which consequently falls with the highest intensity. The area of this catchment is P = 2.08 km^2. The basin elevation is around 840 m a.s.l, and the length of the watercourse is 2,000 m.

The length of the evaluated time series is usually significant and permits observing the influence of the evolution of the vegetation. The changes in vegetation cover affect the demands of evapotranspiration and consequently the complex long-term water regime process. Therefore, the modelling of a relatively long series is not an easy and simple task because the values of the influential model parameters of the basin change over time. There are daily time series of *precipitation*, air *temperature*, and runoff, which are used for the evaluation. The length of the time series is more than 50 years (1953–2011). The average precipitation is 1243 mm/year, and the average runoff is 923 mm/year. However, the observed data are usually burdened with errors, especially long time series because measuring devices have been replaced or upgraded during these long periods.

These additional circumstances contribute to a complicated model calibration of this area. The original area of the Ráztoka catchment was covered with beeches, and in the second half of the 1960s its parts were gradually renewed by spruce stands on more than 75% of the land. This change influenced the evapotranspira-

tion and consumption of the water which also affected the inputs for the rainfall-runoff simulations. Further, the ratio of the observed and simulated flows during floods in 1960, 1966 and 1997 exhibit evident long-term tendencies that are in agreement with the changes of the vegetation cover in the basin. These floods also contributed to the vegetation cover changes. Thus, the values of the model parameters have changed since these flood events, Buchtele and Tesar (2013).

7.2 Liz Catchment

The experimental catchment Liz is part of the southern Vimperk Highlands, which pass into the Šumava Mountains. This basin area represents fully forested watershed covered by mature forest, mainly spruce and beech. The catchment area is 0.99 km^2, and the average altitude is 941.5 m a.s.l. The mean annual runoff is 324 mm/year, annual precipitation is 840 mm/year, and annual temperature is 6.49 °C[2)]. Precipitation, air temperature, and water level, are continuously measured at the closure profile. The time series of hydrological data are available for the season 1976-2006.

Liz is inclined and its geological subsoil forms an impermeable bottom. Despite the soil cover, which is composed of several horizons with different water absorptions, the rainwater mainly leaks down the ground. The soil cover (acid brown soil - Cambisol) is also comprised of several soils with different hydraulic properties, but the infiltrated water mostly flows downwards through the ground. So, the surface and subsurface runoff sloping down is a rare phenomenon only in catastrophic rains, Buchtele *et al.* (2000).

7.3 Elbe River Basin

The Elbe River is one of Europe's largest rivers, springing in the Giant Mountains in the north of Bohemia. The Elbe River flows through Germany and enters the North Sea. The river is 1,094 km long, and its area is 148,268 km^2. In the Czech Republic, its length is 371 km, and the area is 49,933 km^2. The altitude of the river spring is 1,387 m a.s.l, and is located in the peat bog in Labská Louka (in proximity to the state border with Poland), Simon (2005).

Melting of the snow cover causes the highest water levels in spring. The water level descends in summer, but rainfall may cause a sudden rise in water levels during this warm period. The average water flow is 311 m^3/s at the closure profile

2) Values are determined for hydrological years 1976–2006

in the Czech Republic. The mean annual precipitation is 1.82 mm, and annual temperature is 7.56 °C[3)].

The time series of hydrological data are available for season 1895-2000. There were many hydrological, climatic, and vegetation changes during this period. Therefore, the optimisation of this watershed is a complicated issue.

3) Values are determined for hydrological years 1895–2000

8

Main Results and Discussion

This chapter presents the evaluation of the HRNG approach and discusses the achieved results across the informatics and hydrological fields. Sections 8.1 and 8.2 introduce the results of genetic algorithm aspects. Distribution of the randomly generated numbers is a major part of the results. In Section 8.3, we present experiments with the PRNG (uniform distribution) and HRNG (normal distribution) and dependence of the range value on the optimisation quality. The final simulation results of the Sacramento model are introduced in Section 8.4. We analyse the results obtained using the PRNG and HRNG, and we discuss the comparison of observed/simulated discharge and evapotranspiration estimation. The last Section 8.5 shows results of the approaches that apply the continuous functions for defining the UNIT-HG and evapotranspiration.

8.1 Fitness Function Selection

The crucial aspect of the optimisation is the selection of the fitness function. The optimal GA parameter configuration is shown in column 4 of Table 3.3. Several fitness functions were applied and Table 8.1 summarises their results. In this table, there are 8 statistical indicators and 5 fitness functions, all derived from Equations 3.1-3.4. At first, RMSE, R, NASH, and BIAS, were evaluated. If R is used as a fitness function, its value is near 0.90 but other statistical indicators are unsatisfactory. However, RMSE as a fitness function results in low values of most statistical indicators except the Correlation Coefficient. This fitness function seems to be a good choice but the Monthly volume RMSE is still too big.

Table 8.1: Testing of statistical indicators for various fitness functions

Statistic indicator	RMSE	R	NASH	BIAS	MVRMSE
AVG ABS Monthly volume error (mm)	7.087	44.36	12.408	11.401	**0.017**
Monthly volume RMSE (mm)	32.221	160.776	51.453	46.251	**0.073**
Correlation Coefficient (–)	0.8851	**0.8939**	0.8763	0.8708	0.8281
Nash-Sutcliffe coefficient (–)	0.7329	0.6583	**0.7613**	0.7437	0.6652
Monthly ABS volume error (mm)	40.037	250.605	70.0946	64.4091	**0.0946**
RMSE (mm)	**0.0411**	0.0513	0.0429	0.0444	0.0508
Percentage bias (%)	-6.311	-44.36	-11.863	-11.099	**-0.001**
Monthly bias (mm)	-35.65	-250.61	-67.017	-62.703	**-0.005**
Number of the best cases	1	1	1	0	**5**

Consequently, another fitness function derived from RMSE (Equation 3.1) was constructed. This fitness function reflects the high monthly volume RMS error. The new fitness function: monthly volume RMSE (MVRMSE) is

$$MVRMSE = \sqrt{\frac{1}{n}\sum_{i=1}^{n}\frac{1}{30}\left(MQ_i - MS_i\right)^2} \tag{8.1}$$

where MQ is the observed monthly discharge, MS is the simulated monthly discharge, and n is the number of monthly events.

The last column of Table 8.1 shows the results of the testing period. The column indicates that the MVRMSE as a fitness function produces the best results in comparison with other used fitness functions. In particular, the MVRMSE fitness function provides better results in 5 cases of the used statistical indicators. On the other hand, the Correlation Coefficient and the Nash–Sutcliffe coefficient report a slight degradation in quality but not by order of magnitude. A consequence of MQ is that extreme fluctuations of observed flows are averaged within the month. Because of this, the GA does not respond flexibly to those fluctuations caused by floods which can confuse the algorithm. Due to this fact, the MVRMSE has been selected as the fitness function for the optimising of the Sacramento model for the Ráztoka catchment.

When compared, these results suggest that there is an association between the fitness function and simulated watershed. Moreover, the length of the time period of the simulation of the basin is also a significant association aspect. There is no universal procedure how to determine the fitness function yet. It is still necessary

to perform an analysis determining which fitness function is optimal for given basin and even time period. For instance, the MVRMSE is the optimal fitness function for the Ráztoka catchment, while the AAMVE (see Table 4.1) is the optimal fitness function for the Elbe basin but only for long time periods. There are some instances of simulations which require multiple optimisations with several kinds of fitness functions.

A similar statistical analysis as in the case of Ráztoka basin was used for the selection of the fitness function for the Elbe River as was the long period from 1905 to 1970.

Table 8.2: Statistical indicators for the Elbe River with a sequential optimisation using different fitness functions

Statistic indicator	**Initial**	**MVRMSE**	**AAMVE**
AVG ABS Monthly vol error (mm)	6.692	**1.233**	1.99
Monthly volume RMS error (mm)	61.992	**14.333**	23.733
Correlation Coefficient (–)	0.840	0.789	**0.856**
Nash–Sutcliffe coefficient (–)	0.695	0.607	**0.732**
Monthly ABS volume error (mm)	70.925	**13.066**	21.087
RMSE (mm)	9.611	10.087	**9.327**
Daily AVG ABS error (mm)	92.362	101.752	**86.995**
Percentage bias (%)	-6.086	**0.078**	0.279
Monthly bias (mm)	-64.503	**0.826**	2.962
Number of the best cases		**5**	4

However, Table 8.2 shows an example that a sequential optimisation with a different fitness function can provide interesting results. The initial calibration has been derived from previous experiments, Chlumecky *et al.* (2014). We select the MVRMSE as the fitness function for the first optimisation run. The results (column 3) indicate an interesting improvement beside the initial calibration. There are low decreases of some indicators with minimal impact to the model output quality. The optimisation output of the first run was used as an input for the next optimisation run but with the AAMVE (AVG ABS Monthly volume error) fitness function. In comparison with the MVRMSE, the AAMVE has only 4 best cases of statistical indicators but the model output shows better results. The second optimisation run primarily improved the Correlation and Nash-Sutcliffe coefficients, so the course of simulated and optimised discharges is more

similar. It is apparent from the table that the selected fitness function does not guarantee that statistical indicator reflecting the selected fitness function provides the best value. Specifically, if MVRMSE is selected as the fitness function, the value of AAMVE is 1.233. By contrast, the value of AAMVE is 1.99 for AAMVE as the fitness function.

8.2 Optimisation using HRNG

This section describes results of the Sacramento optimisation from the point of view of the GA. In this section, we discuss the results of the sensitivity analysis of the GA parameters, optimisation speed, and other observations. Observed results have been obtained using the PRNG based on the Mersenne Twister generator and the newly presented HRNG. Ráztoka was selected as a simulated catchment for this section and the modelled period was 10 years (1953-1963). The optimisation quality is measured by the MVRMSE fitness function.

8.2.1 Sensitivity Analysis of GA Parameters

The proper setting of GA parameters has a significant effect on the optimisation quality. We will demonstrate that the new HRNG can reduce this impact.

The most significant GA parameters are the *Generation limit* and the *Population size*. We analysed 15 combinations of x and y, where x is the *Population size* and y is the *Generation limit*; x takes the values 100, 125, 150, and 175; y takes the values 400, 450, 500, and 550. The optimisation was carried out for following x-y combinations and both RNGs.

Figure 8.1 illustrates the tendencies of the MVRMSE indicator for each combination (x-y). At first glance, it is evident that the HRNG provides better values of the MVRMSE whose tendency is approximately equal for each x-y combination in comparison with the PRNG. It is apparent that the GA with a PRNG significantly influences the MVRMSE according to the *Population size* parameter, as is shown in Figure 8.1. Another fact is that higher *Population size* does not mean higher optimisation quality. The benefit of the HRNG is a stable value of the MVRMSE for different values of the *Population size*. Moreover, the value of the MVRMSE in the HRNG is one-sixth smaller than the same value in the PRNG. We selected the combination of 175-400 as optimal for Ráztoka catchment.

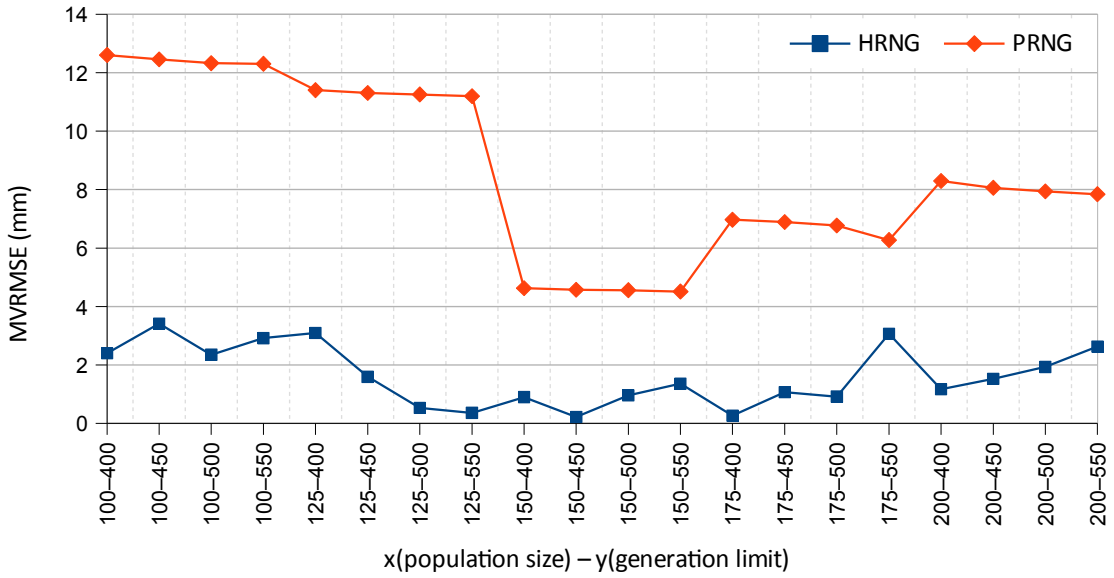

Figure 8.1: Tendency of MVRMSE indicators depending on the *Population size* and the *Generation limit* parameters using both RNGs

Additional GA parameters are crossover, mutation, and elitism, whose influence is illustrated in Figure 8.2. One-point and two-point crossover operations have the same tendency. The figure only shows the one-point operation for clarity. The crossover operations have one argument p, where p is the probability of the crossover operation, and the x-axis of Figure 8.2a that represents the value of the p argument. This value affects the fitness function equally, and therefore, the tendency is the same for both RNGs. The p value is set to 0.8 for this study. The x-axis of Figure 8.2b represents the probability p of the mutation. Again, it is evident that the trend of the fitness function is the same for both generators. If the p value of the mutation is 0, the MVRMSE is higher by several orders of magnitude. The higher value of the mutation unnecessarily prolongs the computing time with zero profit, and therefore the p value is set to 0.03. For elitism, the x-axis of Figure 8.2c represents the percentage of the number of the best individuals transferred to the new generation. It is evident that the tendency is also similar. The p value of the elitism is fixed to 0.04 since a higher value does not bring a significant improvement but prolongs the computing time.

The Sacramento users should only configure the GA parameters which directly influence the optimisation quality while the rest of the GA parameters are screened out from the users. Thus, *Population size* and *Generation limit* are possible to be adjusted in contrast to *crossover*, *mutation* and *elitism* parameters, which are fixed.

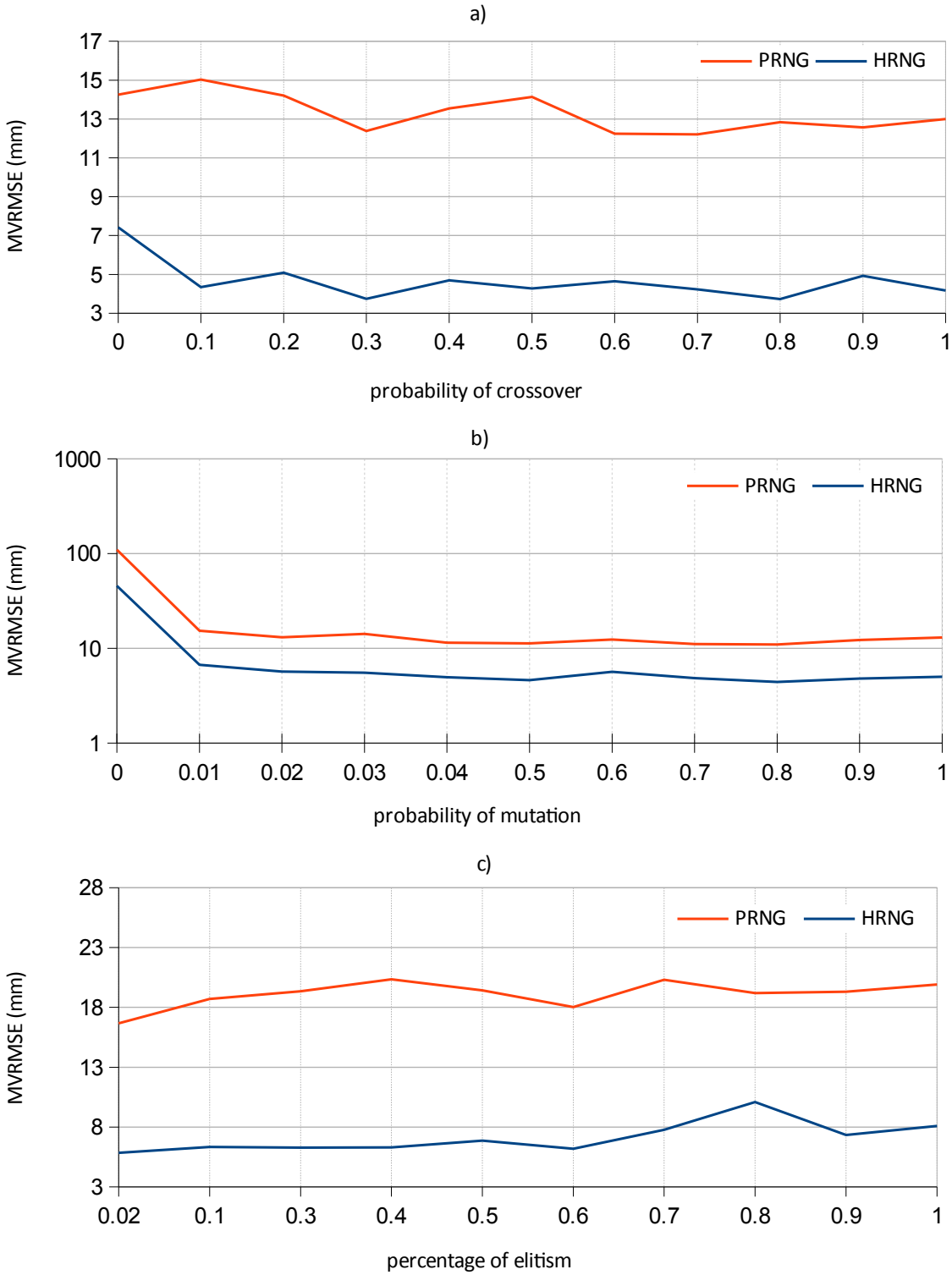

Figure 8.2: Tendencies of the fitness function value depending on (a) crossover, (b) mutation, (c) elitism

8.2.2 Optimisation Speed

The optimisation speed is the most interesting finding of this study. Figure 8.3 illustrates the course of the fitness function (MVRMSE) depending on the progress of the GA. The GA's progress is expressed by the sequence number of processed interactions (generation): each sequence number is assigned the best fitness function value of the current interaction. The horizontal axis displays the sequence number and the vertical axis shows the best fitness function of that interaction. The HRNG curve decreases almost quadratically; in absolute numbers: the PRNG needs approximately 90,000 iterations to achieve 4.64 of MVRMSE, whereas the HRNG needs only 10,000 iterations to achieve the same result.

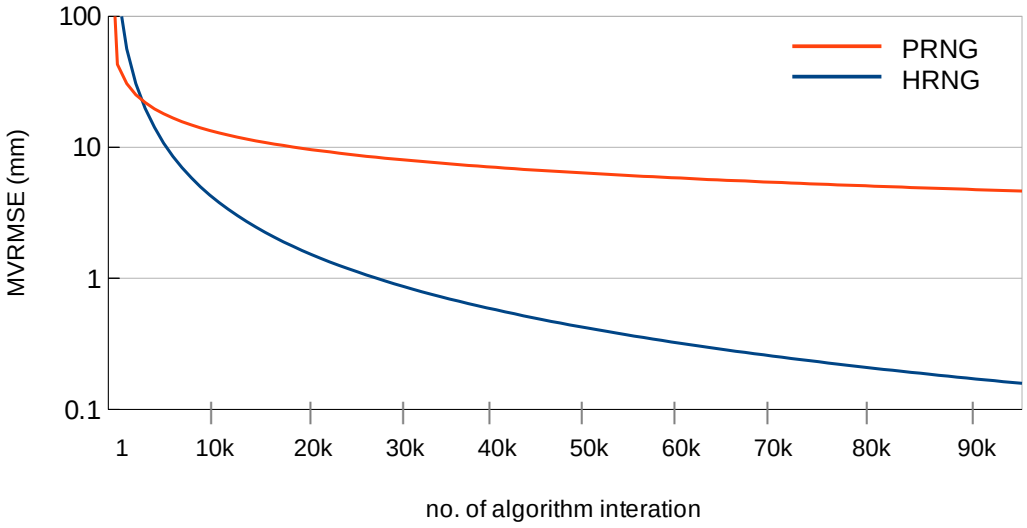

Figure 8.3: Development of the course of MVRMSE depending on the number of iterations

However, the optimisation speed significantly depends on the GA parameters, namely the *Population size* and the *Generation limit*. Figure 8.4 demonstrates the optimisation speed in minutes. The same combinations of x-y are used for this benchmarking, as in Figure 8.1; here, x is the *Population size,* and y is the *Generation limit*. The secondary y-axis shows time differences in the optimisation speed between the PRNG and HRNG in percentages. The optimisation speed of the HRNG is, on average, faster by 30% for the *Population size* interval <125, 175>. For the *Population size* $<$ 125 the HRNG is slower in certain x-y combinations by approximately 8% but only for small absolute values. The biggest acceleration can be observed in the combination of 175-550 where the acceleration is up to 40%. On the other hand, if the combination values rise, the opposite effect occurs and the HRNG drops by up to 40 %, see the

combination 200-450. Nevertheless, combinations higher than 200-y do not have any real use because they do not provide radical improvement of the MVRMSE, as is illustrated in Figure 8.1.

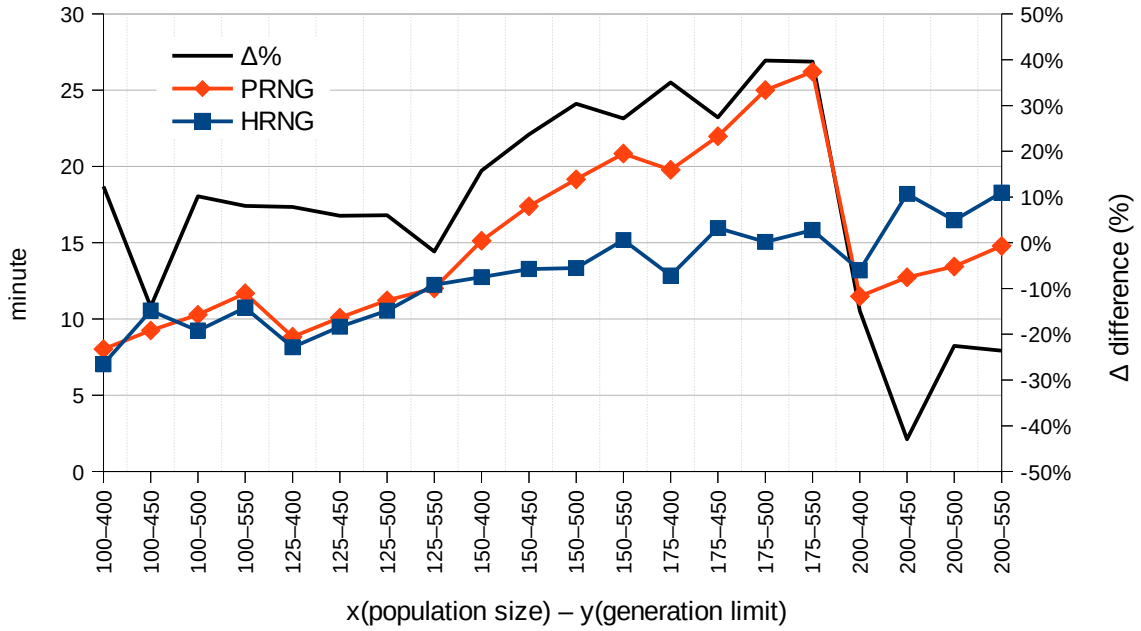

Figure 8.4: Time duration of the optimisation depending on the *Population size* and the *Generation limit*

8.2.3 Multiple Optimisation Runs

Current simulation comparing HRNG to PRNG showed that the PRNG easily gets stuck in local minima. It is interesting to note that the value of the fitness function is the same in all optimisation runs with the same Sacramento and GA parameters; namely initial model calibration, GA parameter configuration, and input data. The value of the fitness function is the same but additional indicators of the optimisation (e.g. highest score, average score, deviation score, the number of legal individuals) are different, so the optimisation algorithm tries several ways. This fact has been tested for each defined fitness function. Figure 8.5 only shows MVRMSE values for 10 optimisation runs for clarity. The figure reveals that the fitness function has constant values using the PRNG in contrast with HRNG. An implication of this might be the possibility that the HRNG can find a better solution whereas the PRNG gets stuck in local minima. However, these results need to be interpreted with caution because the HRNG does not guarantee the optimal solution to be found; but it can find a better solution than the PRNG. Section 8.3 explains this phenomenon.

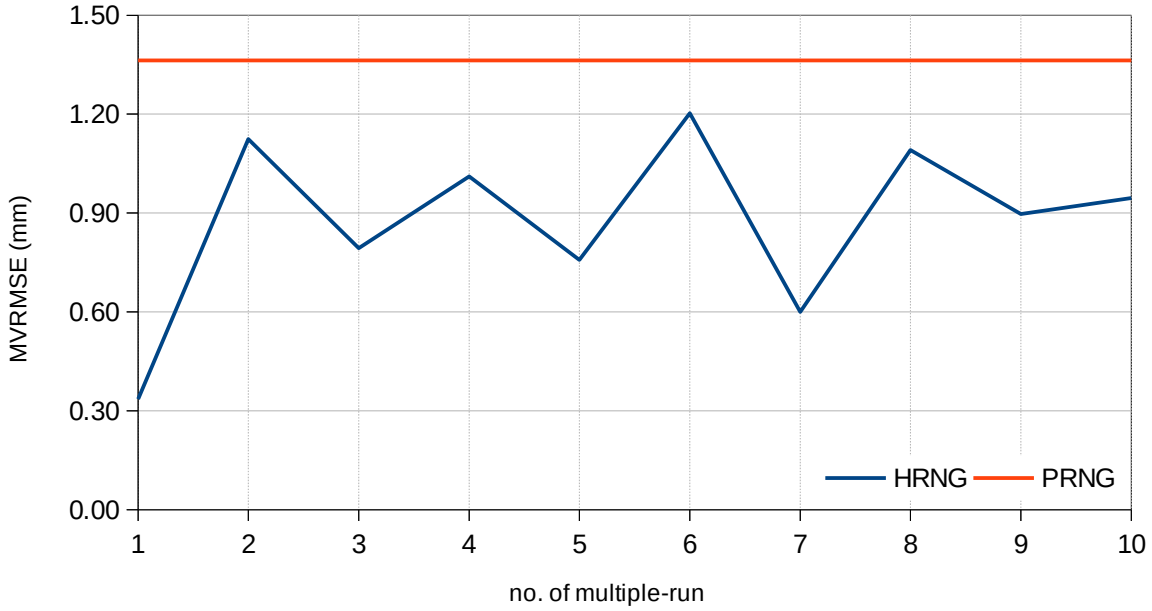

Figure 8.5: Ten multiple-runs of optimisation with a different RNG

8.3 Range and Distribution Function

The Sacramento optimisation includes estimation of many model parameters in the diverse range of parameter values. Moreover, there are model parameters which are in different order of magnitude, which means that to determine the useful course of search space is a complicated issue.

The range determining the interval of estimated values for each model parameter is crucial for a successful model optimisation. The more extensive range interval, the more complicated optimisation, since the GA must search the large search space. If the ranges are too broad, the GA needs more time to achieve the optimum. However, the degeneration of processed populations can occur, Holland (1992). On the contrary, if the range intervals are too narrow, the GA can get stuck in local minima, since the GA cannot continue to the more distant parts of the search space. It follows that the optimisation quality still depends on the Sacramento modeller experiences and, to a certain extent, also intuition.

The major part of the PRNGs operates with a uniform distribution of generated numbers. It has significant impact on the course of search space. If the range is set small enough, the GA is able to thoroughly scan the whole interval because it manages to generate most values in time. More precisely, it is able to do this within one GA run, which is limited by the value of the GA parameter –

Generation limit. It should be noted that the GA can never search the whole interval because it is too broad, since it is a set of real numbers and the *Generation limit* stops the optimisation before the GA processes most values of the interval. If the *Generation limit* is increased, the computation time of the GA is unnecessarily prolonged and the probability of the degeneration is increased. On the other hand, the PRNG estimates the parameter values in the interval *(a, b)* using a uniform distribution. If the GA estimates a value near the optimum value, the probability that the PRNG will select the next value close to this is small; the exact probability is *1/(b-a)*. Therefore, the broader interval, the lower the probability that the GA finds the optimal value.

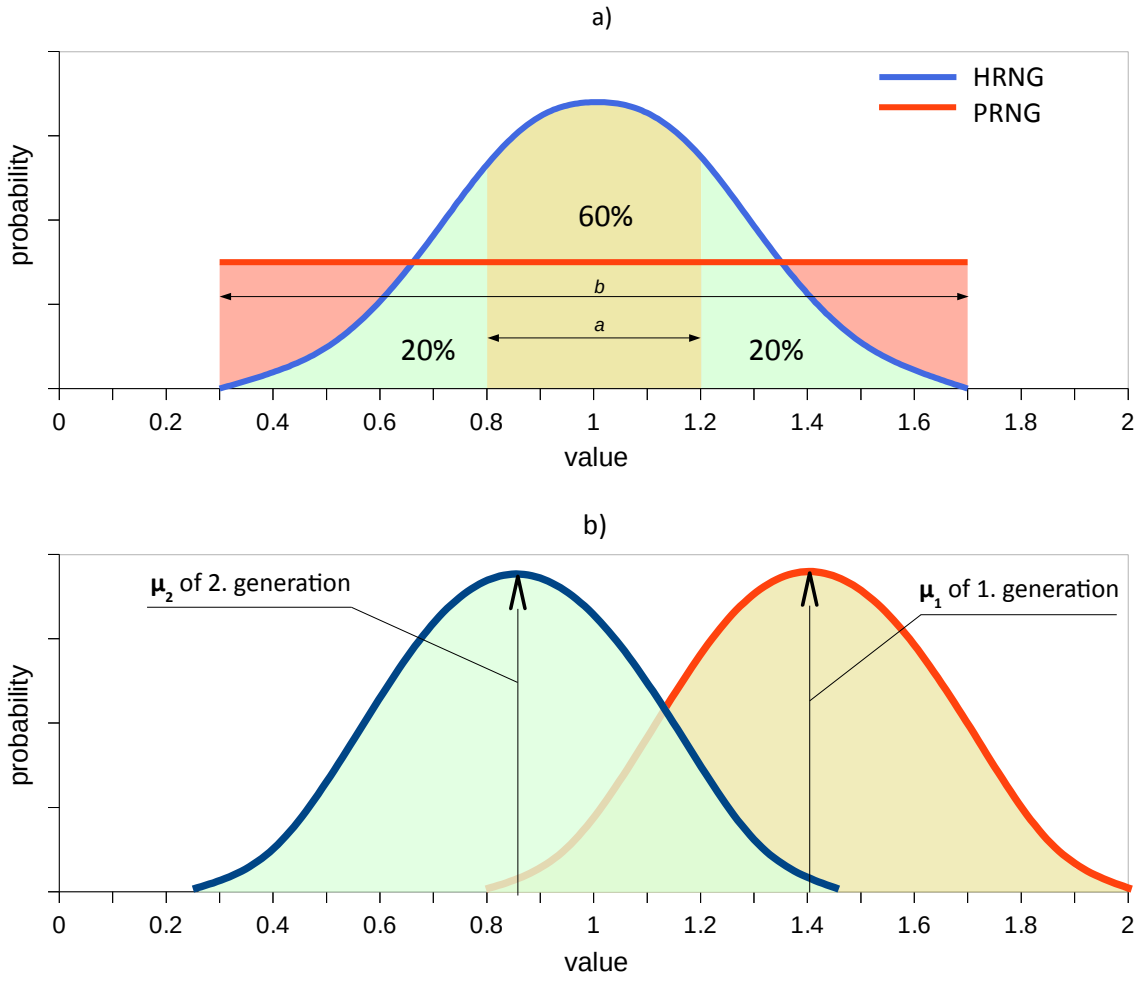

Figure 8.6: Influence of probability distribution (a) probability distribution of HRNG and PRNG, (b) shifting of scanned intervals across the generations

In contrast, the HRNG with a normal distribution brings a different approach to the parameter value estimation. The large interval of estimated model parameters can be set while using the HRNG since random numbers are generated with normal probability. In other words, the whole potential interval of generated numbers is divided into several subintervals with a different probability according to normal distribution. Thus, there is one interval with a higher probability, approximately 60%; it is based on the probability density function of normal distribution, see Figure 8.6a. If the optimal value of the estimated parameter is in this interval, the probability that the optimal value will be selected in this interval, compared to the one with a uniform distribution, is higher. Naturally, the modeller must estimate this interval properly. However, there are other subintervals with a small probability so that the GA can pass to a farther part of the search space represented by these unlikely intervals. In this manner, the GA is able to search significant parts of the search space.

For clarity, Figure 8.6a delineates an example of the parameter estimation using both random number distributions. The modeller has a rough estimate that the parameter value is between 0.8 and 1.2, marked as interval *a*. However, there is a possibility that the parameter value can be in the broader interval *b (0.3-1.7)*. Taken together, these results suggest that the interval *a* and the PRNG with a uniform distribution do not provide acceptable model results because the optimal value may be in the interval *b*. The problem is that interval *b* with the PRNG is too wide for the GA to find the optimal value in time. Whereas, the HRNG with normal distribution is able to process the interval *b* effectively, since the GA scans the interval *a* thoroughly. Moreover, the boundaries of interval *b* have a non-zero probability compared to interval *a*.

There is a significant side effect of the HRNG approach. The interval, where the GA searches for the parameter values, is different for each generation, since the current interval is based on current parameter value, which is shifted across generations. Figure 8.6b illustrates how the GA shifts the scanned interval across the generations.

Figure 8.6b also demonstrates that if a less probable value is selected, then a newly estimated value is searched in the proximity of a point with a higher probability than the one of the previous generation. Due to this, the GA gives the opportunity to the less likely value, since its area is scanned in depth in the next generation. Therefore, improbable values are searched in contrast with the uniform distribution, where these values have zero-probability of being selected due to the small size of the scanned interval. If thus created individuals have high fitness values, the probability of selection into the next generation is higher. If not, these

valueless individuals are removed from the population, but they still have a chance to be selected for the next generation, where they may improve their fitness values. These individuals would not have had an opportunity to be created, if the interval had been too small.

Specifically, the mean value (μ_1) of the estimated parameter in the first generation is 1.4, so the scanned interval is (0.8-2.0) in case of 40 % range. If the best fitness value of the first generation is 0.85, this value is set as the mean value (μ_2) for the next generation. It has several consequences, as follows. In the next generation, the GA scours the proximity of μ_2 more densely, in contrast with the uniform distribution. Therefore, if the optimal value is near μ_2, there is a high probability that the GA finds it. So, either the fitness value of μ_2 will be improved or the more fitness mean value will be found in the next generation. On the other hand, the PRNG with a uniform distribution and with 40 % range has a high probability that the GA strays into the wrong parts of the search space. Thus, looking for the optimal value is prolonged.

In short, the HRNG adopts the advantages of the PRNG but wide intervals of estimated values do not make the optimisation quality worse. The HRNG inspects the most probable parts of the intervals in depth. However, the HRNG can select values from distant parts of the search space in contrast to the PRNG, since the HRNG operates with large intervals. The PRNG can also achieve this by outlying the values but at the expense of decreasing the probability to find the optimal value, since the optimal value is usually in the middle of the interval specified by the modeller. The HRNG uses normal distribution and the probability that the next value will be in small proximity to the previously estimated value is approximately 60%. Although values at the bounds of the scanned interval have a low probability, they have a chance to make it to the next generation selection. The HRNG estimates values primarily in narrow surroundings but does not exclude farther surroundings. Whereas, the PRNG with a small interval of estimated values never achieves same values as HRNG does. For model users, this finding helps to make setting the parameter ranges easier because users can set greater parameter ranges without affecting the optimisation quality.

The shape, or more precisely the parameters of a normal distribution are of high importance for the course of the optimisation since they determine the probabilities of the normal distribution subintervals. The shape of a normal distribution is the topic for a separate research.

8.3.1 Using Two Distributions of the RNG

The following course of actions shows a practical application of different distribution functions in the RNG. The observed basin for this example is Ráztoka and the time period is 1954-1964. We have only a rough estimate of model parameter values from this period so that some optimal values might be far from these estimated values. The initial model validation (see column 2 of Table 8.3) confirms that the rough estimate has big monthly RMS errors despite the Correlation Coefficient. Figure 8.7 illustrates that the curve of the simulated discharge is very similar to the observed discharge but has significant transposition, hence the model validation shows the high error rate.

Table 8.3: Model validation for the Ráztoka basin using different RNGs

Statistic indicator	**Initial**	**HRNG**	**PRNG**
AVG ABS Monthly vol error (mm)	57.135	0.960	0.200
Monthly volume RMS error (mm)	220.3	3.953	0.958
Correlation Coefficient (–)	0.8165	0.783	0.826
Nash–Sutcliffe coefficient (–)	0.4104	0.573	0.677
Monthly ABS volume error (mm)	322.772	5.421	1.129
RMSE (mm)	0.177	0.160	0.152
Daily AVG ABS error (mm)	0.031	0.025	0.023
Percentage bias (%)	-57.135	-0.017	-0.024
Monthly bias (mm)	-322.772	-0.095	-0.138

The first phase of the Sacramento optimisation includes using the broader ranges of parameter values and the HRNG with a normal distribution. It is expected that the optimisation will only find close values of model parameters; therefore, we have to use the wider ranges and the HRNG, namely 80% ranges for each model parameter value. The result of this first phase indicates a significant improvement, see column 3 of Table 8.3. There was only a slight decrease in the Correlation Coefficient. Now, the HRNG estimates the model parameters more accurately. Another phase is the optimisation using the PRNG with a uniform distribution but with narrower ranges of model parameter values, namely 10%. The consequence of these ranges is that the GA just particularises the model parameters, and the probability that the GA being lost in the search space is minimal.

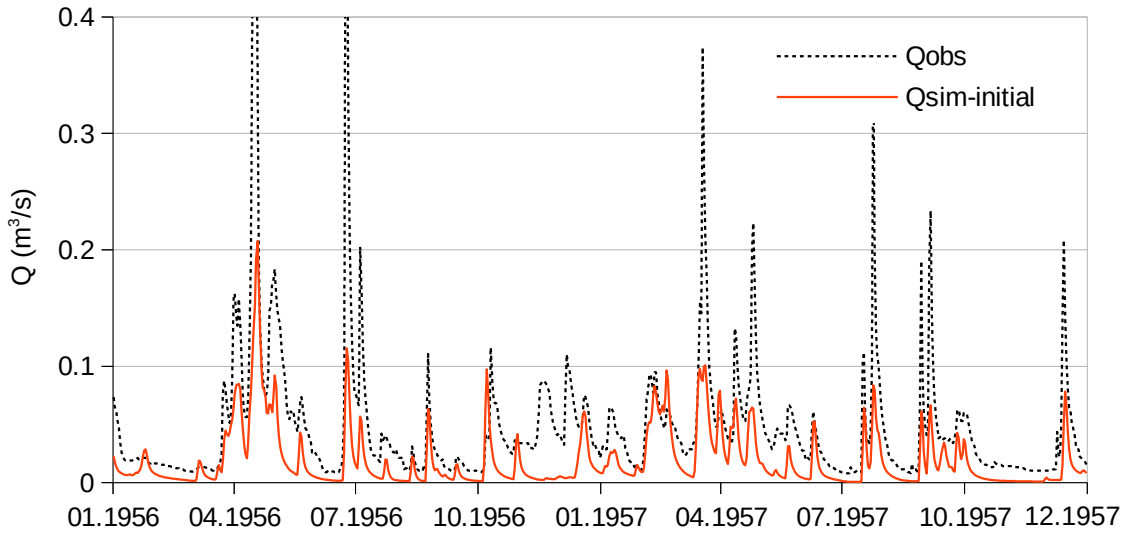

Figure 8.7: Simulation results for a rough estimate of model parameter values in the Ráztoka basin (1956-1957)

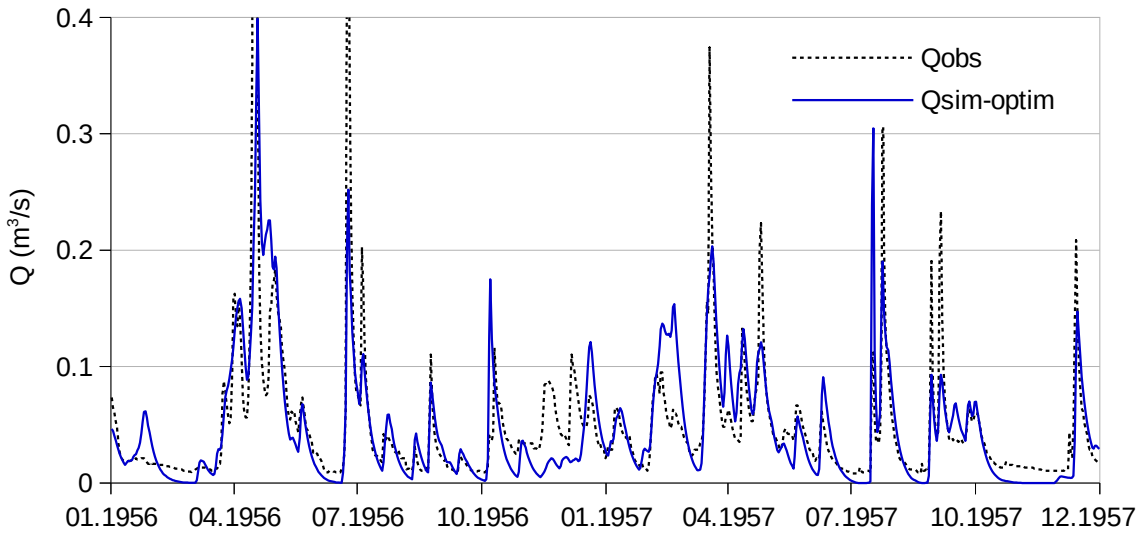

Figure 8.8: The final results of the Ráztoka simulation (1956-1957)

Last column of Table 8.3 and Figure 8.8 illustrate the final result of the Sacramento simulation for the Ráztoka catchment. The vast majority of the model validation indicates a quality improvement. Even the Correlation Coefficient has a higher rate than the initial value. In short, the sequential optimisation using different RNGs and ranges might improve the simulation of the Sacramento model.

8.4 SAC-SMA Results

First of all, we compare the model validations of both RNGs. The present results are significant because the HRNG can find a better solution, as Table 8.4 illustrates. The statistical indicators used in the table are described in depth in Burnash (1995). Column 2 lists the statistical values of the manual calibration which were used as the initial calibration. This result was expected because the iterative manual calibration is very difficult and time-consuming. Finally, columns 3 and 4 summarise the statistical results of the model optimisation with different RNGs. These results might be related to the selection of a fitness function, which is one dimensional so that the other values of the indicators may become less favourable. The differences between manual calibration and automatic optimisation calibrations are another interesting observation. In the case of the PRNG, some indicator values are worse compared to values with the manual calibration: especially the Correlation Coefficient. On the other hand, the HRNG improves all values of indicators compared to the PRNG.

Table 8.4: Statistical indicators for various random number generators (PRNG, HRNG)

Statistic indicators	**Manual calibration**	**Used RNG**		**Δ**
		PRNG	**HRNG**	
AVG ABS Monthly volume error (mm)	61.194	0.226	0.024	0.202
Daily AVG ABS error (mm)	0.038	0.041	0.036	0.005
Daily RMS error (mm)	0.196	0.204	0.0755	0.1285
Monthly ABS volume error (mm)	217.923	7.8018	0.8318	6.97
Monthly volume RMS error (mm)	220.30	4.572	0.240	4.332
RMSE (mm)	0.0751	0.0755	0.0641	0.0114
Correlation Coefficient (–)	0.8266	0.7823	0.7969	0.0146
Nash–Sutcliffe coefficient (–)	0.4015	0.3950	0.5643	0.1693

Figure 8.9 compares the results obtained for the Ráztoka simulation in the period 1956-1966. It is one of the most variable periods concerning *precipitation* because there were several flood events. Moreover, the development of diverse aspects of the vegetation cover (e.g. the strong influence of forest changes due to the bark beetle calamity, increased grain production) frequently occurred. These aspects make the model calibration during this period more complicated. In particular, the consecutive re-forestation in this catchment and the resulting decrease of evapo-transpiration requires precision in the complex component of water balances.

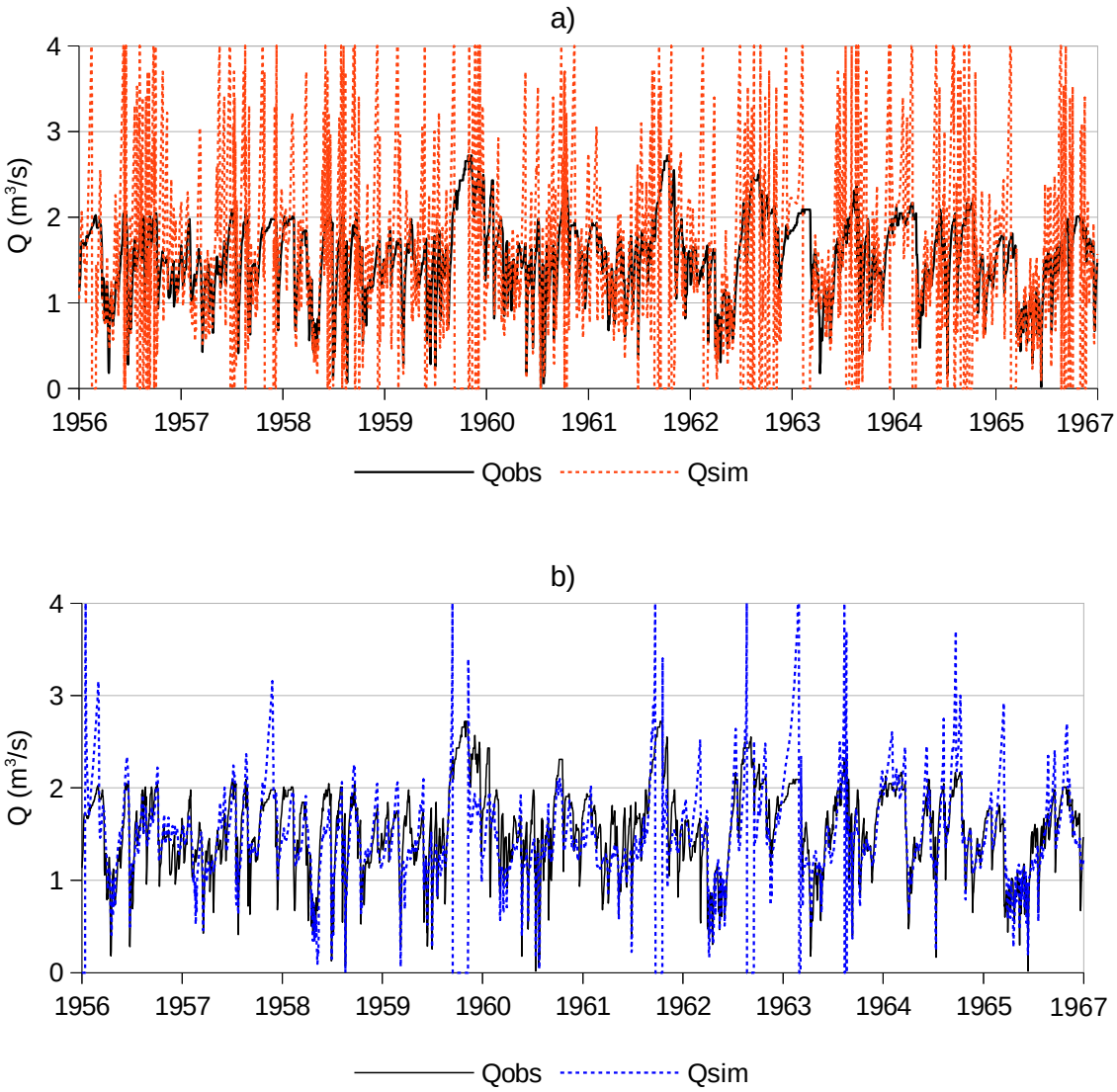

Figure 8.9: Logarithmic scale of observed and simulated discharges using (a) PRNG and (b) HRNG

The shape of the HRNG curve is satisfactory towards the obtained results and it takes the nature of the period into account. In contrast, the PRNG yields high deviations from the observed flow, these deviations are apparent on most peaks. Figure 8.9 also illustrates that the HRNG creates smoother and more continuous shape of the simulated discharge compared to the PRNG. This is the result of the primal optimisation run of the model implementation, and an additional calibration/optimisation can further increase the quality of the model validation; some of our preliminary experiments for partial periods have indicated this phenomenon as a possibility.

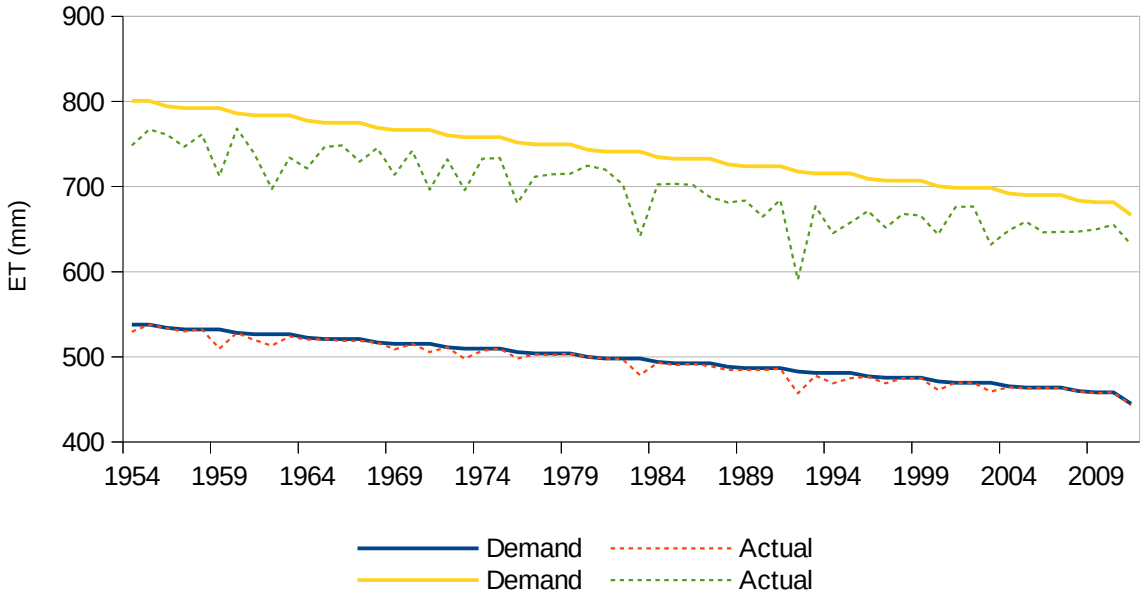

Figure 8.10: Annual trends of the evapotranspiration demand and actual evapotranspiration using both RNGs

Figure 8.10 illustrates the annual trends of the evapotranspiration (ET) demand and actual evapotranspiration using both RNGs. The trends are the same. However, the actual ET of the PRNG is very volatile compared to the HRNG. Another important implication is that the GA with HRNG can more realistically calibrate the Sacramento model. The evapotranspiration of the HRNG reflects the vegetation changes of the Ráztoka catchment, where the water consumption was decreased due to the gradual deforestation.

The abrupt disasters of vegetation cover and its long-term development should be stated in this context as a reason for the surprising course of the evapotranspiration on such occasions (see Appendix C).

8.5 Continuous Function Optimisation

Evapotranspiration (ET) and Unit Hydrograph (UNIT-HG) are defined using discrete values, which are in correlation, but the GA does not take this fact into account. This section describes experiments with continuous functions, defined in Section 6, which improve the optimisation quality. We compare the original definition of ET and UNIT-HG with the new approach using the continuous function.

8.5.1 Evapotranspiration by Gaussian Function

As we mentioned in the introduction (see Section 1.1.4), optimisation of ET can bring the unrealistic ET shape since it is defined by 12 discrete values that are in the correlation, the GA is not able to take these account.

In this section, the Sacramento simulation was performed on Ráztoka basin for the year 1954 since this is a calm season from hydrological point of view. Therefore, we expect a smooth course of evapotranspiration.

Figure 8.11 and Figure 1.1 illustrate the optimisation issue. The blue line represents optimised ET which is defined via 12 discreet values (*et12*). The course of this ET is not smooth at first glance; especially in the 7^{th} month there is a significant slump. However, there is no reason for this slump because the modelled period is hydrologically calm. Too loose ranges of *et12* parameters can be a result of this unrealistic ET shape. The model user must define the proper range for each value of *et12* to achieve a realistic ET course, which is very time-consuming. On the other hand, the red line in Figure 8.11 illustrates a realistic ET shape. It is a result of ET optimisation using Equation 6.3 (*etGauss*).

If we compare the simulated discharges of both ET definitions (*et12* and *etGauss*), the results are very similar and there are no deviations that debase the simulation quality, as Figure 8.12 illustrates. The visible differences can be seen in the 6^{th} and 8^{th} month but with a relatively small disparity. Moreover, the *ET by Gauss* course is more similar to the observed discharge than *ET by 12 values*.

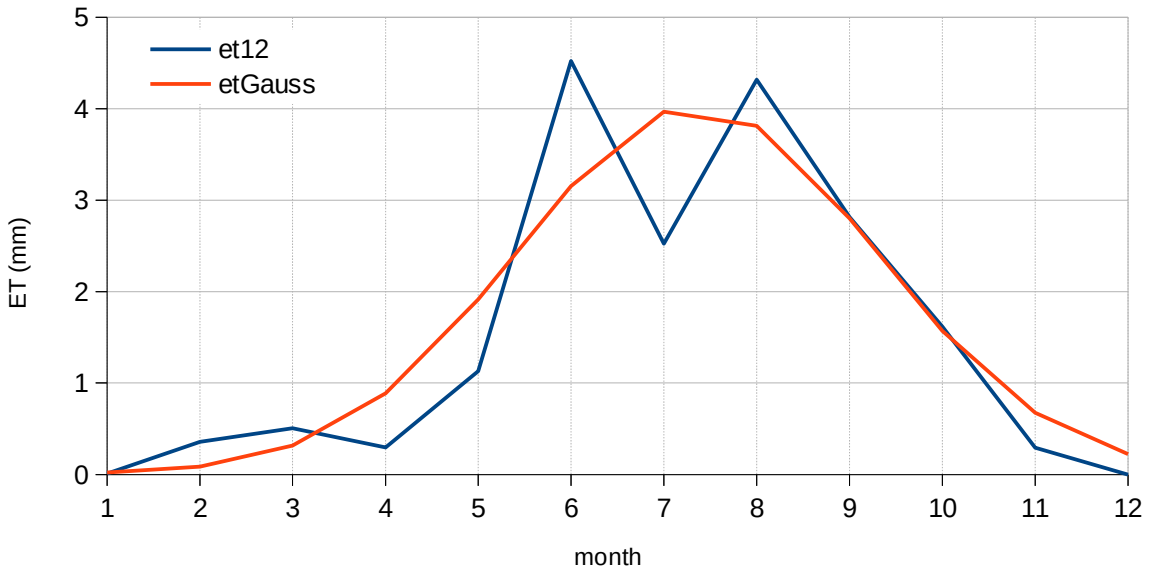

Figure 8.11: Optimised evapotranspiration using 12 discrete values and Gauss function

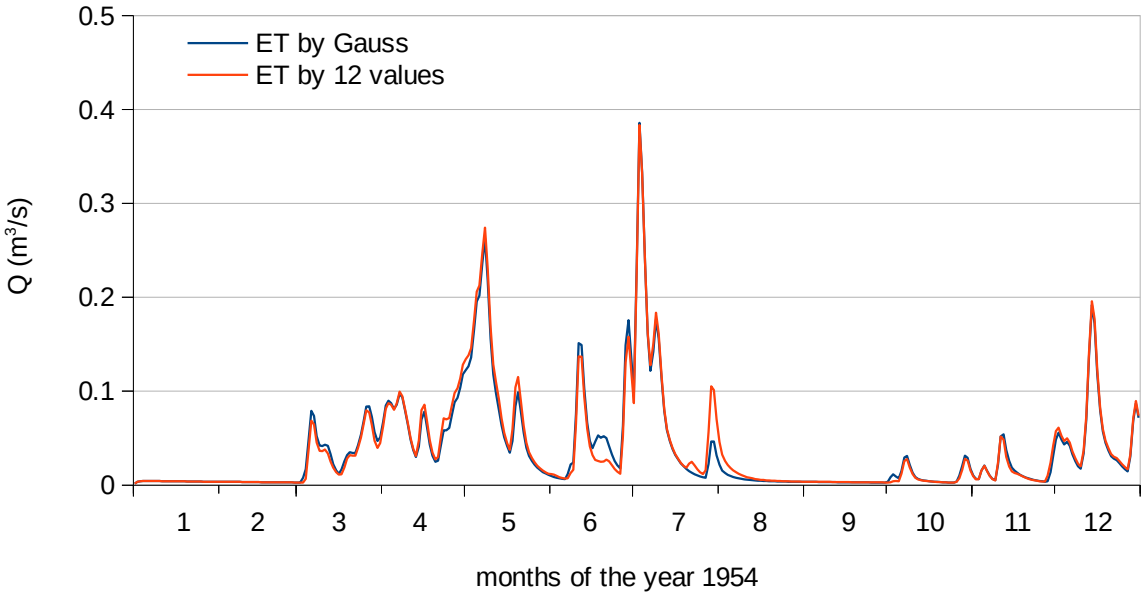

Figure 8.12: Simulated runoff using 12 discrete values and Gaussian function

Table 8.5: Model validation using 12 discrete values and Gaussian function

Statistical indicator	et12	etGauss	Δ
Daily RMS error (mm)	0.116	0.115	0.001
Daily AVG ABS error (mm)	0.013	0.013	0
AVG ABS Monthly vol error (mm)	0.701	10.533	-9.832
Monthly volume RMS error (mm)	1.268	13.743	-12.475
Correlation (–)	0.8699	0.8724	0.0025
Nash-Sutcliffe (–)	0.7555	0.7606	0.0051
Monthly ABS volume error (mm)	0.2679	4.0265	-3.7586

Table 8.5 summarises the model validation for both ET definitions. As can be seen from the table, *etGauss* makes a few statistical indicators worse but not radically. Correlation and Nash coefficients evince a slight improvement in contrast to *et12*. However, achieving the realistic shape of evapotranspiration is more important than these statistical indicators. This finding has important implications for basin information obtained by the Sacramento model since ET influences a filling of the model zones. Therefore, if the evapotranspiration mirrors reality, the rest of the model parameter and model outputs could provide useful information.

8.5.2 Unit Hydrograph by Diffusion Function

Discrete values also define the Unit Hydrograph (UNIT-HG). Therefore, the optimisation of the Unit Hydrograph (UNIT-HG) is similar to ET optimisation. Nevertheless, a number of discrete values defining the UNIT-HG variable make the UNIT-HG optimisation more complicated. Primarily, the more points of UNIT-HG, the more ranges for each point must be defined. It brings a potential issue of an unrealistic course of the UNIT-HG similar to the subject illustrated in Figure 8.11.

For this section, the Elbe basin was selected and its long period of 1905-1970, which includes many hydrological events like floods, vegetation changes, etc. Furthermore, the UNIT-HG of the Elbe basin needs to be defined by approximately 16 UNIT-HG coordinates.

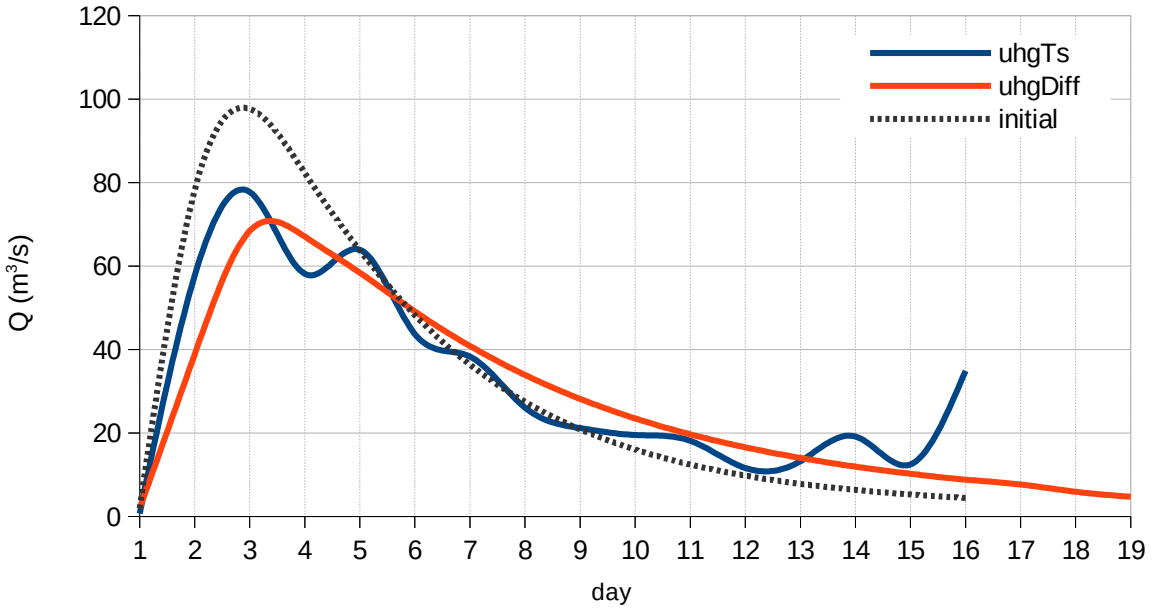

Figure 8.13: UNIT-HG optimisation using coordinates and diffusion equation

As in previous Section 8.5.1, Figure 8.13 illustrates the UNIT-HG optimisation issue. The initial UNIT-HG expects a smooth course with a discharge peak of 100 m^3/s on the 3^{th} day, as the dashed line (*initial*) demonstrates. The blue line represents the UNIT-HG which was optimised using a set of discrete coordinates (*uhgTs*). The course does not meet expectations which might be caused by the ranges of the coordinates being too loose. It is challenging to set proper ranges even for an experienced hydrologist, since it requires several optimisation runs. Finally, the red line of Figure 8.13 represents a realistic UNIT-HG shape because the GA takes the correlation between UNIT-HG coordinates into account using Equation 6.6 (*uhgDiff*). The benefit of this approach is that the course of *uhgTs* and *uhgDiff* is asymptotically same and the *uhgDiff* can smooth out the optimised UNIT-HG.

Moreover, the model validation for both UNIT-HG optimisations is approximately same as Table 8.6 summarises. Differences between *uhgTs* and *uhgDiff* indicators are in the order of tenths, so the simulation quality is not affected by *uhgDiff*.

What is interesting in UNIT-HG optimisation using *uhgDiff* is that the number of UNIT-HG coordinates can also be optimised which is not possible in case of *uhgTs*. The model user estimates a number of coordinates based on modeller's experience and available information about the simulated basin. Our approach easily optimises this number since it defines how many points are taken from Equation 6.6, see Section 6.2.

Table 8.6: Model validation using discrete coordinates and diffusion equation

Statistical indicator	**uhgTs**	**uhgDiff**	**Δ**
Daily RMS error (mm)	9.862	9.898	-0.036
Daily AVG ABS error (mm)	97.256	97.973	-0.716
AVG ABS Monthly vol error (mm)	3.178	3.086	0.092
Monthly volume RMS error (mm)	31.261	30.261	1
Correlation (–)	0.8188	0.8147	-0.0041
Nash-Sutcliffe (–)	0.6585	0.6515	-0.007
Monthly ABS volume error (mm)	33.6802	32.7069	0.9733

9

Conclusion

This thesis proposes the optimisation of the SAC-SMA model calibration using the *genetic algorithm* (GA) with a new random number generator based on hydrological information (HRNG). Compared to the pseudo-random number generator (PRNG), which is the one most frequently used, the obtained results indicate that the HRNG could successfully be applied to the calibration of the rainfall-runoff process. We also present a study of the hypothesis that discrete model parameters can be described by a continuous function as well as its optimisation. This final chapter presents and highlights the most important conclusions of the thesis.

The priority of the dissertation is the potential of the HRNG and range settings of optimised model parameters. The HRNG meets the requirements of the PRNG, which among other things includes a reasonable level of randomness. Moreover, the core of the optimisation quality is the normal distribution of the HRNG which allows more extensive ranges for optimised parameters to be defined without the GA being lost in the search space. One of the more significant findings that emerged from this study is that the HRNG provides more stable results in spite of various GA configurations. Further, the optimisation speed can be increased up to 30%. Multiple regression analyses revealed that the HRNG is more resistant to getting stuck in a local minimum because the PRNG returns the same result for multiple runs of the optimisation with the same configuration of the model calibration and the GA settings. In contrast, the HRNG returns different results for each run of the optimisation.

Subsequently, the results of this study also indicate that the selection of the fitness function considerably affects the quality of the optimisation. The analysis of Ráztoka catchment has determined the MVRMSE as the optimal fitness function across all modelled periods. In contrast, the AAMVE is the optimal function for the Elbe River but only for long time periods. There are several instances

of simulations which require multiple optimisations with different kinds of the fitness function.

The second significant finding was that the continuous functions specifying discrete model parameters might guide the optimisation process in a more appropriate direction. These functions take into account the correlation between the model parameters. A more accurate estimate of the SAC-SMA model output has been achieved using these functions without devaluation of the model validation. Specifically, the discrete definition of evapotranspiration (ET) and unit hydrograph (UNIT-HG) has been substituted by the Gaussian function, respectively the diffusion equation. The result is that the SAC-SMA model returns more useful information.

On the other hand, the results of this thesis are not a panacea for all instances of mentioned problems and also have some limitations. The modeller can smooth the shape of ET and UNIT-HG, but this might also distort the modelled reality since some fluctuations are realistic. Here an intervention of a hydrologist who has knowledge about the modelled watershed is necessary. The GA with the HRNG is able to find quality solutions but only for one fitness function. Therefore, the modeller must correctly select the fitness function to achieve the best optimisation. However, the right choice of the fitness function requires an analysis and several auxiliary simulations. In short, the presence of the hydrologist and his experience is still indispensable for the SAC-SMA optimisation.

The presented study makes several noteworthy contributions. Results obtained from our framework have a higher quality and are applicable in practice in terms of hydrology. Moreover, the HRNG can be easily implemented into the legacy framework because it has minimal influence on this legacy framework and user interface. Therefore, this approach can be easily applied to the similarly structured optimisation framework. Another significant contribution is the acceleration of the optimisation speed. Another contribution from the point of view of the user interface is that the HRNG reduces the mutual dependence of the optimisation quality and parameter setting of the GA. Hence, the modeller with basic knowledge of the GA should not distinctively affect the optimisation quality. Additionally, the modeller can use wider ranges for optimised parameters while the optimisation quality is maintained.

This research has thrown up many questions. Further investigation and experimentation into the HRNG and rainfall-runoff optimisation are strongly recommended. More research is required to determine the efficiency of the HRNG since it seems that the shape of the HRNG distribution function may affect

the quality of the optimisation. It is necessary to explore the correlation between the distribution function of the HRNG and the calibrated basin since the first results indicate that a different distribution function can influence the calibration quality for each period and basin. It would be interesting to assess the effects of multi-criteria fitness function when its value is computed using more statistical indicators. Such a multi-criteria fitness function could provide more stable results.

Bibliography

Abdulla, F. A., Lettenmaier, D. P., Liang, X. (1999). Estimation of the ARNO model baseflow parameters using daily streamflow data. Journal of Hydrology, 222(1), 37-54.

Abebe, N. A., Ogden, F. L., Pradhan, N. R. (2010). Sensitivity and uncertainty analysis of the conceptual HBV rainfall–runoff model: Implications for parameter estimation. Journal of Hydrology, 389(3), 301-310.

Abramson, M. A., Audet, C., Dennis, J. E. (2004). Generalized pattern searches with derivative information. Mathematical Programming, 100(1), 3-25.

Anderson E. (2006). Snow accumulation and ablation model-SNOW-17. National Oceanic and Atmospheric Administration.
http://www.nws.noaa.gov/oh/hrl/nwsrfs/users_manual/part2/_pdf/22snow17.pdf (accessed 3 August 2017).

Anderson, M. G., Bates, P. D. (2001). Model validation: perspectives in hydrological science. John Wiley & Sons Ltd.

Anderson, R. M., Koren, V. I., Reed, S. M. (2006). Using SSURGO data to improve Sacramento Model a priori parameter estimates. Journal of Hydrology, 320(1), 103-116.

Andréassian, V., Perrin, C., Michel, C., Usart-Sanchez, I., Lavabre, J. (2001). Impact of imperfect rainfall knowledge on the efficiency and the parameters of watershed models. Journal of Hydrology, 250(1), 206-223.

Arsenault, R., Poulin, A., Côté, P., Brissette, F. (2013). Comparison of stochastic optimisation algorithms in hydrological model calibration. Journal of Hydrologic Engineering, 19(7), 1374-1384.

Bastos-Filho, C. J., Oliveira, M. A., Nascimento, D. N., Ramos, A. D. (2010). Impact of the random number generator quality on particle swarm optimization algorithm running on graphic processor units. In Hybrid Intelligent Systems (HIS), 2010 10th International Conference on (pp. 85-90). IEEE.

Beer, J. (2005). Solar variability and climate change. Memorie-Societa Astronomica Italiana, 76(4), 751.

Berga, L., Buil, J. M., Bofill, E., De Cea, J. C., Perez, J. G., Mañueco, G., Yagüe, J. (Eds.). (2006). Dams and Reservoirs, Societies and Environment in the 21st Century, Two Volume Set: Proceedings of the International Symposium on Dams in the Societies of the 21st Century, 22nd International Congress on Large Dams (ICOLD), Barcelona, Spain, 18 June 2006. CRC Press.

Bergstrom S. (1976). Development and Application of a Conceptual Runoff Model for Scandinavian Catchments. Report RHO 7, Swedish Meteorological and Hydrological Institute, Norrkoping, Sweden, 134 pp.

Bergström, S. (1991). Principles and confidence in hydrological modelling. Hydrology Research, 22(2), 123-136.

Bi, W., Dandy, G. C., Maier, H. R. (2015). Improved genetic algorithm optimisation of water distribution system design by incorporating domain knowledge. Environmental Modelling & Software, 69, 370-381.

Bronstert, A., Niehoff, D., Bürger, G. (2002). Effects of climate and land-use change on storm runoff generation: present knowledge and modelling capabilities. Hydrological processes, 16(2), 509-529.

Brown, T. (1997). Clearances and clearings: deforestation in Mesolithic/Neolithic Britain. Oxford Journal of Archaeology, 16(2), 133-146.

Buchtele J., Tesar M. (2013). Evaluation of the appearing changes in water regime at Ráztoka and Červík basins in the Beskydy Mts. Beskydy. The Beskids Bulletin, 6(2), 135-148. http://dx.doi.org/10.11118/beskyd201306020135.

Buchtele, J., Košková, R. (2008). Approaches to credible identification of reliable parameters in rainfall-runoff model from long time series. HydroPredict, 241-244.

Buchtele, J., Tesař, M. (2009). The time variability of evapotranspiration and soil water storage in long series of rainfall-runoff process. Biologia, 64(3), 575-579.

Buchtele, J., Kulasová, A., Tesař, M.. Šír, M. (2000). Long-term experimental monitoring and theoretical modelling of the surface runoff formation in the Šumava and Jizera Mts. (Czech Republic). In: Monitoring and Modelling Catchment Water Quantity and Quality (ed. by N.E.C. Verhoest & Y.J.P. van Herpe & F.P. De Troch). European Network of Experimental and Representative Basins and IHP NE FRIEND Project 5 Conference, Ghent

Buchtele, J., Tesař, M., Krám, P. (2009). Variability of the water regime in the forested experimental catchments. Soil & Water Research, 4(2), 93-101.

Burnash R. J. C. (1995). The NWS river forecast system-Catchment modeling. In: Computer Models of Watershed Hydrology, V. P. Singh (ed.), Water Resources Publications, Colorado, USA, pp. 311-366.

Calder, I. R., Newson, M. D., Walsh, P. D. (1982). application of catchment, lysimeter and hydrometeorological studies of coniferous afforestation in Britain to land-use planning and water management. In Hydrological research basins and their use in water resources planning: proceedings of the international symposium held in Berne, Switzerland September 21-23, 1982. Bern: Landeshydrologie, 1982.

Clark, M. P., Nijssen, B., Lundquist, J. D., Kavetski, D., Rupp, D. E., Woods, R. A., Arnold, J. R. (2015). A unified approach for process-based hydrologic modeling: 1. Modeling concept. Water Resources Research, 51(4), 2498-2514.

Crawford, N. H., Burges, S. J. (2004). History of the Stanford watershed model. Water Resources Impact, 6(2), 3-5.

Diersch, H. J. (1990). Fletcher, CAJ, Computational Techniques for Fluid Dynamics. Vol. I: Fundamental and General Techniques. Vol. II: Specific Techniques for Different Flow Categories. Berlin etc., Springer-Verlag 1988. XIV, 409 pp., 183 figs./XI, 484 pp., 183 figs., DM 198, 00 as a Set. ISBN 3-540-18151-2/3-540-18759-6 (Springer Series in Computational Physics). ZAMM-Journal of Applied Mathematics and Mechanics/Zeitschrift für Angewandte Mathematik und Mechanik, 70(9), 409-410.

Donigian, A. S., Huber, W. C. (1991). Modeling of nonpoint source water quality in urban and non-urban areas. Environmental Research Laboratory, Office of Research and Development, US Environmental Protection Agency.

Duan, Q., Schaake, J., Andreassian, V., Franks, S., Goteti, G., Gupta, H. V., Hogue, T. (2006). Model Parameter Estimation Experiment (MOPEX): An overview of science strategy and major results from the second and third workshops. Journal of Hydrology, 320(1), 3-17.

Dubrovský, M., Buchtele, J., Žalud, Z. (2004). High-frequency and low-frequency variability in stochastic daily weather generator and its effect on agricultural and hydrologic modelling. Climatic Change, 63(1), 145-179.

Dumenil, L., Todini, E., (1992). A rainfall-runoff scheme for use in the Hamburg climate model. In: O'Kane, P. (Ed.). Advances in Theoretical Hydrology, a Tribute to James Dooge, European Geophysical Society, Series on Hydrological Sciences 1, Elsevier, Amsterdam, pp. 129–157.

Fischer, V., Drutarovsky, M. (2002). True random number generator embedded in reconfigurable hardware. In CHES (Vol. 2, pp. 415-430).

Flajolet, P., Gardy, D., Thimonier, L. (1992). Birthday paradox, coupon collectors, caching algorithms and self-organizing search. Discrete Applied Mathematics, 39(3), 207-229.

Franchini, M. (1996). Use of a genetic algorithm combined with a local search method for the automatic calibration of conceptual rainfall-runoff models. Hydrological Sciences Journal, 41(1), 21-39.

Franchini, M., Galeati, G., Berra, S. (1998). Global optimisation techniques for the calibration of conceptual rainfall-runoff models. Hydrological Sciences Journal, 43(3), 443-458. 26.

Friedman, M. (1937). The use of ranks to avoid the assumption of normality implicit in the analysis of variance. Journal of the american statistical association, 32(200), 675-701.

Gallagher, K., Sambridge, M. (1994). Genetic algorithms: a powerful tool for large-scale nonlinear optimization problems. Computers & Geosciences, 20(7-8), 1229-1236.

Gandomi, A. H., Alavi, A. H., Ryan, C. (Eds.). (2015). Handbook of genetic programming applications. Switzerland: Springer.

Ghanea-Hercock, R. (2013). Applied evolutionary algorithms in Java. Springer Science & Business Media.

Gupta, H. V., Sorooshian, S., Yapo, P. O. (1998). Toward improved calibration of hydrologic models: Multiple and noncommensurable measures of information. Water Resources Research, 34(4), 751-763.

Gupta, V.K., Sorooshian, S., (1985). The automatic calibration of conceptual catchment models using derivative-based optimisation algorithms. Water Resour. Res. 21 (4), 473–485.

Haahr, M. (n.d.), (2017). True Random Number Service. Retrieved December 08, 2017, from https://www.random.org/analysis.

Hamed, K. H. (2008). Trend detection in hydrologic data: the Mann–Kendall trend test under the scaling hypothesis. Journal of hydrology, 349(3), 350-363.

Hansen, J., Sato, M., Ruedy, R., Lacis, A., Asamoah, K., Borenstein, S., Curran, B. (1996). A Pinatubo climate modeling investigation. In The Mount Pinatubo Eruption (pp. 233-272). Springer, Berlin, Heidelberg.

Hansen, N., Ostermeier, A. (2001). Completely derandomized self-adaptation in evolution strategies. Evolutionary computation, 9(2), 159-195.

Hanson, R. L. (1991). Evapotranspiration and droughts. US Geological Survey Water-Supply Paper, 2375, 99-104.

Hartmann, A., Lange, J., Weiler, M., Arbel, Y., Greenbaum, N. (2012). A new approach to model the spatial and temporal variability of recharge to karst aquifers. Hydrology and Earth System Sciences, 16(7), 2219-2231. doi:10.5194/hess-16-2219-2012.

Hathaway, D. H., Rightmire, L. (2010). Variations in the Sun's meridional flow over a solar cycle. Science, 327(5971), 1350-1352.

Hejzlar, J., Dubrovský, M., Buchtele, J., Růžička, M. (2003). The apparent and potential effects of climate change on the inferred concentration of dissolved organic matter in a temperate stream (the Malše River, South Bohemia). Science of the Total Environment, 310(1), 143-152.

Holland, J. H. (1992). Genetic algorithms. Scientific american, 267(1), 66-73. Holland (1992)

Hooke, R., Jeeves, T.A., (1961). Direct search solution of numerical and statistical problems. J. Assoc. Comput. Mach. 8 (2), 212–229.

Hughes, D. A., Kapangaziwiri, E., Sawunyama, T. (2010). Hydrological model uncertainty assessment in southern Africa. Journal of hydrology, 387(3), 221-232.

Hurst, H. E. (1951). Long-term storage capacity of reservoirs. Trans. Amer. Soc. Civil Eng., 116, 770-808.

Chlumecký, M., Tesař, M., Buchtele, J. (2014). The appraisals of long time series of evapotranspiration using modelling rainfall-runoff with optimized parameters. In: International work-Conference On Time Series: Proceedings ITISE (pp. 1280-1291).

Ingber, L., Petraglia, A., Petraglia, M. R., Machado, M. A. S. (2012). Adaptive simulated annealing. In Stochastic global optimisation and its applications with fuzzy adaptive simulated annealing (pp. 33-62). Springer Berlin Heidelberg.

Jandora J., Stará V. Starý M., Hydraulika a hydrologie. Brno: Akademické nakladatelství CERM, 2011. ISBN 9788072047390 (in Czech).

Jayawardena, A. W. (2014). Environmental and hydrological systems modelling. CRC Press.

Keller, R. (1970). Water-balance in the Federal-Republic of Germany. In Symp. on World Water Balance, IAHS/UNESCO Publ, vol. 92, pp. 300-314.

Kemel, M. (1994). Hydrologie. Praha: České vysoké učení technické, ISBN 8001005097, (in Czech).

Koren, V., Smith, M., Duan, Q., (2003). Use of a priori parameter estimates in the derivation of spatially consistent parameter sets of rainfall-runoff models. In: Duan, Q., Sorooshian, S.,Gupta, H., Rosseau, H., Turcotte, H. (Eds.), Calibration of Watershed Models Water Science and Applications, vol. 6. AGU, pp. 239–254.

Krause, P., Boyle, D. P., Bäse, F. (2005). Comparison of different efficiency criteria for hydrological model assessment. Advances in geosciences, 5, 89-97.

Kuczera, G. (1997). Efficient subspace probabilistic parameter optimization for catchment models. Water resources research, 33(1), 177-185.

Kundzewicz, Z. W. (2007). Prediction in ungauged basins—a systemic perspective. Predictions in unengaged basins: PUB Kick-off. IAHS Publ, 309.

L'Ecuyer, P. (2012). Random number generation. In Handbook of Computational Statistics (pp. 35-71). Springer Berlin Heidelberg.

Le V. T., Kuo C.-M., Yang T.-C. (2016) Application of non-dominated sorting genetic algorithm in calibration of HBV rainfall-runoff model: a case study of Tsengwen Reservoir catchment in Southern Taiwan. http://www2.hyd.ncku.edu.tw/iche2016/PDF/O.%20Others/15-0056.pdf (accessed 4 August 2017)

Liu, Z., Wang, Y., Xu, Z., Duan, Q. (2017). Conceptual Hydrological Models. Handbook of Hydrometeorological Ensemble Forecasting, 1-23.

Lyon, A. (2013). Why are normal distributions normal?. The British Journal for the Philosophy of Science, 65(3), 621-649.

Marsaglia, G. (1995). The Marsaglia random number CDROM, with the Diehard battery of tests of randomness, produced at Florida State University under flagrant from The National Science Foundation. Access available at www.stat.fsu.edu/pub/diehard, and a revised version of the Diehard tests at www.csis.hku.hk/diehard.

Marsaglia, G., Tsang, W. W. (2002). Some difficult-to-pass tests of randomness. Journal of Statistical Software, 7(3), 1-9.

Merz, R., Blöschl, G., Parajka, J. D. (2006). Regionalization methods in rainfall-runoff modelling using large catchment samples. IAHS publication, 307, 117.

Model Primer. (n.d.), (2017). Sacramento Soil Moisture Accounting Model (SAC-SMA). Retrieved December 08, 2017, from http://www.appsolutelydigital.com/ModelPrimer/chapter5_section10.html.

Montanari, A., Toth, E. (2007). Calibration of hydrological models in the spectral domain: An opportunity for scarcely gauged basins?. Water Resources Research, 43(5).

Mooney, C. Z. (1997). Monte Carlo simulation (quantitative applications in the social sciences).

Moriasi, D. N., Arnold, J. G., Van Liew, M. W., Bingner, R. L., Harmel, R. D., Veith, T. L. (2007). Model evaluation guidelines for systematic quantification of accuracy in watershed simulations. Transactions of the ASABE, 50(3), 885-900.

MACR, (2003). Report on state of water management in the Czech Republic for the year 2002, Prague: Ministry of Agriculture of the Czech Republic, ISBN: 80-86386-40-6.

Nelder, J. A., Mead, R. (1965). A simplex method for function minimization. The computer journal, 7(4), 308-313.

Oracle. (2017). Oracle JDK 9 Documentation. Retrieved December 19, 2017, from https://docs.oracle.com/javase/7/docs/api/java/util/Random.html.

Oudin, L., Andréassian, V., Perrin, C., Michel, C., Le Moine, N. (2008). Spatial proximity, physical similarity, regression and ungaged catchments: a comparison of regionalization approaches based on 913 French catchments. Water Resources Research, 44(3).

Persohn, K. J., Povinelli, R. J. (2012). Analyzing logistic map pseudorandom number generators for periodicity induced by finite precision floating-point representation. Chaos, Solitons and Fractals, 45(3), 238-245.

Pianosi, F., Beven, K., Freer, J., Hall, J. W., Rougier, J., Stephenson, D. B., Wagener, T. (2016). Sensitivity analysis of environmental models: a systematic review with practical workflow. Environmental Modelling & Software, 79, 214-232.

Pitman, W.V., (1973). A Mathematical Model for Generating River Flows from Meteorological Data in South Africa. Report No. 2/73. Hydrological Research Unit, University of the Witwatersrand, Johannesburg, South Africa.

Pykh, Y. A., Hyatt, D. E., Lenz, R. J. (Eds.). (2000). Environmental indices: systems analysis approach-Volume I. EOLSS Publications.

Resende, F. J., Costa, B. V. (1998). Using random number generators in Monte Carlo simulations. Physical Review E, 58(4), 5183.

Roshani, E., Filion, Y. (2012). Using parallel computing to increase the speed of water distribution network optimisation. In WDSA 2012: 14th Water Distribution Systems Analysis Conference, 24-27 September 2012 in Adelaide, South Australia (p. 28). Engineers Australia.

Říha, J. (1997). Matematické modelování hydrodynamických a disperzních jevů. Brno: Vysoké učení technické, ISBN 8021408278, (in Czech).

Sargent, R. G. (2013). Verification and validation of simulation models. Journal of simulation, 7(1), 12-24.

Savenije, H. H. G. (2009). HESS Opinions" The art of hydrology". Hydrology and Earth System Sciences, 13(2), 157-161.

Shahin, M. (2002). Runoff, streamflow, erosion and sedimentation. Hydrology and Water Resources of Africa, 213-270.

Sherman, L. K. (1932). Streamflow from rainfall by the unit-graph method, Eng. News Record, 108, 501-505. http://ci.nii.ac.jp/naid/10023998652.

Simon, M. (2005). Labe a jeho povodí–geografický, hydrologický a vodohospodářský přehled. Mezinárodní komise pro ochranu Labe, Magdeburg, (in Czech).

Singh, V. P., Woolhiser, D. A. (2002). Mathematical modeling of watershed hydrology. Journal of hydrologic engineering, 7(4), 270-292.

Sommer, M. (1973). Aplikovaná hydrologie. Brno: Ediční středisko Vysokého učení technického, (in Czech).

Stipčević, M., Koç, Ç. K. (2014). True random number generators. In: Open Problems in Mathematics and Computational Science (pp. 275-315). Springer International Publishing.

Storn, R., Price, K. (1997). Differential evolution–a simple and efficient heuristic for global optimization over continuous spaces. Journal of global optimization, 11(4), 341-359.

Tang, T., Reed, P., Wagener, T., Van Werkhoven, K. (2006). Comparing sensitivity analysis methods to advance lumped watershed model identification and evaluation. Hydrology and Earth System Sciences Discussions, 3(6), 3333-3395.

Tigkas, D., Christelis, V., Tsakiris, G. (2016). Comparative study of evolutionary algorithms for the automatic calibration of the Medbasin-D conceptual hydrological model. Environmental Processes, 3(3), 629-644. https://doi.org/10.1007/s40710-016-0147-1.

Tolson, B. A., Shoemaker, C. A. (2007). Dynamically dimensioned search algorithm for computationally efficient watershed model calibration. Water Resources Research, 43(1).

Troiano, L., Pasquale, DD., Marinaro, P. (2013). Jenes: Genetic algorithms for Java, JAR package version 2.2.1. https://sourceforge.net/projects/jenes/files/Jenes.

Vicente-Serrano, S. M., Beguería, S., López-Moreno, J. I. (2010). A multiscalar drought index sensitive to global warming: the standardized precipitation evapotranspiration index. Journal of climate, 23(7), 1696-1718.

Vörösmarty, C. J., Green, P., Salisbury, J., Lammers, R. B. (2000). Global water resources: vulnerability from climate change and population growth. Science, 289(5477), 284-288.

Vrugt, J. A., Gupta, H. V., Bouten, W., Sorooshian, S. (2003). A Shuffled Complex Evolution Metropolis algorithm for optimisation and uncertainty assessment of hydrologic model parameters. Water Resources Research, 39(8).

Vrugt, J. A., Gupta, H. V., Dekker, S. C., Sorooshian, S., Wagener, T., Bouten, W. (2006). Application of stochastic parameter optimisation to the Sacramento soil moisture accounting model. Journal of Hydrology, 325(1), 288-307.

Wagener, T., Kollat, J. (2007). Numerical and visual evaluation of hydrological and environmental models using the Monte Carlo analysis toolbox. Environmental Modelling & Software, 22(7), 1021-1033.

Wagener, T., Wheater, H. S., Gupta, H. V. (2004). Rainfall-runoff modelling in gauged and ungauged catchments.

Wallace, J., McJannet, D. (2012). Climate change impacts on the water balance of coastal and montane rainforests in northern Queensland, Australia. Journal of hydrology, 475, 84-96. 6.

Wang, Q.J., (1991). The genetic algorithm and its application to calibrating conceptual rainfall-runoff models. Water Resour. Res. 27 (9), 467–2471. Wang (1991)

Wang, Y. C., Yu, P. S., Yang, T. C. (2010). Comparison of genetic algorithms and shuffled complex evolution approach for calibrating distributed rainfall–runoff model. Hydrological processes, 24(8), 1015-1026. DOI: 10.1002/hyp.7543.

Wu, S. J., Lien, H. C., Chang, C. H. (2012). Calibration of a conceptual rainfall–runoff model using a genetic algorithm integrated with runoff estimation sensitivity to parameters. Journal of Hydroinformatics, 14(2), 497-511.

Yu, P. S., Jeng, Y. C. (1997). A study on grid based distributed rainfall runoff models. Water resources management, 11(2), 83-99.

Zhang, C., Wang, R. B., Meng, Q. X. (2015). Calibration of conceptual rainfall-runoff models using global optimisation. Advances in Meteorology, 2015.

Zhao, R., Zhuang, Y., Fang, L., Liu, X., Zhang, Q. (1980). The Xinanjiang model. Hydrological Forecasting Proceedings Oxford Symposium, IASH 129, 351-356. National Center for Atmospheric Research, Computational and Information Systems Laboratory. http://rda. ucar. edu/datasets/ds083, 2.

Zvára, K., Štěpán, J. (2006). Pravděpodobnost a matematická statistika. Praha: Matfyzpress, ISBN 80-86732-71-1, (in Czech).

Publications of the Author

Publications Relevant for the Thesis

Articles in journals, with IF:

[A 1] Chlumecký, M. (62%), Buchtele, J. (33%), Richta, K. (5%). **Application of Random Number Generators in Genetic Algorithms to Improve Rainfall-Runoff Modelling.** *Journal of Hydrology.* 2017, 553, pp 350-355. ISSN 0022-1694. (WoS, Scopus), IF=3.483

The paper has been cited in:

Zeng, M.; Cheng, W.; Guo, P., **Modelling and Metaheuristic for Gantry Crane Scheduling and Storage Space Allocation Problem in Railway Container Terminals**. *DISCRETE DYNAMICS IN NATURE AND SOCIETY*, 2017. ISSN 1026-0226. (WoS, Scopus), IF=0.711

Articles in journals, indexed by WoS, Scopus:

[A 2] Chlumecký, M. (100%). **Simulation of Hydrological Processes by Optimization Algorithm using Continuous Function**. *Advances in Intelligent Systems and Computing.* 2016, 511 pp 110-121. ISSN 2194-5357. (WoS, Scopus)

[A 3] Chlumecký, M. (34%), Tesar, M. (33%), Buchtele, J. (33%). **Ascertaining of Evapotranspiration Series by Optimized Rainfall-Runoff Model.** *Boletin Geologico y Minero.* 2016, (in print) ISSN 0366-0176. (Scopus)

In proceedings, indexed by WoS, Scopus:

[A 4] Chlumecký, M. (34%); Tesař, M. (33%), Buchtele, J. (33%). **The Appraisals of Long Time Series of Evapotranspiration Using Modelling Rainfall-Runoff with Optimized Parameters**, In: *International work-conference on Time Series 2014.* Granada: Universidad de Granada, 2014, pp. 1280-1291. ISBN 978-84-15814-97-9. (WoS)

In proceedings:

[A 5] Chlumecký, M. (34%), Tesař, M. (33%), Buchtele, J. (33%). **Evaluation of Changes in Water Regime Caused by Long-term Development of Vegetation Cover,** In: *Hydrologie malého povodí 2014.* Praha: Ústav pro hydrodynamiku AVČR, 2014, pp. 160-165. ISBN 978-80-02-02525-2.

[A 6] Chlumecký, M. (100%). **Optimizing of Parameters Soil Moisture Accounting Model (SAC-SMA)**, In: *POSTER 2013 – 17th International Student Conference on Electrical Engineering.* Prague: Czech Technical University, 2013, pp. 1-6. ISBN 978-80-01-05242-6.

Publications with Partial Relevance to the Thesis

Articles in journals:

[A 7] Chlumecký, M. (80%), Buchtele, J. (20%). **Analysis of Water Regime Modification Induced by Long-Term Development of Vegetation Cover**. *Int J Hydro*, 2017, 1(6). ISSN 2576-4454

In proceedings, indexed by WoS, Scopus:

[A 8] Chlumecký, M. (100%). **Methods and Approaches for Reverse Engineering**. In: *38th Software Development 2012*. Ostrava: VŠB - Technická univerzita Ostrava, 2012. pp. 36-42. ISBN 978-80-248-2669-1. (WoS)

In proceedings:

[A 9] Chlumecký, M. (100%). **Case Study of Legacy Systems: Converting and Improvement** In: *SDOT 2013*. Praha: Vysoká škola manažerské informatiky a ekonomiky, a.s., 2013. pp. 61-70. ISBN 978-80-86847-66-5.

[A 10] Chlumecký, M. (100%). **Practice Use of GXL in Reverse Engineering**. In: *Objekty 2012*. Praha: Vysoká škola manažerské informatiky a ekonomiky, a.s., 2012, pp. 84-94. ISBN 978-80-86847-63-4.

[A 11] Chlumecký, M. (100%). **Call Graph of FORTRAN Captured by GXL**. *Business & IT*. 2013, 2012(2), 91-103. ISSN 1805-3777.

[A 12] Chlumecký, M. (100%). **Using reverse engineering to re-implementing procedural source code**. In: *Objekty 2011*. Žilina: Žilinská univerzita v Žiline, Fakulta riadenia a informatiky, 2011, pp. 131-136. ISBN 978-80-554-0432-5.

Unreferenced Publications

In proceedings:

[A 13] Chlumecký, M. (100%). **History of the Temelín Nuclear Power Plant**. In: *POSTER 2012 – 16th International Student Conference on Electrical Engineering*. Praha: Czech Technical University in Prague, 2012, pp. 1-4. ISBN 978-80-01-05043-9.

Appendix A

Input Data

01.1.1954	3.1	-8.0	0.0032
02.1.1954	0.8	-12.0	0.0032
03.1.1954	0.2	-10.3	0.0032
04.1.1954	0.7	-7.2	0.0032
05.1.1954	0.0	-12.2	0.0037
06.1.1954	0.0	-9.8	0.0037
07.1.1954	0.3	-5.6	0.0037
08.1.1954	4.5	-8.3	0.0037
09.1.1954	2.3	-9.8	0.0037
10.1.1954	5.3	-8.0	0.0037
11.1.1954	0.6	-8.5	0.0037
12.1.1954	0.6	-7.9	0.0037
13.1.1954	1.8	-2.5	0.0037
14.1.1954	0.0	-0.5	0.0037
15.1.1954	0.0	-3.1	0.0037
16.1.1954	5.6	-3.0	0.0037
17.1.1954	0.0	1.7	0.0037
18.1.1954	1.1	-1.9	0.0037
19.1.1954	0.0	-1.8	0.0037
20.1.1954	6.1	0.0	0.0037

Statistical Information

Month	Sim. Mean	Obs. Mean	% bias	Mth bias %	avg Abs err
[1]	0.023	0.023	0.256	0.049	23.812
[2]	0.029	0.029	-1.244	-0.282	30.328
[3]	0.063	0.062	0.547	0.291	74.025
[4]	0.122	0.122	-0.222	-0.223	118.656
[5]	0.086	0.085	0.261	0.190	63.571
[6]	0.073	0.073	-0.343	-0.207	73.573
[7]	0.072	0.072	0.228	0.141	63.833
[8]	0.038	0.038	-0.729	-0.236	31.495
[9]	0.023	0.022	1.989	0.368	22.566
[10]	0.028	0.029	-1.025	-0.250	25.849
[11]	0.035	0.034	0.703	0.200	23.975
[12]	0.036	0.037	-1.255	-0.394	36.958
Total	0.052	0.052	-0.067	-0.353	49.075

Daily RMS error	0.160
Daily AVG ABS error	0.026
AVG ABS Monthly vol error	0.539
Monthly volume RMS error	1.829
Correlation	0.775
Nash-Sutcliffe	0.574
Monthly ABS volume error	2.830
RMSE-W	0.119

Model parameters

```
[sacramento]
tile = Raztoka 1953-1954
from = 1.1.1953
  to = 31.12.1954

[snow17]
card1 = 880.00; 50.00;
card2 = 24.00; 0.9640;
card3 = 24.00; 242.0446; 0.6179; 0.3030;
card4 = 0.8196; 0.2309; 0.3127; 0.1081; 32.2998;
card5 = 0.1863; 0.0897; -0.9240; 1.4976; 0.4930; 0.00;
  adc = 0.3724; 0.4777; 0.5839; 0.7920; 0.8960; 0.9480; 0.9740; 0.9870; 0.9935;

[sacsma]
card1 = 0.3325; 3.3495; 674.8948; 12.1411; 0.3423; 0.00; 0.0404; 0.3046; 0.00; 1.00;
card2 = 23.785; 2.603; 599.433; 66.4411; 22.5932; 0.0518; 0.0122; 0.129; 0.079; 0.00;
card3 = 76.4009; 0.00; 158.5981; 0.00; 8.0760; 169.3168;
   et = et12
 etTs = 1.00; 1.00; 1.00; 1.00; 1.00; 1.00; 1.00; 1.00; 1.00; 1.00; 1.00; 1.00
 et12 = 0.07; 0.44; 0.67; 0.25; 1.07; 1.73; 0.84; 1.48; 4.76; 0.53; 0.147; 0.01;
etGauss = 55.00; 35.00; 6800.00; 0.05

[unithg]
card1 = 2.5400; 0.0
uhg = uhgDiff
uhgDiff = 10.00; 3.15; 130.00; 0.65; 36.00; 0.01;
uhgTs = 0.0090; 0.0010; 0.0010
```

Parameter ranges

```
[snow17]
card1 = 0.00; 0.00;
card2 = 0.00; 0.80;
card3 = 0.00; 0.80; 0.80; 0.80;
card4 = 0.80; 0.80; 0.80; 0.80; 0.80;
card5 = 0.80; 0.80; 0.80; 0.80; 0.80; 0.80;
  adc = 0.80; 0.80; 0.80; 0.80; 0.80; 0.80; 0.80; 0.80; 0.80;

[sacsma]
card1 = 0.80; 0.80; 0.80; 0.80; 0.80; 0.80; 0.80; 0.80; 0.00; 0.80;
card2 = 0.80; 0.80; 0.80; 0.80; 0.80; 0.80; 0.80; 0.80; 0.80; 0.80;
card3 = 0.80; 0.80; 0.80; 0.80; 0.80; 0.80;
   et = et12
 et12 = 0.80; 0.80; 0.80; 0.80; 0.80; 0.80; 0.80; 0.80; 0.80; 0.80; 0.80; 0.80;

[unithg]
card1 = 0.00; 0.00;
  uhg = uhgTs
uhgTs = 0.00; 0.00; 0.00;
```

Appendix B

Importance of Evapotranspiration

The evapotranspiration is one of the essential hydrological phenomena for modelling of the rainfall-runoff process, which is needed and extensively used for the evaluation of water regime mainly in basins with vegetation cover, Hanson (1991). Unfortunately, the measuring devices for evapotranspiration are scarcely realistic and available for large river basins. If longer and older time series are analysed, then there are no values of evapotranspiration at all, Kuczera (1997). Therefore, the simulation of the rainfall-runoff process still has to be used to obtain the appropriate values of evapotranspiration.

However, the various water changes in runoff caused by natural variability and unexpected events are significant and require further inspection. The historical changes in the land use should be reconsidered, due to the influence of water reservoirs, such as ancient fishing ponds, canals, rivers regulations, etc. The illustration of the situation with the extraordinary large fish-pond affecting water regime is demonstrated in Figure 9.1, which was built 500 years ago. The notion concerning the displayed destructive and extensive effect of the flood is indicated in Figure 9.2, which also documents the extent of this flood. Moreover, these pictures, together with Figure 9.5, document the retention and evaporation effects of the floods.

Figure 9.1: Retention of the Rožmberk pond during the flood in August 2002, *MACR (2003)*

The total retained volume is estimated at about 70 million cubic meters. Inflow Q_{max}=700 m^3/s, runoff Q_{max}=270 m^3/s, i.e. ΔQ=430 m^3/s. Achieved water levels: H_{max}=860 cm, $H_{overfall}$=571 cm.

Altogether, the instance in Figure 9.2 provides an example of a stage of the main stream of the Vltava river. It needs to be noted that the dams and reservoirs on the Vltava river play a significant role in flood protection of Prague.

Figure 9.2: Water reservoir Orlík st Vltava - flood August 2002, *MACR (2003)*

The intention to decrease uncertainties in the water regime caused by different oscillations requires the evaluation of the appearing natural fluctuations and the abrupt seeming random changes in the basin. This consecutive variability of water regime is usually influenced by changes of the vegetation cover, its growth and also other natural events, e.g. wind and insect disasters. Figure 9.3 and Figure 9.4 document long-term and random changes in both local and regional processes in the water regime.

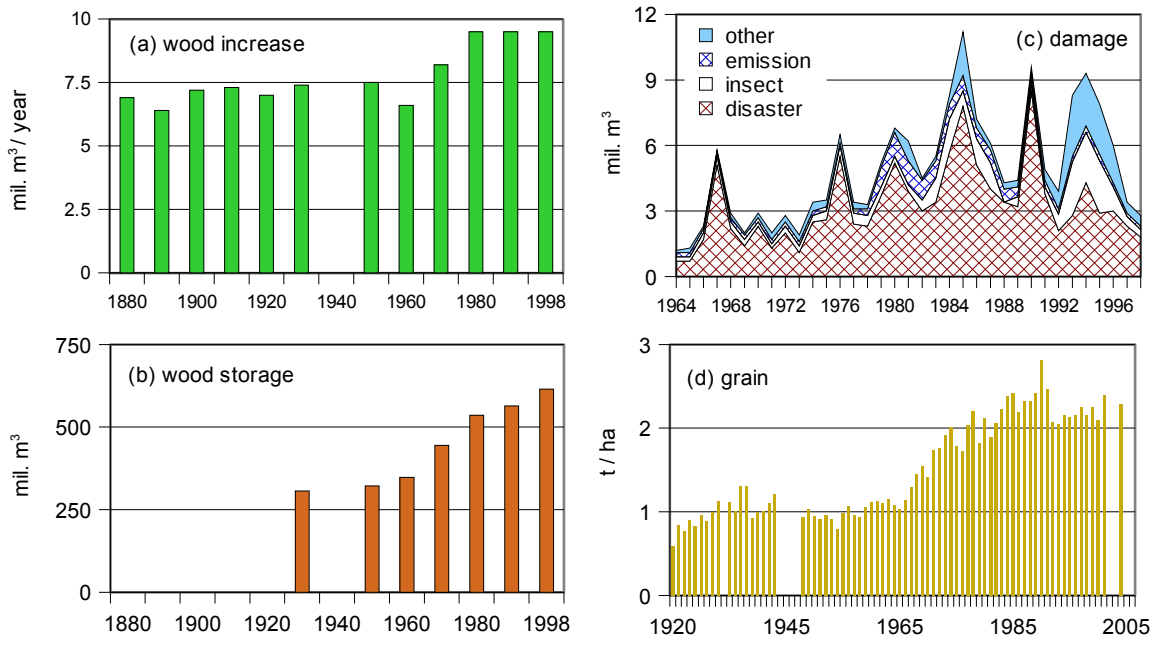

Figure 9.3: Czech forests stage and grain production during past more than 100 years

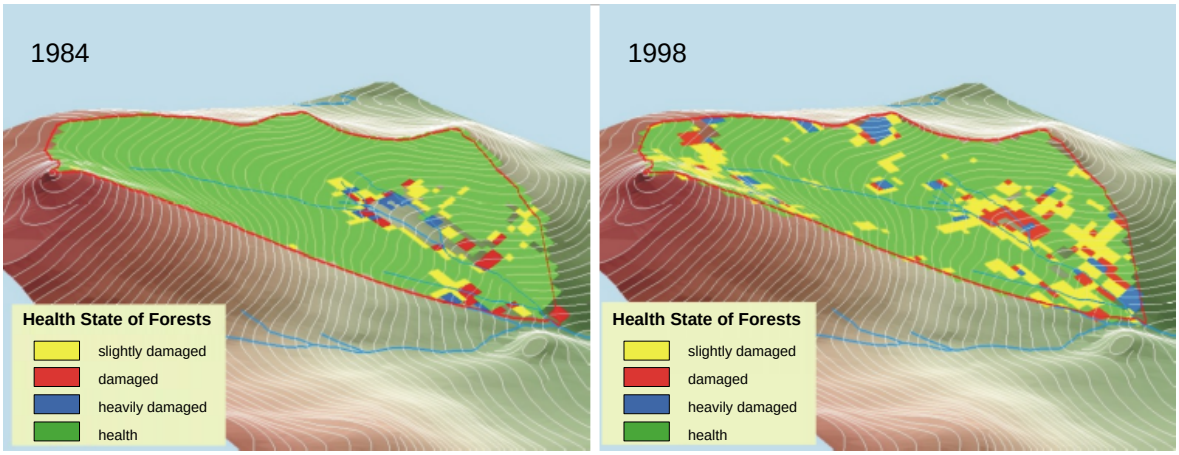

Figure 9.4: Forest disasters in experimental Liz basin in Šumava Mts., *Buchtele et al. (2009)*

The changes of vegetation cover and the desirable appraisals of the interactions between evapotranspiration demand (evapotranspiration needs) and sub-surface water storage seem to be rather significant processes. The agricultural production, e.g. increased yields of grain, has already been labelled a significant phenomenon for water balance several years ago, Keller (1970). The desirable attention on the higher variability of evapotranspiration demands is caused by solar radiation correlated with solar activity, Beer (2005).

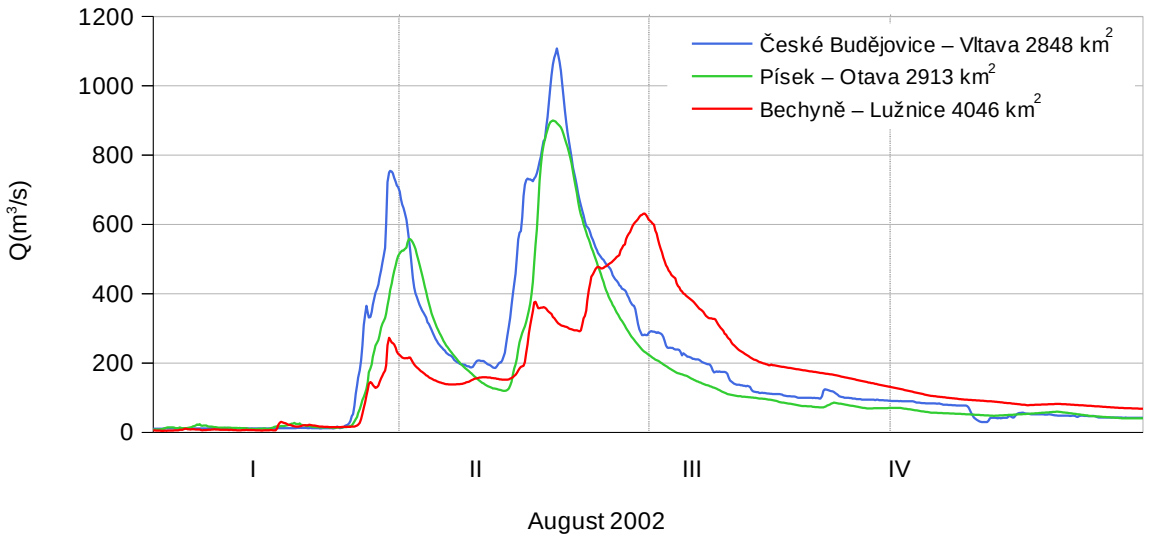

Figure 9.5: Main inflows of reservoir Orlík at Vltava river

The length of evaluated time series is generally significant. When daily time series of several decades to the past are available, these circumstances enable the observation and assertion of the influences of the vegetation development on the evapotranspiration demand and it could significantly influence runoff, Calder *et al.* (1982). In Great Britain, the role of ensuing deforestation has been viewed positively in terms of it providing more water for overall water supply. Figure 9.5 is an illustration of expressive regional floods with high areal diversity caused by the activities of our ancestors, e. g. building dams, ponds, etc.

The evolution of the vegetation cover is usually perceived as one of the natural causes of the usual annual oscillations in water resources. However, another reason for these fluctuations could also be the development of the vegetation cover during decades. It means that this might affect the long-term evaporation variability, e.g. due to the wind disasters in forests. The precise modelling of the rainfall-runoff process appears helpful in the efforts to decrease uncertainties in the water regime. Figure 9.6 is a relevant example of the situation in the catchment where deforestation and other similar interventions, influencing evaporation and runoff, appeared. The course of differences between observed and simulated discharge helps us follow the dynamics in current modifications. It helps to identify the intervals for which the evapotranspiration demand could be expected to be a stable process. Hence, the model implementation and optimal simulation are attainable.

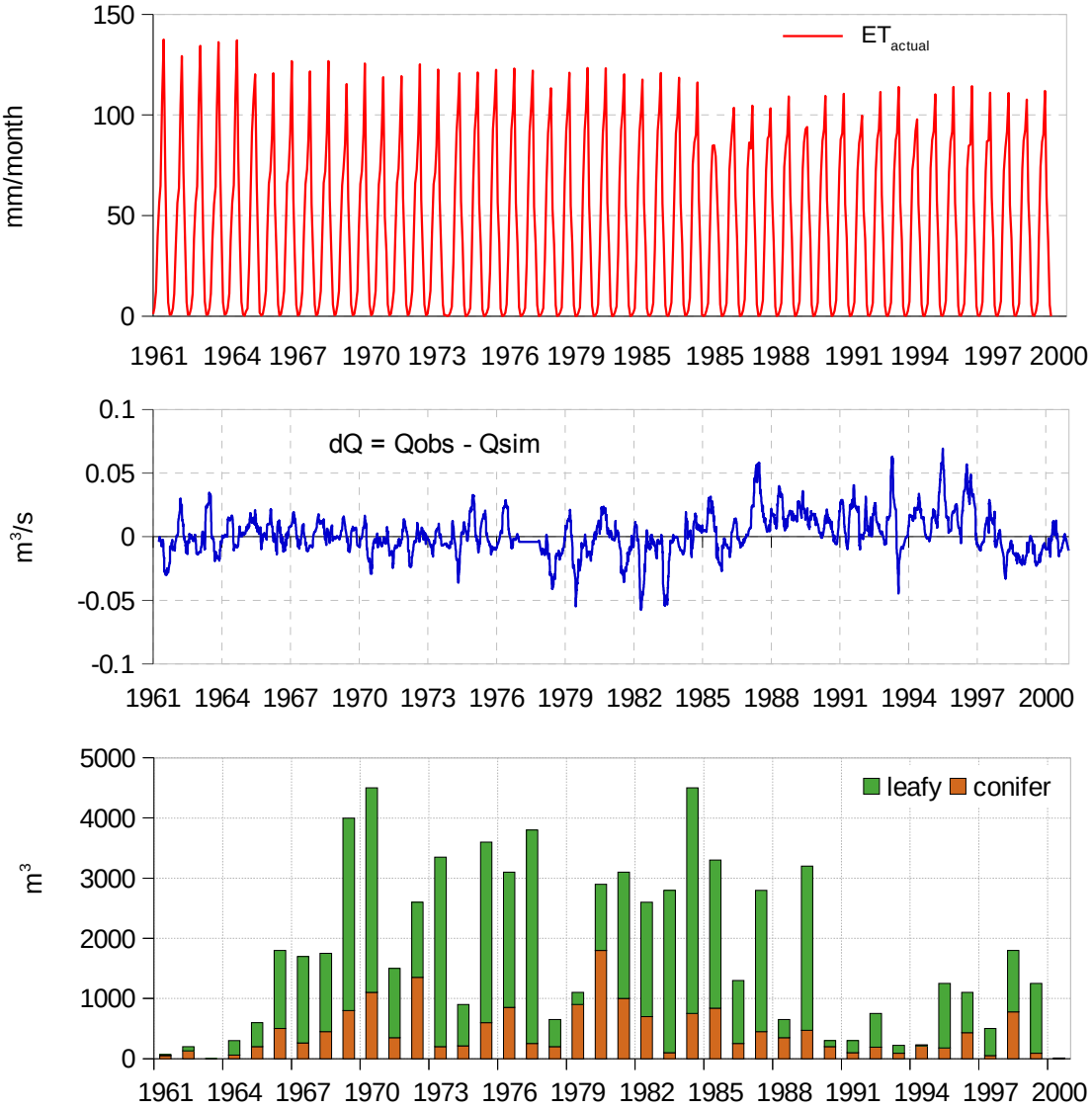

Figure 9.6: Evapotranspiration decreasing and runoff variation in Raztoka basin as respond to cutting trees in the forest

Appendix C

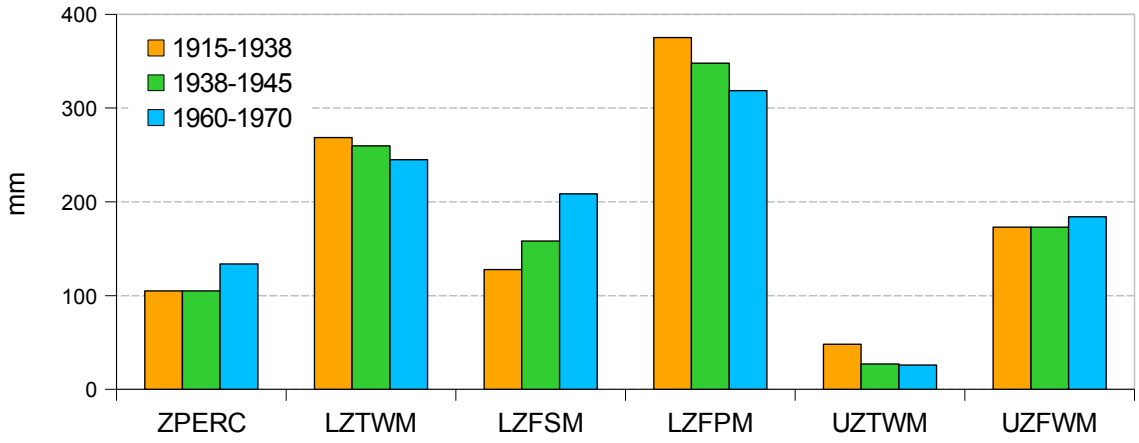

Figure 9.7: SAC-SMA model parameters for the Labe River during different time periods

Moreover, Figure 9.7 indicates that the changes in vegetation cover could be the reason for the changes in the parameters of conceptual models and not for the changes in evapotranspiration.

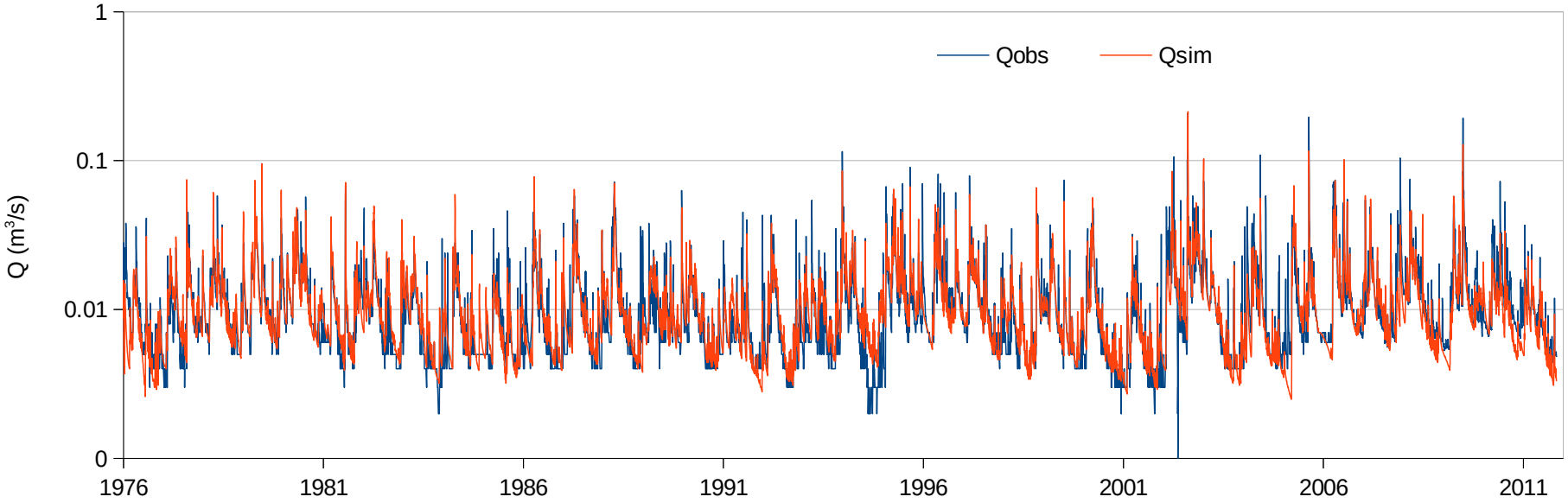

Figure 9.8: Logarithmic scale of observed and simulated discharges of the Liz catchment

Influence of diverse parameters for partial intervals whole period years 1976–2011 of the Liz catchment (as is depicted by distinct colours in the graphs).

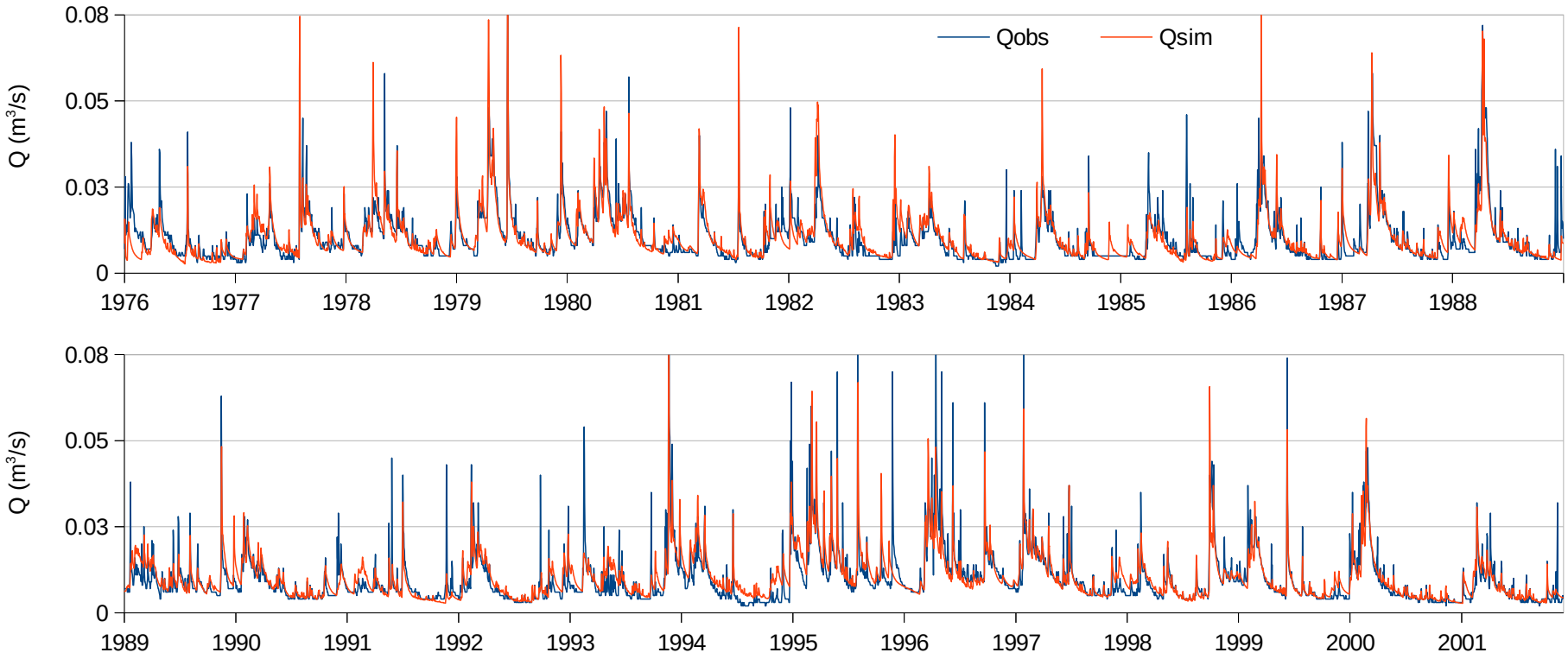

Figure 9.9: ΔQ of the Liz catchment for two time periods with some changes in the basin

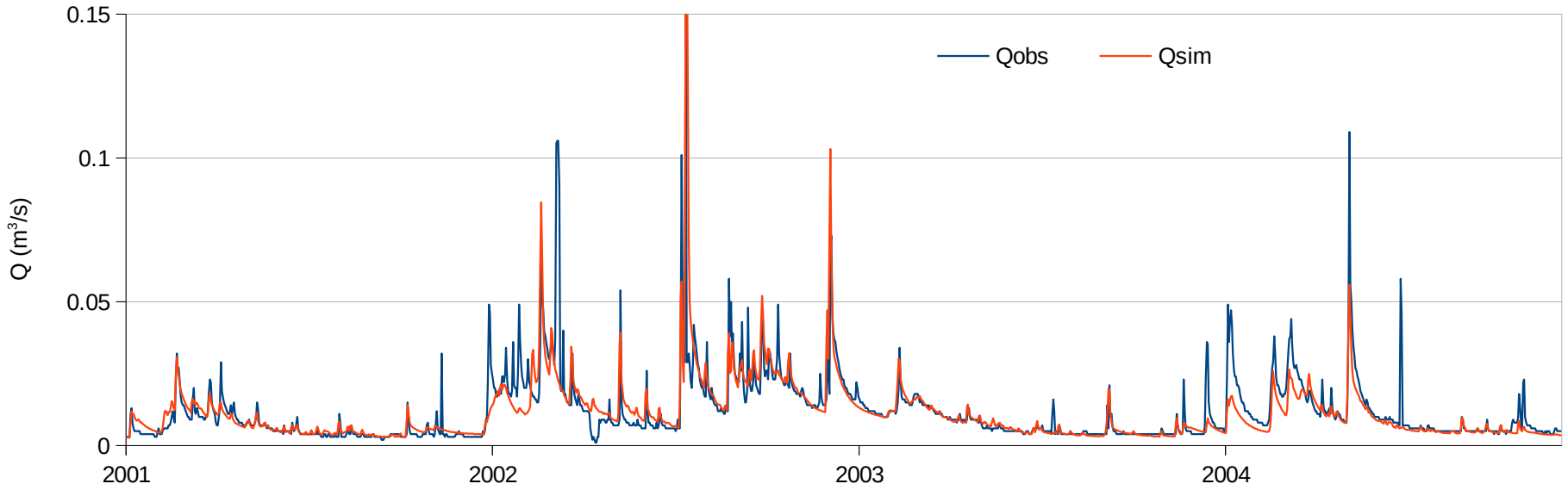

Figure 9.10: ΔQ of the Liz catchment during the flood event in 2002

In Figure 9.10 the runoff changes are typical for the year 2002 with three flow waves and one extraordinarily strong flood. It indicates the realistic estimation of the main model parameters. Moreover, the Sacramento model searches for the reasons for corrections of the input data in some short intervals. This proves the quality of the model calibration in the year cycle in the frame 2002–2003.

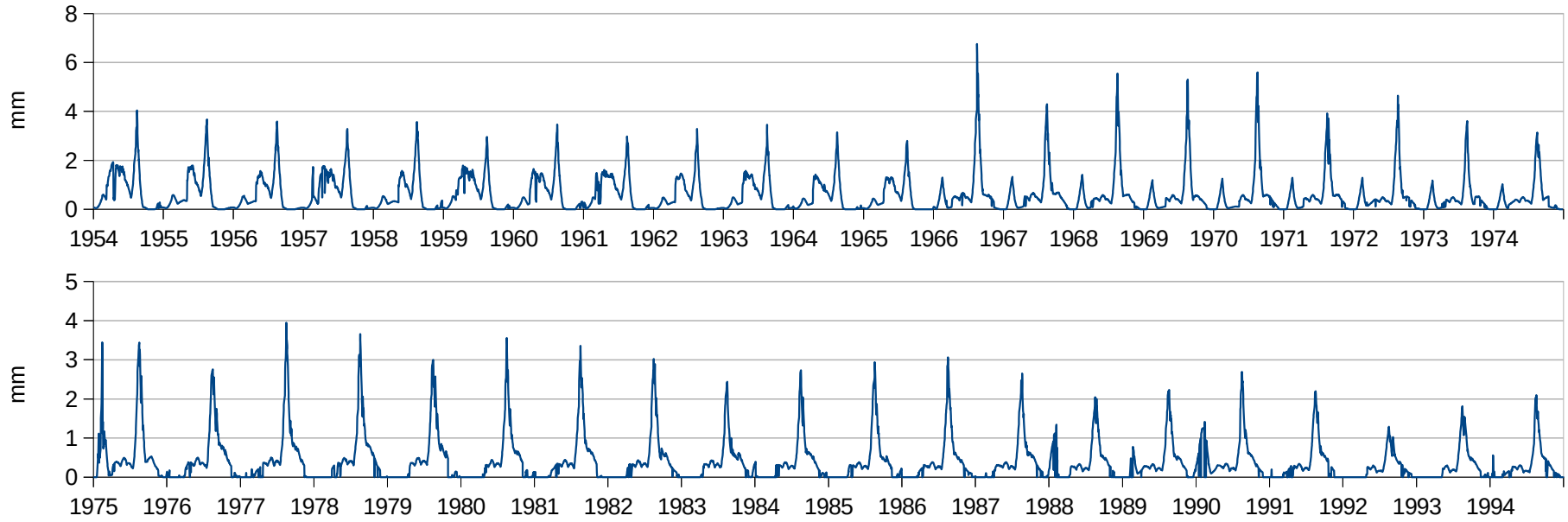

Figure 9.11: Annual development of Ráztoka evapotranspiration

Differentiated courses of Ráztoka evapotranspiration in sundry intervals. It suggests the development of the vegetation cover over the annual cycle and long-term courses.

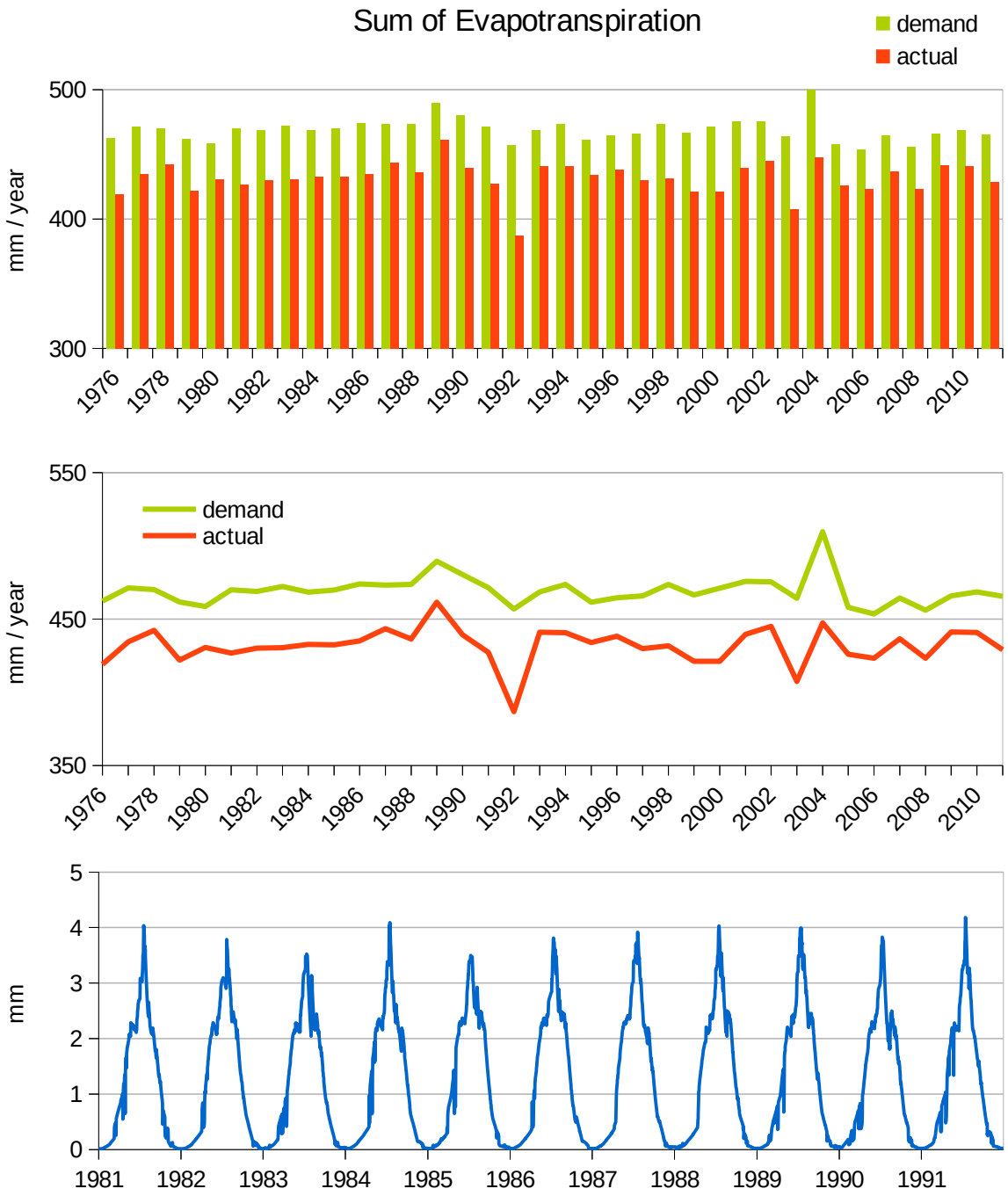

Figure 9.12: ET_{atc} and ET_{dem} of the Liz catchment

Figure 9.12 illustrates oscillations of the occurrence of the disaster periods caused by the insect damage in this forested basin (see Appendix B, Figure 9.3 and Figure 9.4).

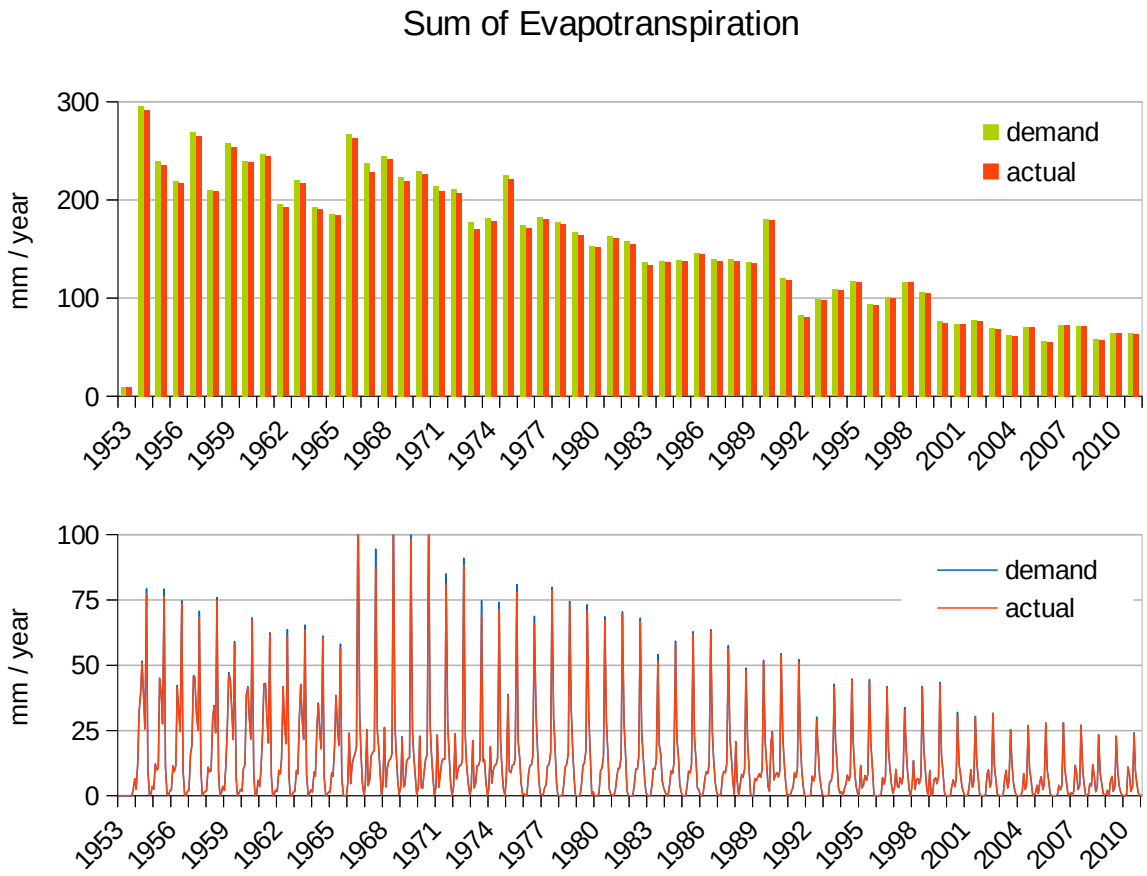

Figure 9.13: Course of Ráztoka evapotranspiration in annual cycles

Figure 9.13 represents the sum of evapotranspiration in annual cycle and a long-term tendency in the forested basin of the Ráztoka catchment. Perhaps it appeared due to consecutive re-forestation.

Acronyms

AAMVE	Average Absolute Monthly Volume Error
ADC	Areal Depletion Curve
ET	Evapotranspiration
ET_{act}	Current Evapotranspiration
ET_{dem}	Demand Evapotranspiration
GA	Genetic Algorithm
HRNG	Hydro-Random Number Generator
CHI	Czech Hydrometeorological Institute
LCG	Linear Congruential Generators
MCS	Monte Carlo Simulation
MTG	Mersenne Twister Generator
MVRMSE	Monthly volume Root Mean Square Error
NOAA	National Oceanic Atmospheric Administration
NWS	National Weather Service
NWSRFS	National Weather Service River Forecast System
PRNG	Pseudo-Random Number Generator
R	Correlation Coefficient
RMSE	Root Mean Square Error
RNG	Random Number Generator
SAC-SMA	Sacramento Soil Moisture Accounting Model
SNOW-17	Snow Accumulation and Ablation Model
TDE	Translation Diffusion Equation
TRNG	True Random Number Generator
UNIT-HG	Unit Hydrograph